

**LIFT-OFF DETECTION SYSTEM USING
ERROR COMPENSATED EDDY CURRENT
TESTING BASED ON FUZZY LOGIC**



KHARUDIN BIN ALI

MASTER OF SCIENCE

UNIVERSITI MALAYSIA PAHANG

UNIVERSITI MALAYSIA PAHANG

DECLARATION OF THESIS AND COPYRIGHT

Author's Full Name : KHARUDIN BIN ALI

Date of Birth : 09 November 1981

Title : LIFT-OFF DETECTION SYSTEM USING
ERROR COMPENSATED EDDY CURRENT TESTING
BASED ON FUZZY LOGIC

Academic Session : 2/ 2016-2017

I declare that this thesis is classified as:

- CONFIDENTIAL (Contains confidential information under the Official Secret Act 1997)*
- RESTRICTED (Contains restricted information as specified by the organization where research was done)*
- OPEN ACCESS I agree that my thesis to be published as online open access (Full Text)

I acknowledge that Universiti Malaysia Pahang reserves the following rights:

1. The Thesis is the Property of Universiti Malaysia Pahang
2. The Library of Universiti Malaysia Pahang has the right to make copies of the thesis for the purpose of research only.
3. The Library has the right to make copies of the thesis for academic exchange.

Certified by:

(Student's Signature)

(Supervisor's Signature)

New IC/Passport Number
Date:

Name of Supervisor
Date:

NOTE : * If the thesis is CONFIDENTIAL or RESTRICTED, please attach a thesis declaration letter.

SUPERVISOR'S DECLARATION

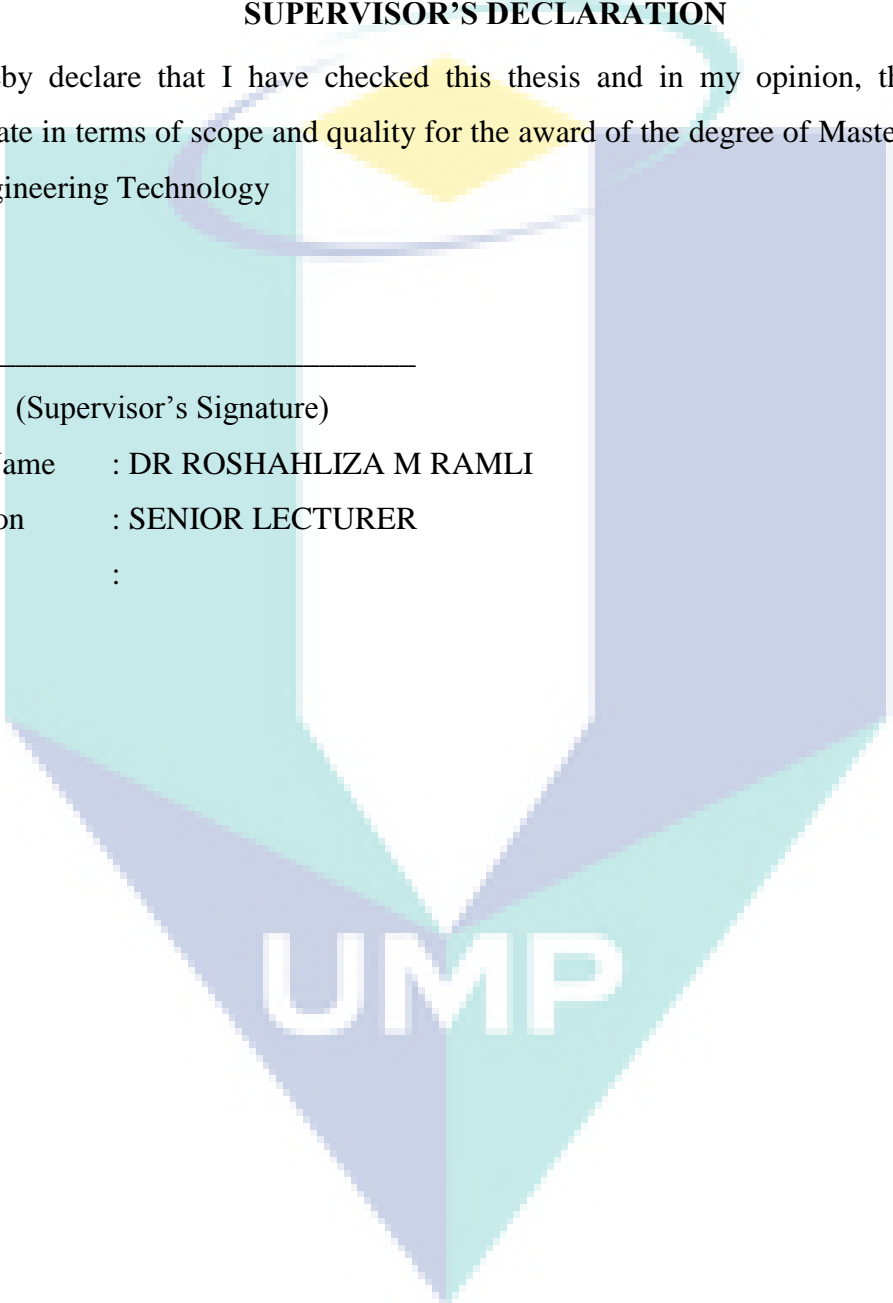
I hereby declare that I have checked this thesis and in my opinion, this thesis is adequate in terms of scope and quality for the award of the degree of Master of Science in Engineering Technology

(Supervisor's Signature)

Full Name : DR ROSHAHLIZA M RAMLI

Position : SENIOR LECTURER

Date :



UMP

STUDENT'S DECLARATION

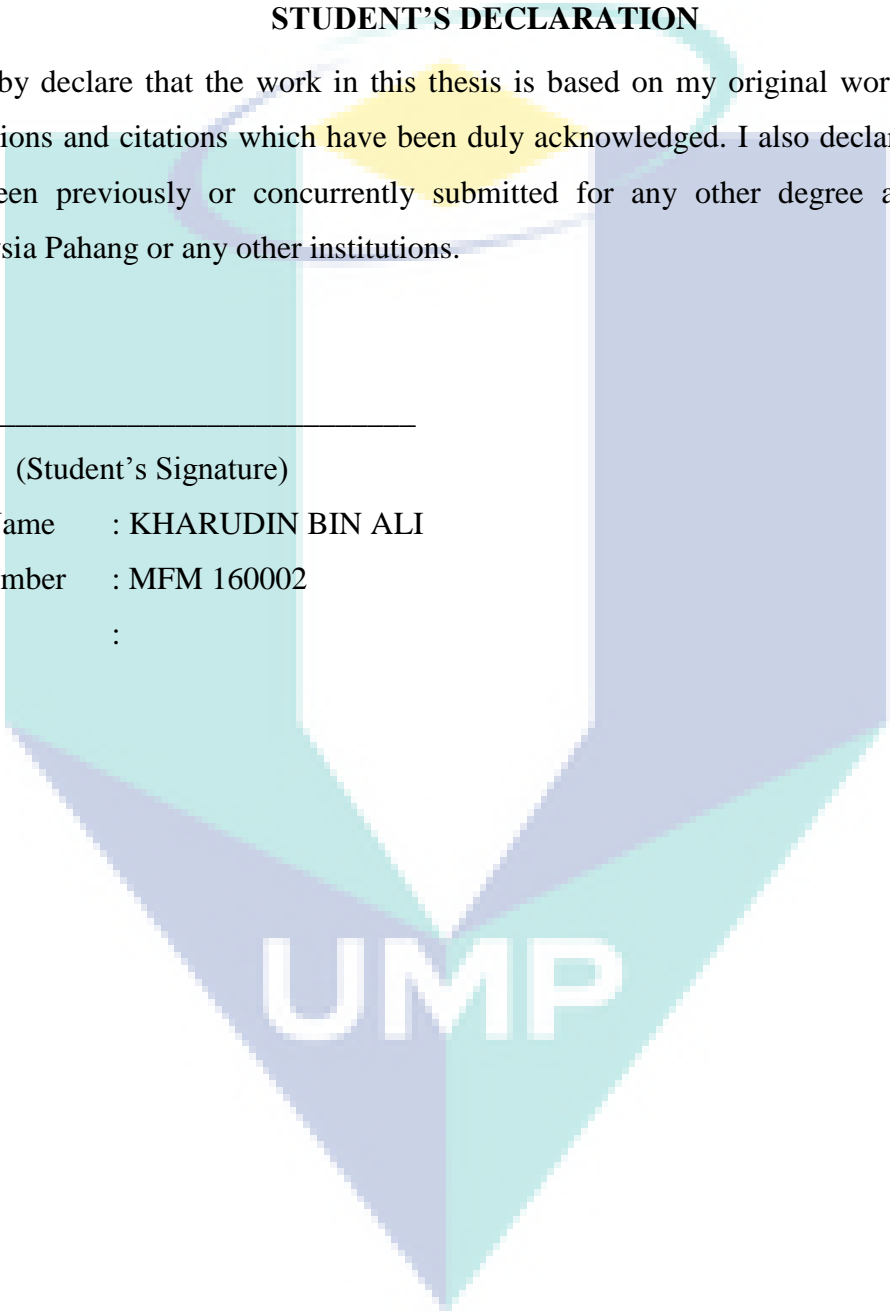
I hereby declare that the work in this thesis is based on my original work except for quotations and citations which have been duly acknowledged. I also declare that it has not been previously or concurrently submitted for any other degree at Universiti Malaysia Pahang or any other institutions.

(Student's Signature)

Full Name : KHARUDIN BIN ALI

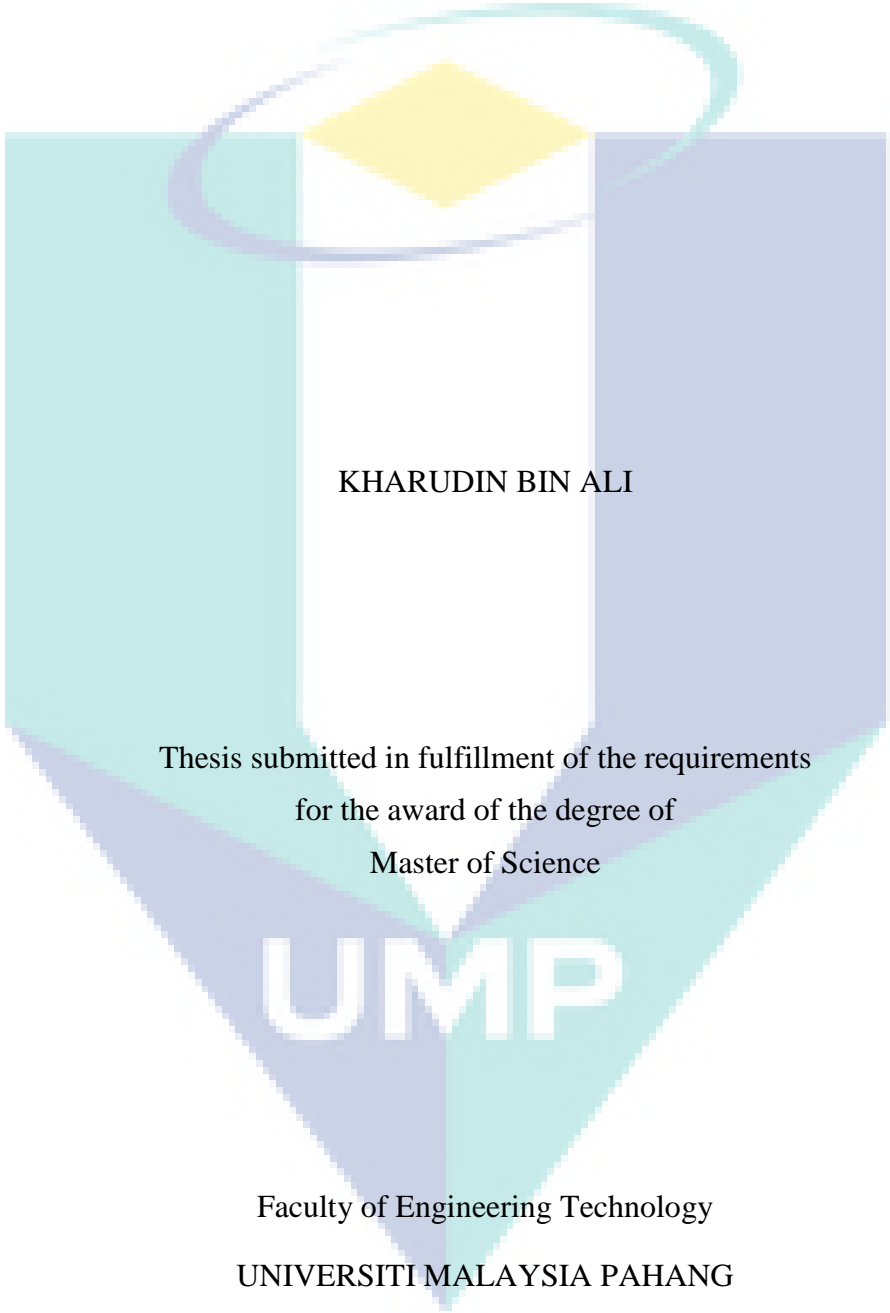
ID Number : MFM 160002

Date :



UMP

LIFT-OFF DETECTION SYSTEM USING ERROR COMPENSATED EDDY
CURRENT TESTING BASED ON FUZZY LOGIC



KHARUDIN BIN ALI

Thesis submitted in fulfillment of the requirements
for the award of the degree of
Master of Science

UMP

Faculty of Engineering Technology
UNIVERSITI MALAYSIA PAHANG

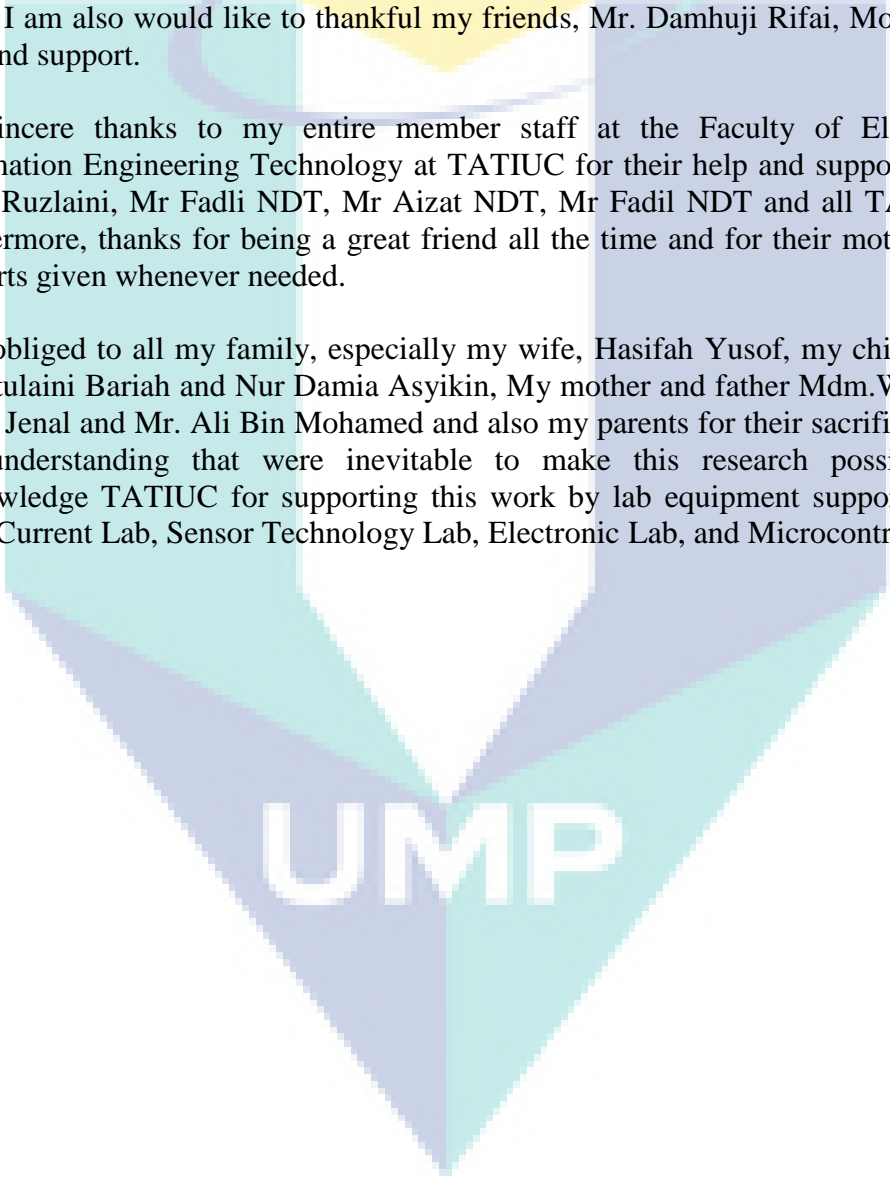
MAY 2017

ACKNOWLEDGEMENTS

All praise to Allah for giving me the inner strength in completing the thesis. I am grateful and would like to express my sincere gratitude and appreciation to my supervisor, Associate Professor Dr. Ahmed N. Abdalla and for the support, invaluable guidance and continuous encouragement throughout this research. Besides, he has offered me invaluable helps in writing and publishing the research works. Not forget for my main supervisor Dr Roshahliza M Ramli for guidance and suggestion to completing this thesis. I am also would like to thankful my friends, Mr. Damhuji Rifai, Moneer, for his help and support.

My sincere thanks to my entire member staff at the Faculty of Electrical and Automation Engineering Technology at TATIUC for their help and support especially to Dr Ruzlaini, Mr Fadli NDT, Mr Aizat NDT, Mr Fadil NDT and all TATIUC staff Furthermore, thanks for being a great friend all the time and for their motivations and supports given whenever needed.

I am obliged to all my family, especially my wife, Hasifah Yusof, my children, Nurul Qurratulaini Bariah and Nur Damia Asyikin, My mother and father Mdm.Wan Fatimah Bt W. Jenal and Mr. Ali Bin Mohamed and also my parents for their sacrifice, patience, and understanding that were inevitable to make this research possible. I also acknowledge TATIUC for supporting this work by lab equipment supported through Eddy Current Lab, Sensor Technology Lab, Electronic Lab, and Microcontroller Lab.



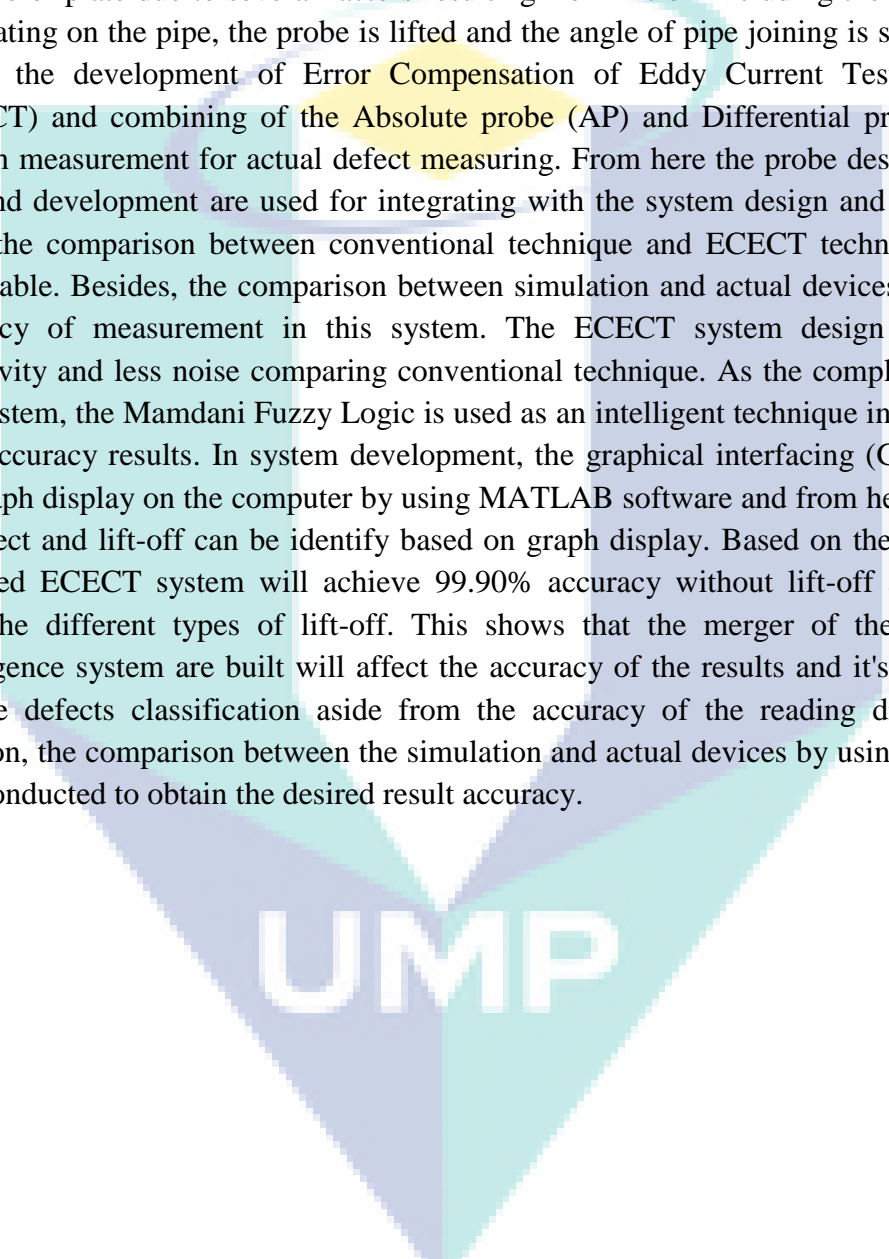
UMP

ABSTRAK

Ujian tanpa musnah (NDT) merujuk kepada pemeriksaan objek untuk menentukan sifat-sifatnya tanpa memusnahkan fungsinya. Aplikasi termasuklah bagi pengesanan keretakan dalam salutan industri, wap penjana tiub di loji kuasa nuklear, kapal terbang dan lain-lain. Sebagai salah satu keadah NDT, ujian eddy current digunakan bagi mengesan lift-off pada paip atau plat selain pelbagai faktor yang terhasil dari lift-off termasuklah ketebalan cat pada paip, probe yang terangkat dan sudut penyambung paip yang kecil. Dalam tesis ini pembangunan Error Compensation of Eddy Current Testing system (ECECT) dan pengabungan Absolute probe (AP) dan Differential probe (DP) digunakan dalam pengukuran bagi memperolehi bacaan kecatatan yang sebenar. Dari itu reka bentuk dan pembangunan probe (2D dan 3D) digunakan bagi menggabungkan sistem yang dibina dan pada masa yang sama perbandingan antara teknik konvensional dan teknik ECECT dapat dijalankan. Selain itu perbandingan antara simulasi dan alat yang sebenar digunakan bagi ketepatan bacaan didalam sistem. Reka bentuk sistem ECECT sangat sensitif dan kurang gangguan berbanding teknik conventional. Sebagai pelengkap bagi sistem ini Mamdani Fuzzy Logic digunakan sebagai teknik kepintaran ECECT bagi memperolehi ketepatan data yang tinggi. Didalam reka bentuk sistem, pengantaraan muka grafik (GUI) digunakan bagi memaparkan graf pada computer dengan menggunakan perisian MATLAB dan dari sini bacaan kecatatan dan lift-off dapat dikenalpasti berdasarkan graf yang dipaparkan. Berdasarkan hasil yang diperolehi ketepatan ECECT system boleh mencapai sehingga 99.90% tanpa lift-off dan 99.00% dengan lift-off yang berbeza. Ini menunjukkan pengabungan probe dan sistem kepintaran yang dibina akan mempengaruhi ketepatan hasil dan ianya amat berguna bagi pengelasan kecatatan selain kejituan bacaan yang dipaparkan. Selain itu perbandingan diantara simulasi dan juga secara nyata dengan menggunakan ECECT juga dilaksanakan bagi memperolehi ketepatan hasil yang diinginkan

ABSTRACT

Nondestructive testing (NDT) deals with the inspection of an object for determining its properties without destroying its usefulness. Applications include detection of cracking in coating industries, steam generator tubing in nuclear power plants, aircraft and etc. As a method for NDT, the eddy current testing is also used for detection the lift-off in the pipe or plate due to several factors resulting from lift-off including the thickness of the coating on the pipe, the probe is lifted and the angle of pipe joining is small. In this thesis, the development of Error Compensation of Eddy Current Testing system (ECECT) and combining of the Absolute probe (AP) and Differential probe (DP) is used in measurement for actual defect measuring. From here the probe design (2D and 3D) and development are used for integrating with the system design and at the same time, the comparison between conventional technique and ECECT technique can be executable. Besides, the comparison between simulation and actual devices is used for accuracy of measurement in this system. The ECECT system design has higher sensitivity and less noise comparing conventional technique. As the complementary in this system, the Mamdani Fuzzy Logic is used as an intelligent technique in ECECT for high accuracy results. In system development, the graphical interfacing (GUI) is used for graph display on the computer by using MATLAB software and from here the value of defect and lift-off can be identify based on graph display. Based on the results was obtained ECECT system will achieve 99.90% accuracy without lift-off and 99.00% with the different types of lift-off. This shows that the merger of the probe and intelligence system are built will affect the accuracy of the results and it's very useful for the defects classification aside from the accuracy of the reading displayed. In addition, the comparison between the simulation and actual devices by using ECECT is also conducted to obtain the desired result accuracy.



UMP

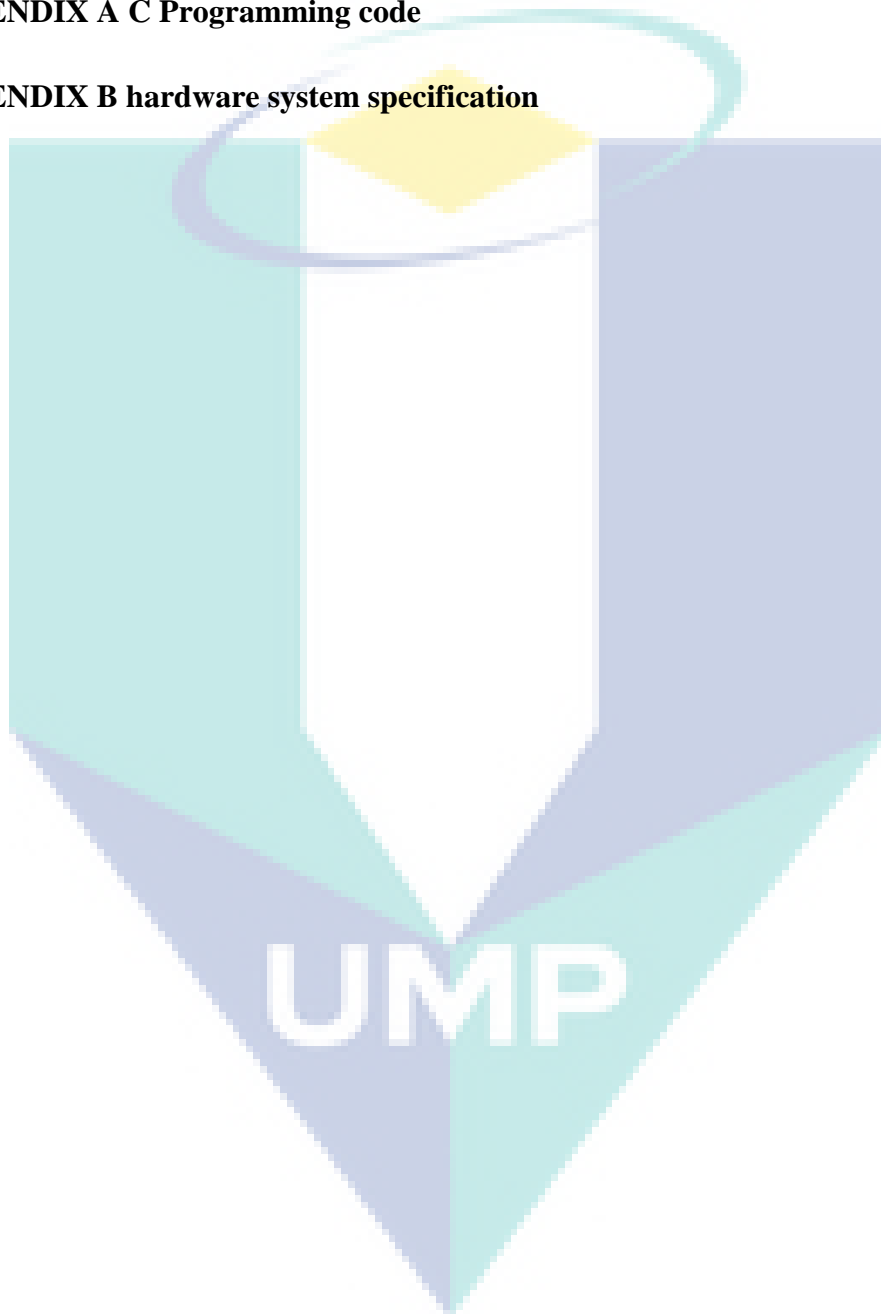
TABLE OF CONTENT

DECLARATION	
TITLE PAGE	
ACKNOWLEDGEMENTS	ii
ABSTRAK	iii
ABSTRACT	iv
TABLE OF CONTENT	v
LIST OF TABLES	ix
LIST OF FIGURES	x
LIST OF SYMBOLS	xiii
LIST OF ABBREVIATIONS	xv
CHAPTER 1 INTRODUCTION	1
1.1 Introduction	1
1.2 Background	3
1.3 Problem Statement	3
1.4 Objective of Thesis	4
1.5 Scope of Thesis	4
1.6 Thesis Outline	5
CHAPTER 2 LITERATURE REVIEW	7
2.1 Introduction	7
2.2 Overview of Eddy Current Testing	8
2.3 Magnetic Characterization Excitation Source	14

2.3.1	Sinusoidal Excitation Signal	14
2.3.2	Pulsed Excitation Signal	17
2.4	Eddy Current Testing Probe	20
2.4.1	Air Coil Probe	20
2.4.2	GMR Probe	25
2.5	Crack Defect Classification	28
2.6	ECT Defect Measuring	31
2.6.1	Air-Coil for Lift-Off Measuring	31
2.6.2	Intelligent Technique in Defect Measuring	32
2.7	Summary	35
CHAPTER 3 METHODOLOGY		36
3.1	Introduction	36
3.2	Proposed ECT Technique Using Fuzzy Logic	36
3.3	Step of Development Fuzzy Logic	39
3.3.1	Rules Of Fuzzy Logic	41
3.3.2	Surface Viewer for Fuzzy Logic	42
3.3.3	Graph Surface Viewer For Fuzzy Logic	43
3.4	Flow Chart	45
3.5	Simulation Model of ECECT system	45
3.5.1	Input For Fuzzy Logic	46
3.5.2	Conditioning Function For Fuzzy Logic	46
3.5.3	Fuzzy Logic Process and Feedback	47
3.6	Proposed Probe Design	48
3.6.1	3-D Probe Design	48
3.6.2	Design Probe Drive Circuit	49

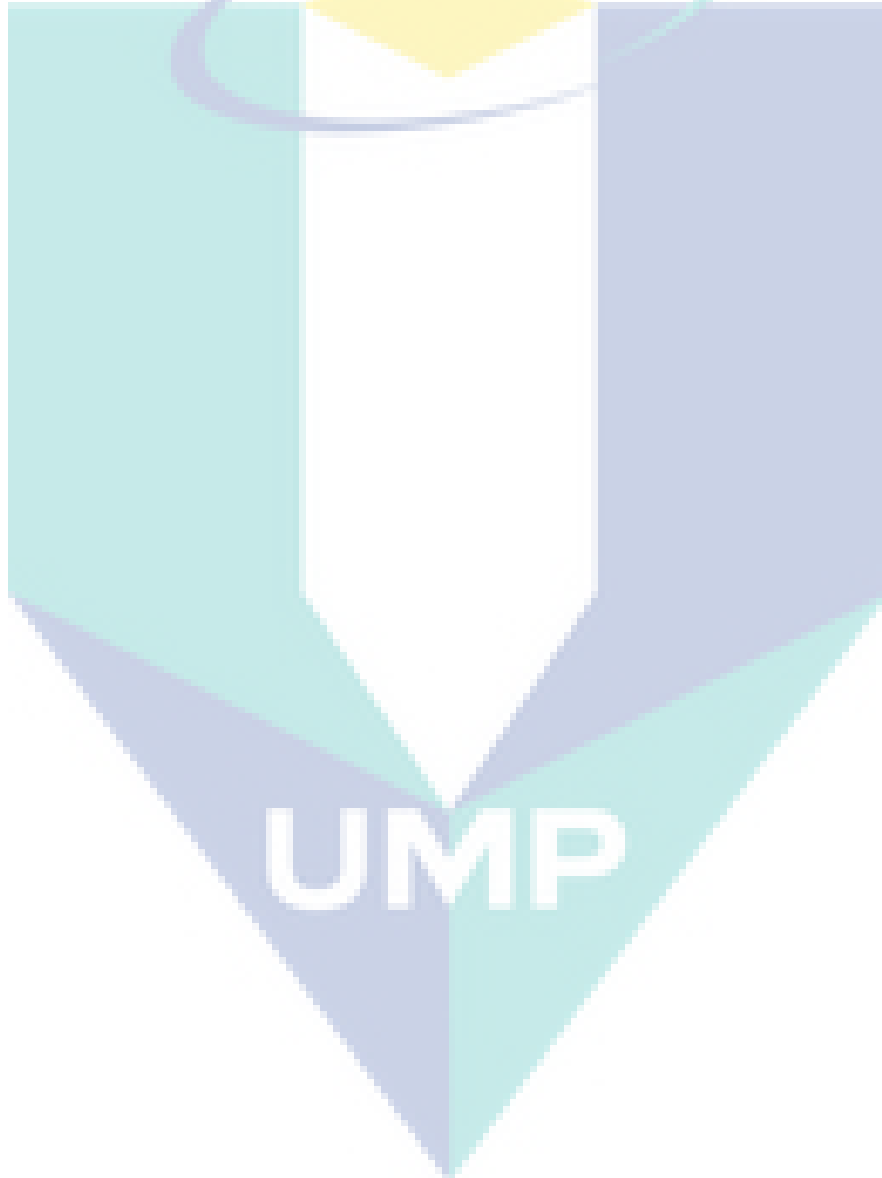
3.7	Error Compensation Eddy Current Setup (ECECT)	50
3.8	Calibration Block Sample Testing	51
3.8.1	Sample Testing	53
CHAPTER 4 RESULTS AND DISCUSSION		54
4.1	Introduction	54
4.2	Simulation Result and Discussion	54
4.3	Experimental Conventional Probe Result	56
4.3.1	Differential Probe by Using ECECT	56
4.3.2	Absolute Probe Signal Using ECECT	57
4.3.3	Differential / Absolute Probe without coating thickness	57
4.3.4	Differential / Absolute Probe with coating thickness	58
4.4	Comparison with Fuzzy Model	59
4.4.1	Differential Probe with Fuzzy Model	59
4.4.2	Absolute Probe with Fuzzy Model	60
4.4.3	Differential / Absolute Probe with Fuzzy Model	61
4.5	Comparisons with other technique	63
4.6	ANOVA analysis	64
4.6.1	Data Testing ECECT	64
4.6.2	Comparing Output Peak Effecting by Coating Thickness in ECECT Technique	66
4.6.3	Response Surface Linear Model	68
4.6.4	Final Equation in Terms of Actual Factors	69
4.7	Summary	72
CHAPTER 5 CONCLUSIONS AND FUTURE WORK		74

5.1	Conclusions	74
5.2	Future Work	75
	REFERENCES	76
	APPENDIX A C Programming code	86
	APPENDIX B hardware system specification	89



LIST OF TABLES

Table 2.1	Summary of research in ECT hardware and software	9
Table 2.2	Geometric parameters of the coils	27
Table 2.3	Intelligent Technique In Defect Measuring	32
Table 4.1	Comparison of liftoff with different coating thickness	63
Table 4.2	Table of Parameter Effecting Defect Measuring	64
Table 4.3	Response Output Peak	69

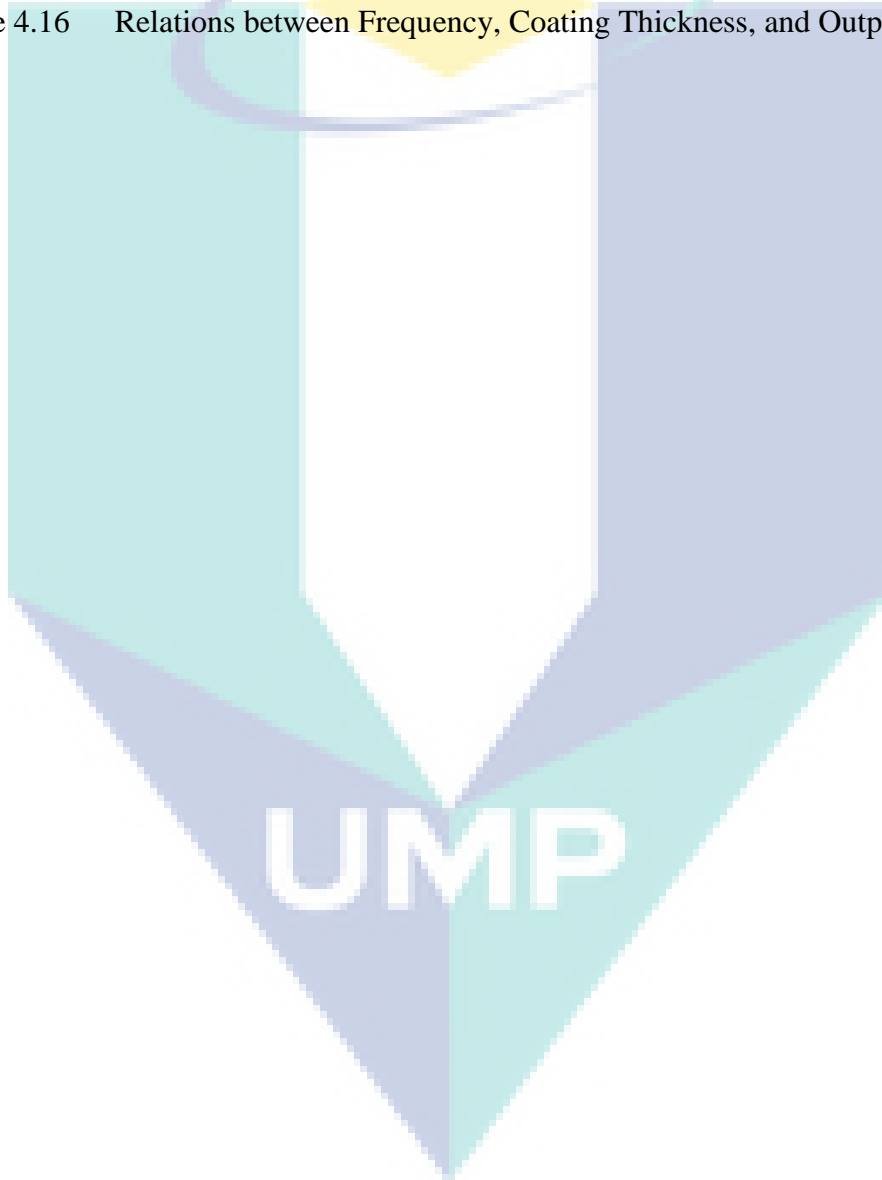


LIST OF FIGURES

Figure 2.1	The peak factor and Hardware Flowchart a) The peak factor values versus the multi-sine signal's tones, b) Hardware flowchart.	15
Figure 2.2	The Multi-frequency stimulus amplitude and characteristic of measuring channel a) Multi-frequency stimulus generator b) The amplitude–frequency characteristic of the measuring channel.	17
Figure 2.3	Positioning of exciting coil and signal and the excitation period waveform, a) Excitation coil and the test-piece schematic, b) Repeating ideal for square wave excitation pulse in a period, c) PEC excitation period, d) PEC response for a half of period of the normalized.	18
Figure 2.4	Two placements testing for conductivity, 24 processed signals and Reconstruction the thermal image.	20
Figure 2.5	The block diagram of ECT excitation probe, a) ECT probe and PCB lines coil array sensor, b) The designed ECT probe in front view	22
Figure 2.6	Coil arrangement and carbon steel collar	23
Figure 2.7	Specimen coil orientation and experiment setup, a) Coil's orientations, b) Experimental setup	24
Figure 2.8	ECT Common type probe and Diagonal type probe	25
Figure 2.9	Block diagram of signal conditioning and eddy current ECP probe, a) Measuring system in Depicts block diagram, b) The architecture of 3D uniform eddy current ECP probe.	26
Figure 2.10	GMR-based ECT probe's schematic and configuration, a) Configuration of the sensor for GMR magnetometers are connected with Wheatstone bridge, b) The biaxial sensors arrangement and the permanent magnet and coil excitation.	28
Figure 2.11	Topological gradient plot with reconstructed slot for performances of two optimization models, a) Rectangular slot in the topological gradient plot. b) Reconstructed slot for final shape. c) Reconstructed slot for impedance signal. d) Performances of two optimization models.	30
Figure 2.12	ECT principle in random variables output quantities and lift-offs simulation results, a) ECT Principle in random with (red) input variables and (blue) output quantities, b) The lift-offs simulation results	32
Figure 3.1	Proposed the Architecture of ECECT System.	37
Figure 3.2	Flow chart of fuzzy logic (a) Basic block for Fuzzy Logic, (b) Internal block function in Fuzzy Logic.	38
Figure 3.3	Command Window	39
Figure 3.4	(a) MF Differential Probe, (b) MF Absolute Probe, (c) Output Actual Depth Defect.	41

Figure 3.5	(a) Rule viewer, (b) Surface viewer	43
Figure 3.6	(a) Differential probe graph for surface viewer, (b) Absolute probe graph for surface viewer	44
Figure 3.7	Flow Chart of Fuzzy ECT Compensation Scheme	45
Figure 3.8	The Simulink Block Diagram Model for ECECT. 1) Input source, 2) Conditioning process, 3) Fuzzy logic process and feedback, 4) Output display	46
Figure 3.9	Input Block Diagram	46
Figure 3.10	Conditioning Block Diagram	47
Figure 3.11	Error Compensation Feedback	48
Figure 3.12	Dimensioning of Eddy Current Probe	49
Figure 3.13	The view of Eddy Current Probe (a) Front View, (b) Top View,	49
Figure 3.14	Designing of ECECT Drive Circuit. 1) AC signal, 2A) Absolute Probe, 2B) Differential Probe, 3A) LCD Display, 3B) Differential Probe, 4) ATMEGA 2560 microcontroller, 5) Computer.	50
Figure 3.15	ECECT System Components Setup. 1) Computer, 2) ATMEGA 2560 microcontroller, 3) Absolute and Differential probe combining 4) LCD display, 5) Function generator, 6) Calibration block	51
Figure 3.16	Eddy Current Set Unit.	52
Figure 3.17	Calibration block with different depth	52
Figure 3.18	Coating thickness shield.	53
Figure 3.19	A Plate Sample	53
Figure 4.1	Simulation result for output voltage ECECT (a) Input Signal, (b) Output voltage value of Differential and Absolute Probe simulation	55
Figure 4.2	(a) Differential Probes Testing by Using Calibration Block, (b) The signal from the differential probe.	56
Figure 4.3	Absolute Probes Testing by Using Calibration Block	57
Figure 4.4	Integrated Probe Output without Coating Thickness	58
Figure 4.5	Integrated Probe Output with Coating Thickness	59
Figure 4.6	Output for Fuzzy Logic by using the Differential Probe	60
Figure 4.7	Output for Fuzzy Logic by using the Absolute Probe	61
Figure 4.8	Fuzzy Logic for Error Compensation Signal Output without Coating Thickness	62
Figure 4.9	Fuzzy Logic for Error Compensation Signal Output with Coating Thickness	63
Figure 4.10	Depth Of Defect (mm) vs Testing Sampling By Using 3khz Frequency	66

Figure 4.11	Depth Of Defect (mm) vs Testing Sampling By Using 6khz Frequency	67
Figure 4.12	Depth Of Defect (mm) vs Testing Sampling By Using 9khz Frequency	68
Figure 4.13	Residuals vs Predicted	70
Figure 4.14	Relations between Depth of Defect, Frequency and Output Peak	70
Figure 4.15	Relations between Depth of Defect, Coating Thickness, and Output Peak	71
Figure 4.16	Relations between Frequency, Coating Thickness, and Output Peak	72



LIST OF SYMBOLS

A	Cross sectional area
B	Magnetic flux density
c	Circumference at the reference radius
D	Eddy current L-R ladder diffusion network
d_p	Depth of infinite plate
E	Energy
F_{EM}	Electromagnet force
$F_{friction}$	Friction force
F_{MMF}	Magnetomotive force
F_{spring}	Spring force
F_{wal}	Wall force
g	Air gap (armature position)
h	Axial dimension
H	Magnetic field intensity
i	Current
i_{cp}	Primary coil current
i_e	Eddy current
i_p	Permeance current
l	Length
L	Inductance
l_{eff}	Effective length
l_{eff*}	Linearized effective length
l_p	Length of infinite plate
m_r	Normalized magnitude of reversed current pulse
N_{cp}	Number of primary coil turns
N_{cs}	Number of search (secondary) coil turns
N_r	Node radial dimension
N_x	Node axial dimension
n_z	Number of discretized flux tube elements
P	Magnetic permeance
P_g	Air gap permeance

P_{go1}	Air gap 1st outer fringing permeance
P_{go2}	Air gap 2nd outer fringing permeance
P_l	Leakage permeance
R	Radial dimension / Electrical resistance
R_{bobbin}	Eddy current resistance of the bobbin
R_{cp}	Resistance of primary coil
R_e	Eddy current resistance of a flux tube
t	Time
t_r	Normalized duration of reversed current pulse
U	step function
V	Voltage
V_{cp}	Voltage across the primary coil
V_{cs}	Voltage generated by the search coil
w	Width of plate or thickness of tube shaped armature
W_b	Magnetic reluctance
w_p	Half width of infinite plate
y	Integration dimension
z	Depth into plate

UMP

LIST OF ABBREVIATIONS



A/D	Analog To Digital Converter
AC	Alternating Current
BOB	Bottom Of Bottom
BOT	Bottom Of Top
EC	Conventional Eddy Current
ECECT	Error Compensation of Eddy Current Testing
ECT	Eddy Current Testing
EM	Expectation-Maximization
FE	Feature Extraction
GMR	Giant Magneto Resistive Sensor
KL	Karhunen Loeve Transform
LPI	Liquid Penetrate Inspection
NDT	Non-Destructive Testing
NI	National Instrument
PCA	Principal Component Analysis
PEC	Pulsed Eddy Current
PSD	Power Spectral Density
STFT	Short Time Fourier Transforms
TFD	Time–Frequency Distribution
TOB	Top Of Bottom
Tzc	Arrival Time
UT	Ultrasound
Vp	Voltage Peak
Vpp	Voltage Peak-Peak/ Peak Heigh

CHAPTER 1

INTRODUCTION

1.1 Introduction

Various techniques are used in science and industry to evaluate and study the properties of the material things and one of them was a non-destructive testing (NDT) that does not cause damage to the material. Controlling quality standards in the various fields of NDT have been applied to a variety of processes, including metal detection, process control inspection and maintenance of some parts and etc. The examinations necessary for the workpiece are done by using nondestructive testing methods to determine the material without damaging its usefulness.

The eddy current testing is an accurate, widely used and well-understood inspection technique, particularly in the aircraft and nuclear industries. Eddy current testing is also used as a quality control tool in a variety of industries. Eddy current methods are mostly used for two types of applications. One is to detect a defect and inspect the condition of samples (Enokizono et al.,1998). The condition of samples may be related to the surface cracks, sub-surface flaw (Bowler, 1992) and degradation of samples. For this kind of application, the nature of the defect must be well understood in order to obtain good inspection results. Since eddy currents tend to concentrate at the surface of a sample, they can only be used to detect defects close to the surface. Another important application of eddy current testing is to measure the properties of samples, including the electrical conductivity (Lambert et al., 2011) magnetic permeability (Voulgaraki, Poulakis, & Theodoulidis, 2013) and thickness of samples (Båvall, 2007). Eddy currents are affected by the electrical conductivity and magnetic permeability of materials. Therefore, eddy current measurements can be used to sort conductive materials (usually different metals have different conductivity) and to

characterize heat and stress treatment, which normally lowers the conductivity. Since the electrical conductivity and magnetic permeability of materials may be related to structural features such as hardness, chemical composition, grain size and material strength, we can also apply eddy current techniques to differentiate coating properties related to coating structure and depositing conditions which will be described in detail in this thesis. Eddy current methods are also able to measure the thickness of thin coatings or thin paint. The thickness range that eddy current testing can handle is usually from the level of micrometers to the level of millimeters. Since corrosion might change the thickness of coatings, eddy current testing can also be a method to detect corrosion.

Eddy current testing is a widely applied non-destructive technique in different sections of industries (Abbas et al., 2016). Recent progresses in Superconducting Quantum Interference Device (SQUID) magnetometer for quantitative measurements in eddy-current nondestructive evaluation and examined involve the coil in lift-off condition (Krause et al., 2003; Pipis et al., 2016; Voulgaraki et al., 2013) by using pulsed eddy current signal (Y. Li & Chen, 2012; Shejuan Xie et al., 2013; Tian, et al., 2013) have been report in the literature making eddy current testing more attractive in quality control and inspecting field (Barbato et al., 2015; François Cairel et al., 2015; Stubendekova et al., 2014). Michael Faraday's discovery of electromagnetic induction in 1831 opened the possibility to develop eddy current testing instrumentation and continued with Hughes in 1879 with apply eddy current testing (Morozov et al., 2010). Considerable work was done in the 1950's and 1960's in the development of the theory and experiments with eddy currents.

Coupling of the magnetic field to the material surface is important in Eddy Current Testing (ECT). For surface probes, it is called "lift-off" which is the distance between the probe coil and the material surface. In general, uniform and very small lift-off are preferred for achieving better detection sensitivity to defects. Similarly, the electromagnetic coupling in the case of tubes/bars/rods is referred to as "fill-factor". It is the ratio of the square of coil diameter to the square of tube diameter, in the case of encircling coils and is expressed as a percentage (dimensionless). Usually, 70-90% "fill-factor" is targeted for reliable inspection (Nelligan & Calderwood, 2014).

1.2 Background

A variety of nondestructive methods are used currently depending on the application and the type of energy source used. Some of the important methods are ultrasonic, magnetic flux leakage, radiographic, penetrate and eddy current techniques. A brief introduction to these methods follows.

For ultrasonic testing is based on the principle that solid materials are good conductors of sound waves. Therefore any waves reflected are by interfaces or internal material dislocations.

In Radiographic Technique the energy used comes from gamma ray source or X-rays propagates through a test specimen and the pattern of the energy received on the opposite side is evaluated. Once radiation passes through the object, an image is projected on the receiver or recording plane on the opposite side.

Lastly Eddy Current Technique by based on the electromagnetic technique used to inspect electrically conducting materials for discontinuities, irregularities in structure and etc. Eddy current testing can be used to inspect non-magnetic but conducting materials

Another important advantage of eddy current testing over other methods, such as ultrasonic, magnetic particle and potential drop techniques, is that there is no need for physical contact with the surface of the samples. Thus, careful surface preparation is unnecessary.

1.3 Problem Statement

The impact of coating thickness or lift-off will affect the reading of defect depth at pipes or plates. It will be uncertainly decision condition on the workpiece either the defect are crack or scratch. This problem will be inviting the occurrence of pipes leakage besides can causing the deterioration of a company's productivity and at the same time endangering the safety of workers.

Other than that the coating thicknesses on the pipes are not the same on each side due to coating process is done manually. The combination absolute and the

differential probe should be in sync to get the actual measuring of defect's depth that occurs in addition taking into consideration of prevailing error compensation.

The defect measuring will be identified after the coating thicknesses on the pipe are taken into consideration by using an absolute probe. After that, the differential probe is required to measure the depth of defects after taking into account the thickness of the paint and classify defects such as crack pipes or ordinary scratches will be identified.

From here the combination of hardware and software with including the intelligent technique should be carried out to ensure the accuracy of the data obtained is high with regard to the lift-off and error compensation. Huang.C & Wu, (2014) Signal EC highly effective in reducing the lift-off to 2.16% based on the thickness of the plate. The method of compensation is made for liftoff in the rate inversely scheme. Tian et al., (2009) High sensitiveness for defect measuring, and develop eddy current detector for duplex operates specified sampling surface from measuring and defect detection.

1.4 Objective of Thesis

The thesis objectives are as follows:

To develop an integrated differential and absolute probes for an accurate eddy current system.

To proposed a fuzzy controller for error measurement with lift-off compensation in increasing the accuracy of data.

To validate the effect of lift-off at eddy current technique signal by using Fuzzy Compensation Scheme.

1.5 Scope of Thesis

The scope of this thesis includes:

- In hardware development, the C programming language is embedded into the Arduino controller (ATMEGA 2560).

- Implement error compensation using Mamdani fuzzy logic.
- The carbon steel plate material is used as a test sample.
- Measuring the changes in coating thickness, lift-off in the crack.

1.6 Thesis Outline

The rest of the thesis is organized as follows:-

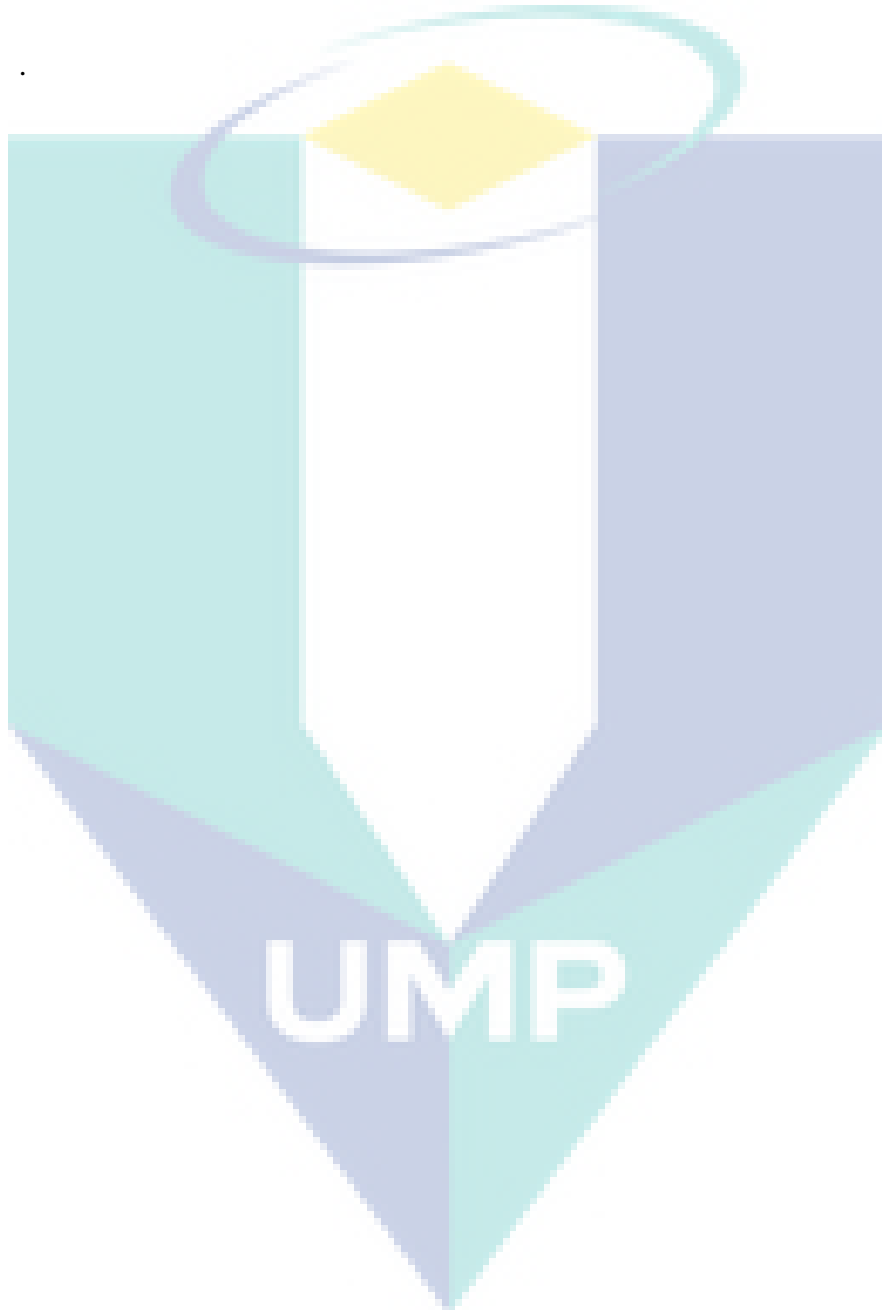
Chapter 2, a review of system development in Eddy Current testing and technique with methods were used for defect classification and characterizations are explained. From here the previous researcher was considering and the criticism is made by based on the method are used. It is followed by the description of Magnetic Characterization Excitation Source. Here the review is based on the types of excitation signal where including an AC/sinusoidal excitation signal and pulse excitation signal. For eddy current testing probe the enforcement is based on the types of the probe are used where including air coil probe or differential and absolute probe and Giant Magnetoresistance (GMR) probe. Other than that the crack defect classification also explaining by based on the method are used in identifying. Finally, more detail of the eddy current testing (ECT) defect measuring with the lift-off measuring by using intelligent techniques has studies by the previous researcher.

Chapter 3 introduces a general description of the proposed ECT technique including the detail of system design, intelligent fuzzy logic design, and Simulink block development design. The detailed description of the probe selection, design, and instrumentation of the error compensation of eddy current testing (ECECT) along with absolute probe and differential probe relevant to the present research work is presented. The ECECT simulation and hardware design are proposed by using the Fuzzy Logic technique for development of new methodology. Finally, more detail of hardware development, the probe development, and connection between input, controller and output are explained. The calibration block, coating shield, and testing plate also explained in the process for inspection for ECT.

Chapter 4, presented the result and discussion including the simulation by using Simulink is used for measuring the defect according to the input waveform. In addition,

the experimental result of comparison with the conventional technique of ECT and ECECT was developed.

Chapter 5 Conclusion and summary of research are presented with a recommendation for future study.



CHAPTER 2

LITERATURE REVIEW

2.1 Introduction

Eddy current testing (ECT) technique is a widely applied non-destructive testing in different sections of industries (Bernieri, A., et al., 2000; Rifai et al., 2016). ECT is also used as a quality control tool in various industries. Eddy current methods are mostly used in two types of applications. One is to detect a defect and inspect the condition of samples (Enokizono et al., 1998). The condition of samples may be related to the surface cracks, sub-surface flaw (Bowler, 1992; Rifai et al., 2016) and degradation of samples. Eddy current methods are also able to measure the thickness of coatings or paint. The range of thickness that eddy current testing can handle is usually from the level of micrometers to the level of millimeters. Since corrosion might change the thickness of coatings, eddy current testing can also be used as a method to detect corrosion.

ECT is an NDT method is used according to the electromagnetic principle as a basis for performing inspections. Remote Field Testing and Flux Leakage are other methods (Bernieri, A., et al., 2001) based on the use of electromagnetic theory. Eddy current testing is originated from Faraday's principle of electromagnetic induction. The changes are the maker of Hughes that recorded differential in the properties of a coil in conductivity and permeability condition when placed in contact with metals (Center, 2016). However, more work in testing materials was done later, especially in the aerospace and nuclear industries. Inspection ECT mostly used in inspection technique that involves deficiency measurement. One of the essential uses of eddy current scrutiny is for defect detection, thus the character of the flaw can be identified. The technique is employed to examine a comparatively tiny space. The probe style and

check parameters should be chosen with a deep understanding of the flaw that the technique is applied to investigate(Center, 2016). Since eddy currents concentrate at the fabric surface, they will solely be wanted to discover defects near the surface.

Additionally, the eddy current technique is helpful in detecting corrosion detects and dilution. The technique is employed for corrosion and dilution measurements on aircraft caused due to warmth exchanges(Center, 2016). Eddy currents are a unit struck by the electrical physical phenomenon and magnetic porosity of materials. Therefore, eddy currents (EC) are often used for investigation of various working materials especially toward fabric that exposed to high temperatures since such treatment changes the physical phenomenon of bound materials.

2.2 Overview of Eddy Current Testing

ECT has its origins from Michael Faraday's discovery of electromagnetic induction in 1831. He is personified and accredited as an English chemist in 1800's with his contribution on finding electromagnetic inductance, electromagnetic revolutions, the magneto-optical consequence, diamagnetism, and other phenomena(Jack Blitz, 1998). In the presence of French physicists Leon Foucault, he carried on the eddy current breakthrough in 1851, and since then, eddy currents are sometimes known as Foucault currents. Foucault expanded a device that applied a copper disk actuating in a hard magnetic field to display generated eddy currents (magnetic fields) while substantial travel inside a implemented magnetic field(García-Martín, 2011). At this point, it cost a lot of valuable application and equipment for materials categorization for only an acting hypothesis which was inadequate. This lead to the German Foerster in 1950s processed the hypothesis for ECT and formulated the essential techniques(Brauer et al.,2014; Forster, 1952). Table 2.1 shows the research summary of ECT hardware and software started from 2011-2016 with more focusing on the hardware and devices development. From here the development including of probe and sensor used, the circuit development, types of the excitation signal, an application on rotation part and liftoff measuring.

Table 2.1 Summary of research in ECT hardware and software

Hardware Development					Software Development				Experimental
Excitation Signal	Probe/Sensor	Circuit	Rotation	Lift-Off	Intelligent	Simulation /3D	Optimization	Sampling	Analysis
Circuit for constant current AC signal pump (Abbas et al., 2014)	An air-core or ferrite-core coil as EC probe.(Zeng et al.,2015)	Develop circuitry to measurement and functioned a particular type of probe(Agum et al.,2014)	The PWM carrier eddy current for estimation of magnet(Yamazaki et al.,2012)	Multi-frequency mode for the triple-coil sensor in lift-off detection. (Yin & Xu, 2016)	System by using artificial neural network(Rosado, L. S., et al.,2013)	Simulations for the three-dimensional finite element (Chudacik et al.,2015)	Topological shape optimization . (M. Li & Lowther, 2011)	Simplex-mesh refinement is proposed for creating a forward database(Gymóthy, 2015)	Lorentz force eddy current testing(Weise, Carlstedt, Ziolkowski, & Brauer, 2015)
Pulsed eddy current signal in inspection technique(Wu et al., 2014)	Probe development of the detection system (Xiaolei CHEN, 2008)	Feeding devices which are used in the eddy current detection of titanium alloy tube (Liu, Y., et al., 2015)	An induction motor 's loading being controlled by eddy current brake(Gulbahce et al.,2013)	Lorentz force eddy current testing. (Weise et al., 2015)	Image processing with 2D defect profile reconstruction technique (G. Betta et al., 2015)	Enables the detection of defects lying and deep inside a conducting material with Computation 3D with Lorentz force technique in eddy current testing (Zec et al., 2013)	Swarm algorithm is performed wherein the exact forward computations (Douvenot, et al.,2011)	Characterization of defects on rivets(Rocha, T., et al.,2012)	Non-invasive inspection of large conductive structures(Salucci et al., 2016)

Table 2.1 Continued

Hardware Development					Software Development				Experimental
Excitation Signal	Probe/Sensor	Circuit	Rotation	Lift-Off	Intelligent	Simulation /3D	Optimization	Sampling	Analysis
Constant Current AC Source for excitation of the probe(Abbas et al., 2015)	Type sensor is introduced based on the eddy current principle(Cao et al., 2013)	Filtrate the suspension of multi-walled Carbon nanotubes CNTs (Hsu, et al.,2011)	The braking torque and force analysis in eddy current using axial flux permanent magnet- type (Shin et al.,2013)	Effectively eliminate the distance effects between the surface of the coil (Dziczkowski, 2013)	Modeling of the measured response in feature extraction for non-linear regressions for(Rosado, L., et al., 2012)	Simulated of three-dimensional diagnosis of real cracks from two-dimensional (Janousek & Smetana, 2014)	Imperialist competitive algorithm in solve the problem of natural crack shape reconstruction(Zhang et al.,2014)	Characterization of the crack depth (Ida, 2014)	The numerical solution in NDE configuration (Barbato et al., 2015)
Multi-frequency ECT for sizing accuracy of a deep Stress Corrosion Cracks (Wang, L.,2013)	The air-core coil is located above a conducting (Koliskina & Kolyshkin, 2015)	Electromagnetic inspection (Chady et al.,2013)	Rotating magnetic field in composed of three windings (Junjun et al., 2011)		A real-time Digital Signal Processing architecture (Rosado, L. S., et al.,2014)	Finite-element model for three-dimensional simulation (Huang, L., et al., 2012)	Optimal control parameters (Mengelkamp et al., 2016)	Eddy current testing Signals in crack size (Chelabi et al.,2013)	Eddy Current Position Sensor has been conceptualizing to detect the diverse Safety Rods (Vijayashree et al., 2011)

Table 2.1 Continued

Hardware Development				Software Development				Experimental	
Excitation Signal	Probe/Sensor	Circuit	Rotation	Lift-Off	Intelligent	Simulation /3D	Optimization	Sampling	Analysis
Low-frequency eddy current testing (Coil et al., 2016)	Lift-off effect and probe direction(Liu, X., et al.,2014)	A portable low-cost system capable of detecting metallic surfaces' defects (Pasadas et al.,2011)	EC measurement over affected by depletion of aluminum in combustion turbine blade coatings(Lambert et al., 2011)		Neural network data fusion(Dashtbani et al., 2015)	Finite element simulations in numerical modeling for a crack in stress corrosion (Wang, J., et al., 2012)	Particle Swarm Optimization algorithms (Duca et al., 2015)	Sinusoidal magnetic field with fixed-inversion are applied in EC inspection (Ribeiro et al., 2012)	A numerical model was used to verify the progression of eddy currents (Rocha, T., et al., 2015)
Difficult cases are explored by used sinusoidal measurement, detection supporting and quantification stages (Giovanni Betta et al., 2014)	Magneto-resistive sensors for subsurface crack detection (Wang Chen et al.,n.d)	Instrument to detect cracks and defects in a conductive plate material. (Pasadas et al.,2011)	Development of a new method in eddy currents induced by velocity(Ramos et al.,2014)		Artificial prosthesis by eddy current method (Stubendekova, A., et al.,2014)	Nested Sampling methods (CaP, C., et al., 2015)			Conductivity invariance in the impact the random distribution in the vertical direction(Yu, et al.,n.d.)

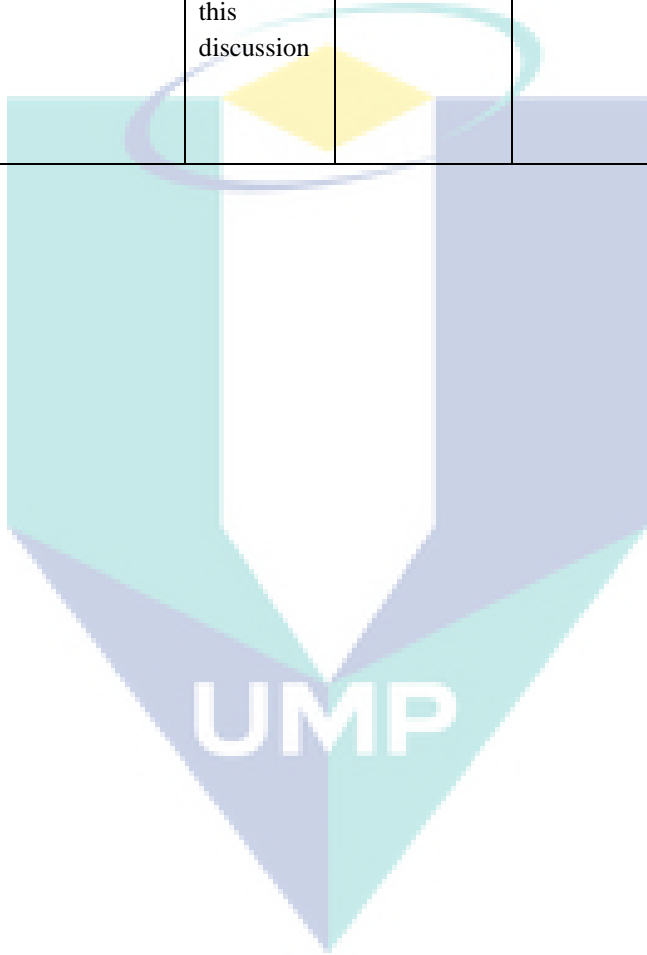
Table 2.1 Continued

Hardware Development					Software Development				Experimental
Excitation Signal	Probe/Sensor	Circuit	Rotation	Lift-Off	Intelligent	Simulation /3D	Optimization	Sampling	Analysis
Capabilities of pulsed eddy-current testing method defect's detecting and material evaluating(Xie et al., 2011)	Magnetometer sensor for uniform eddy current probe architecture (Postolache et al., 2011)	Forces and torques acting upon a magnetic dipole interacting (Thess et al.,2013)			The fuzzy inference by using theory of Dempster–Shafer(Guohou et al., 2011)	A numerical model based on the solution of the Maxwell equations (Homberg et al., n.d.)			Calculate the magnetic field, based on the Maxwell equations (Zhang et al., 2015)

Criticizing For Citation

The research more about the excitation signal and how to improved but very lack the discussion about minimum frequency can be used in inspection	Discussion about the various probe application is very good but combination sensor in one measurement does not discuss from previous	Circuit developme nt is discussion detail in filtering process and amplified the signal from probe used but very low	The application of eddy current at rotating part is very good in the development of rotating probe but the detail of design and impact design in	Lift-off measureme nt is based on the probe design developme nt very useful to get the accurate data but the	Intelligent used in inspection very helping in research but more discussion about the theory and simulation	Crack simulation in 3D picture is based on graphic computing and image only and not actual	Several methods are used in optimization and algorithms process but more in simulation	Sampling process is based on method of measuring of defect and signal by based on size of defect but very low in discussion of combination of intelligent	The experimental is based on conceptual in eddy current technique and practically but the very low explanation in practically.
--	--	--	--	--	---	--	--	---	--

		enforcement about processing circuit in process the data from probe	measurement not deeply discussed.	intelligent technique very low in this discussion				technique for defect identification	
--	--	---	-----------------------------------	---	--	--	--	-------------------------------------	--



2.3 Magnetic Characterization Excitation Source

This section is focusing on the application of input signal for eddy current in inspection and appropriate frequency that could be applied according to the types of material and system used. The feedback of output signal will be shown following the applied input signals. In eddy current testing there are 2 types of signal input characterization that usually used and applied in eddy current testing which is AC eddy current signal and pulse eddy current (PEC) signal.

2.3.1 Sinusoidal Excitation Signal

Various sinusoidal tones are combined to produce a multi-frequency signal, which aims to increase the frequency component as peak to peak amplitude. Equation 2.1 for the general signal of multi-sine is described below. Figure 2.1(a) shows the peak factor values versus the multi-sine signal's tones. The ϕ_k accuracy is selected through the effect resulting peak factor of $S_M(t)$ ratio and minimized square root peak to peak value. Limit peak power is important in practical applications that exist in the generator. By reducing the peak power and maximize total energy delivered at a fixed time t it will also maximize of the SNR (Giovanni Betta et al., 2014; Schroeder, 1970).

$$S_M(t) = \sum_{k=1}^{N_s} S_k * \sin(2 * \pi * f_k * t + \phi_k) \quad 2.1$$

Where:

ϕ_k and f_k : phase and frequency sinusoid

k -th and N_s : number of tones

S_k : amplitude and sinusoidal k -th.

Magnet coil generated is directly proportional to the current drawn. AC characterization current is required to generate a magnetic field inside the coil during the examination process. Tests must be conducted according to the type of metal tested. The Howland Pump is designed to maintain the main magnetic field (as an input wave) fixed so that the signal obtained and the result output can be measured (Abbas et al., 2014). The basic hardware of flowchart is shown in Figure 2.1(b) below. Reaction to pump instrumentation can be seen on a test made as an example. ECT probe impedance will change each time when there are cracks in the material tested subsequently causes a change in the input and output of measured amplitude.

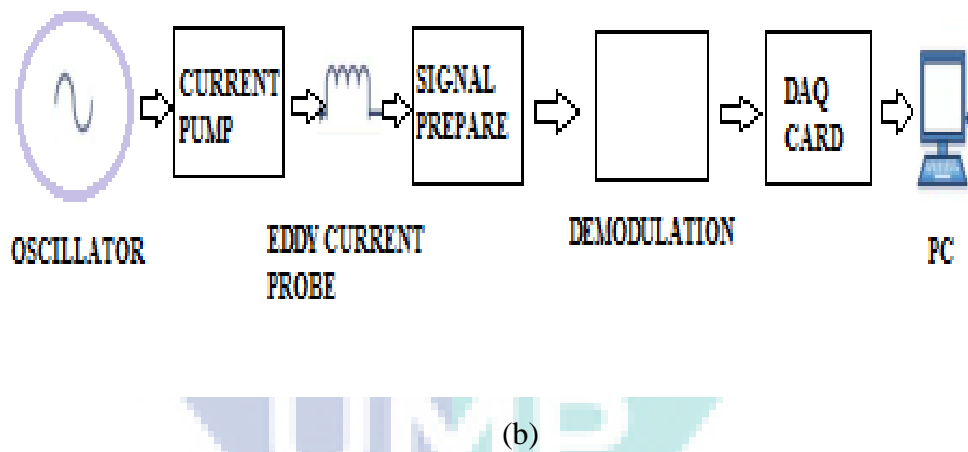
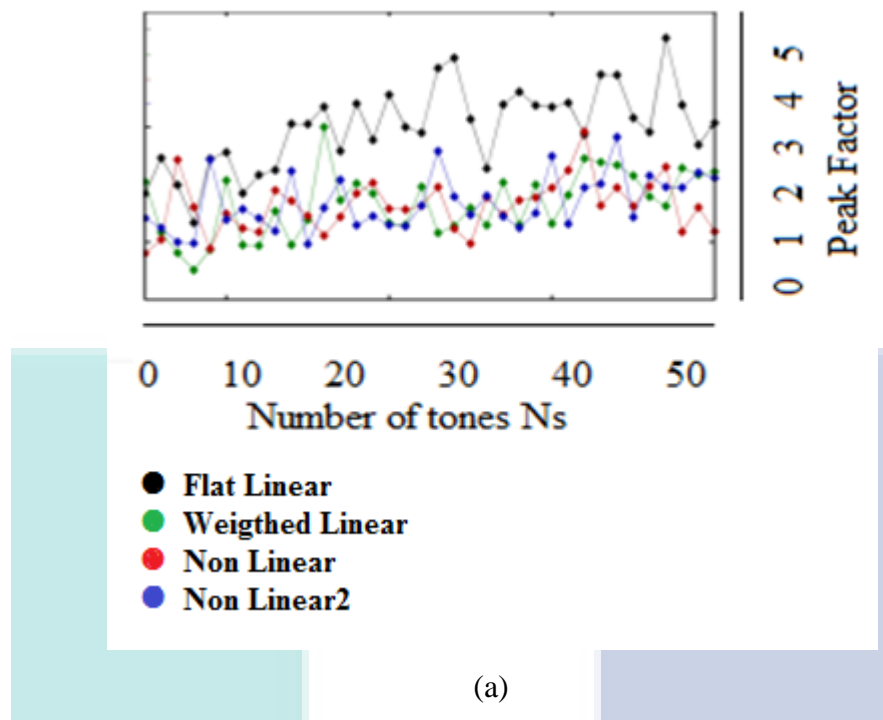


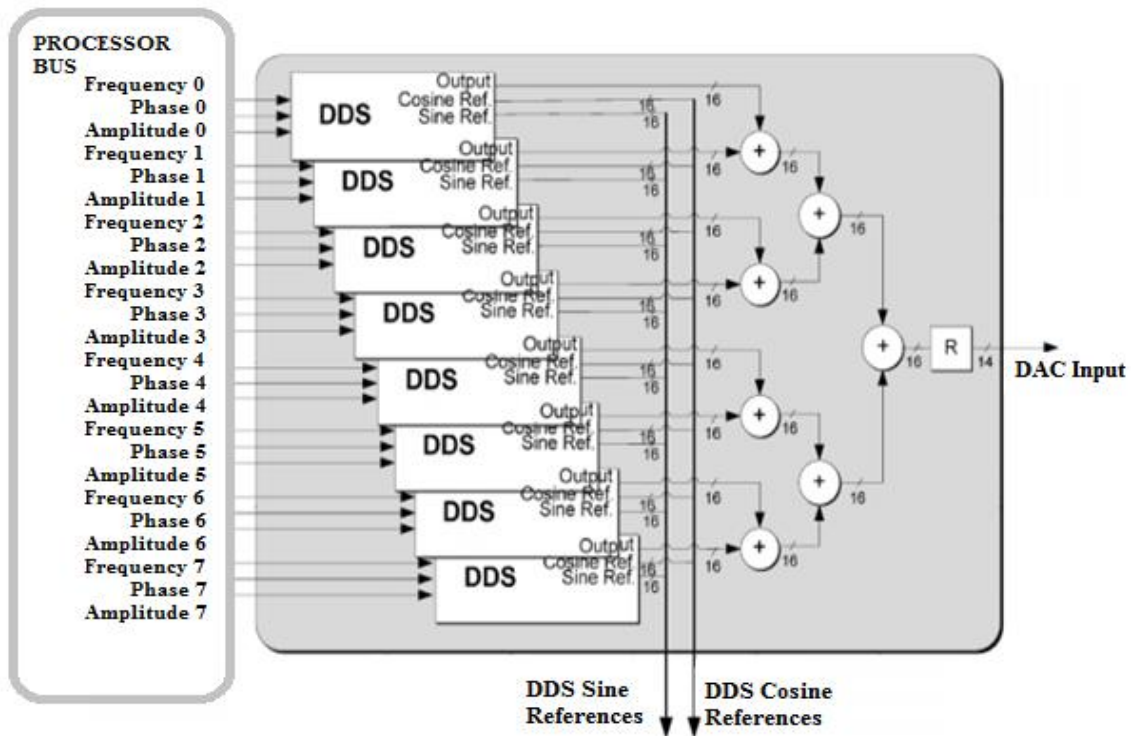
Figure 2.1 The peak factor and Hardware Flowchart a) The peak factor values versus the multi-sine signal's tones, b) Hardware flowchart.

Source: Abbas et al., (2014)

A low-frequency eddy current method used to estimate internal deep defects in ferromagnetic material and iron plate (Lee et al., 2012). (Coil et al., 2016) One of the methods in ECT uses a single coil for both excitation and detection. In this case, changes in coil impedance are used in detecting the presence of conductive materials. ECS has been designed and developed based on multiple frequencies to measure cracks in metal structures. This includes the peak AC source and remains capable of operating within the frequency range for the metal surface and sub-surface near the crack metal.

The resulting output is inversely proportional to the given frequency change. (Abbas et al., 2016).

The analysis of amplitude-frequency response for basic measurement channels $\omega 0$ shown in Figure 2.2(a) (on line 1) displays the dependency analysis of $K(\omega)$ containing null for different frequencies via w_i as the value and multiple to $\Delta \omega$. Line 2 displays the signal modulated by changing the route that crossed the channel frequency measurement ω_i practically without interruption. The modulated signal spectrum over frequency is displayed on the 3rd line, rejected more than 10 times (Goldshtein, et al., 2012). The designing, execution, and evaluation of processing architecture in real-time digital signaling are needed in operation the eddy currents testing signal with multi-frequency has applied on an ordained instrument which working on the core of programmable gate array area. Stimulation generation can be achieved practically through direct digital synthetic processing and also by significant improvements on reduced inauthentic frequency elements. The multi-frequency generation stimulant is handled with the outputs combination from different direct digital synthesis (DDS) and sinusoidal waveform generators inside the FPGA as shown in Figure 2.2(b) (Rosado, L. S., et al., 2014).



(a)

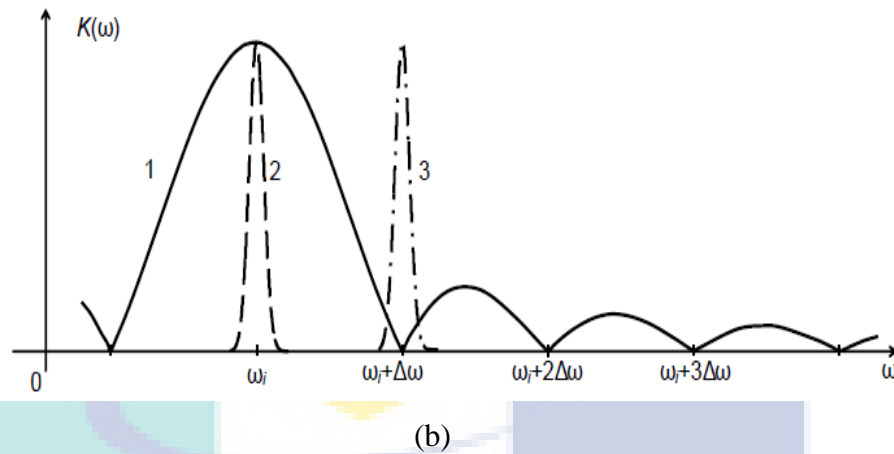


Figure 2.2 The Multi-frequency stimulus amplitude and characteristic of measuring channel a) Multi-frequency stimulus generator b) The amplitude–frequency characteristic of the measuring channel.

Source: Rosado, L.S., et.al., (2014)

2.3.2 Pulsed Excitation Signal

The PEC respond to corrosion involve multi Complicated elements, admitting conduction, permeability and material heaviness fluctuation. When the exposure time growths, then the decrement of mean electrical conduction and permeability means there is the growth of erosion heaviness. Supported the relationship between the PEC characteristics and exposure time, the fitted line and expression could be applied for exposure time rating of coated and uncoated erosion (He et al., 2012).

The eddy current testing (ECT) signal is to simulate the pulses on the procedure frequency domain summation is as follows. Then, a sinusoidal wave signal is a response to the excitation pulses signal with use of difference harmonic frequencies. Figure 2.3(a) shows a schematic of test pieces and excitation coil and Figure 2.3(b) shows a period of ideal square wave excitation pulse repetition(Xie et al., 2011). Hall sensor function is to measure the response of the magnetic field that centered on the ferrite core.

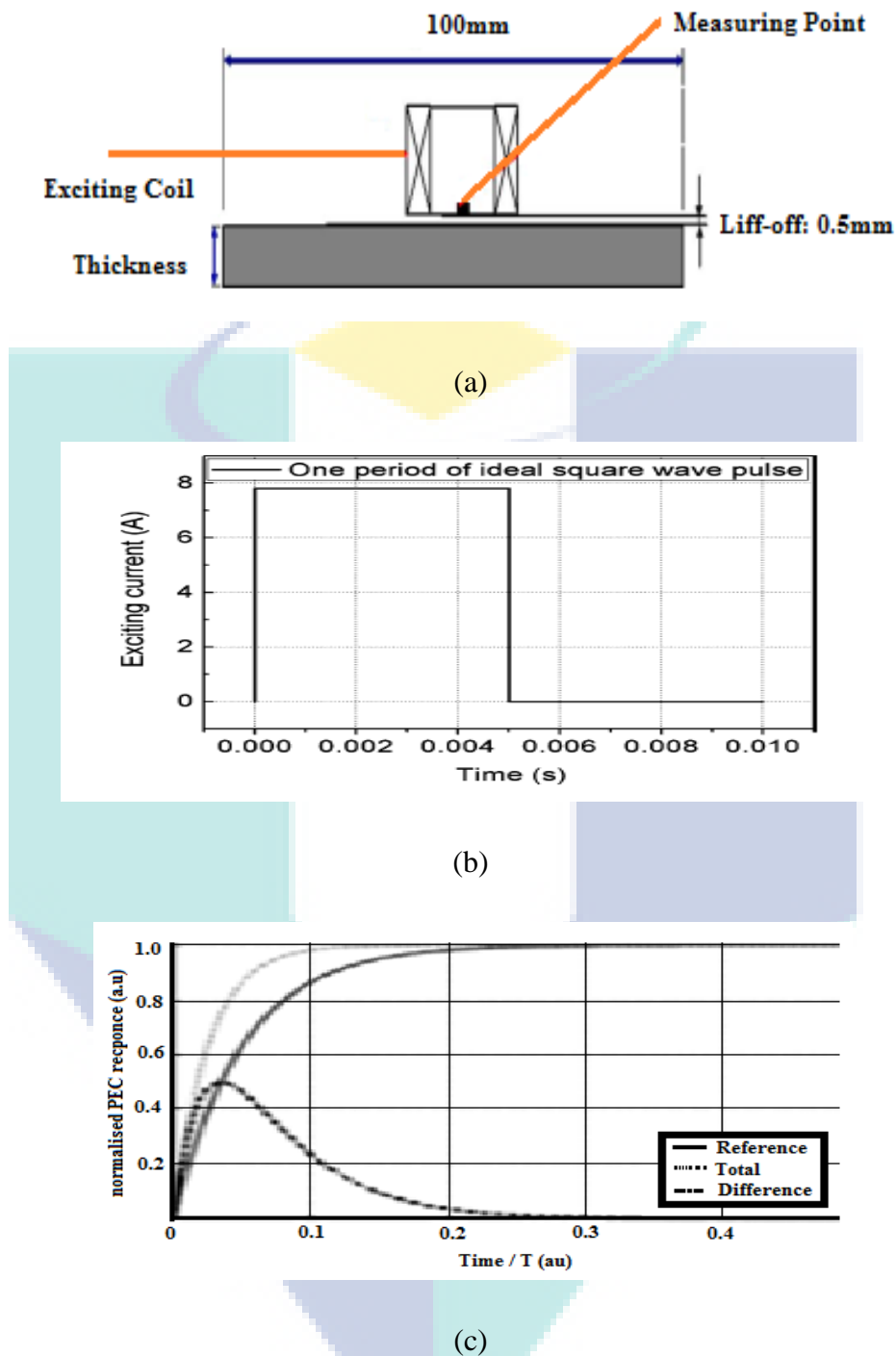


Figure 2.3 Positioning of exciting coil and signal and the excitation period waveform, a) Excitation coil and the test-piece schematic, b) Repeating ideal for square wave excitation pulse in a period, c) PEC excitation period, d) PEC response for a half of period of the normalized.

Source: Xie et al., (2011)

The total magnetic field is measured by the probe represents the superposition of PEC low excitation field and the magnetic field due to the EC. Total reaction PEC can

be divided into two parts in the time domain transient segment (between the initial half of the current period increase) as in Figure 2.3(c) (after half of the time up to start of the next period). PEC response to the transient segment is determined by the time constant, which has a complex dependence on both electrical conductivity and magnetic permeability in the test piece. Although the changes in the magnetic permeability may be weak, the EC changes in the steel for cold work, because they are stronger than non-ferrous materials(McKeehan, 2015). Therefore, in order to improve the resolution of the signal and the signal-to-noise(Sophian A., et al.,2003; Sophian, 2005), it is convenient to make the difference between a normal signal in which the reference signal has B_{ref} obtained in the rolling direction of 90 degrees.

PEC testing is useful in a different position against the defect. Peak waves of response signals present with the same shape in direction of magnetic induction flux, but with different shapes in direction of exciting current, thus different classes of defects can be identified and classified effectively by selecting the rising time as the time domain feature in both directions(He et al., 2010).

The needs of various factory and industry are to examine the carbon fiber reinforced (CFR) plastic components, as used in wind turbine blades and aircraft so that the issues that could potentially lead to failure can be identified. In order to identify the surface defects of CFR composite materials, pulsed eddy current test defect investigations rectangle are recommended as a powerful assessment technique.

The PEC response in the range of heat treatable and non-heat treatable aluminum alloys applied stress well below the elastic limit. The effect prior to the heat treatment plastic deformation on the stress dependency of the pulsed eddy current response is quantified using the peak value of the PEC difference signal(Morozov et al., 2010). Two features of PEC were investigated, the magnetic field intensity and conductivity. These features were used to characterize the different types of defects in carbon fiber reinforced plastics using scanning PEC and the feature representing the magnetic field intensity variation(He et al., 2013.). (Wu et al., 2014)Experimental appliances mainly consist of inquiries of rectangular hall sensor, generator module for pulse signal, module power amplification, signal conditioning circuits, specimen and module of data acquisition and various types Hall sensors.

Figure 2.4 shows the reconstructed image for four divisions' representatives showing the main characteristics of the original infrared images have been exhibited. Based on the analysis about the specific physical meanings, representative parts in the ICs which highlight the marked positions are the significant ones(He et al., 2013; Zhu,P., et al., 2015).

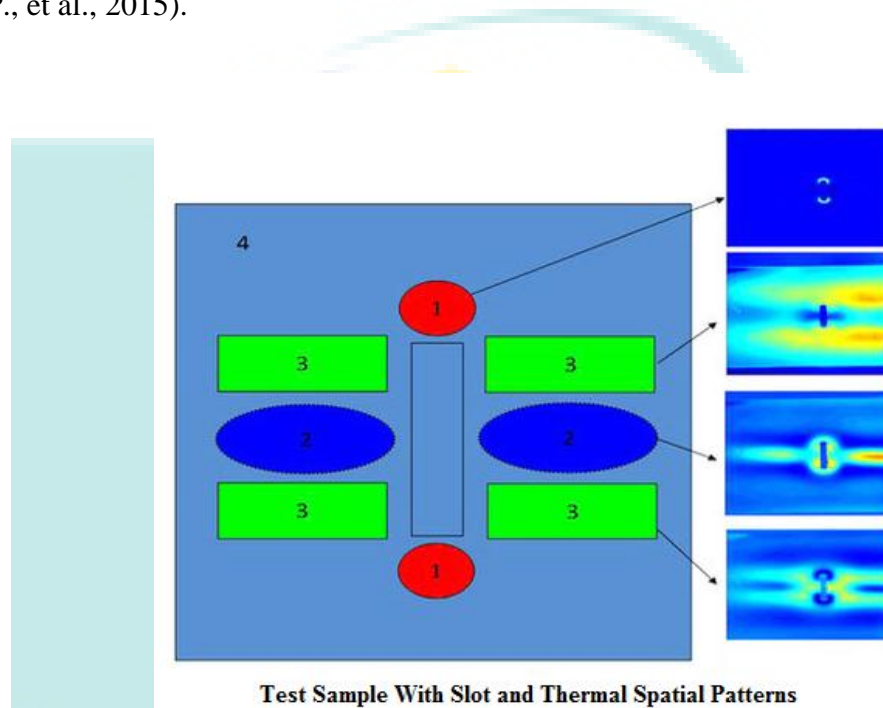


Figure 2.4 Two placements testing for conductivity, 24 processed signals and Reconstruction the thermal image.

Source: Zhu, P., et al.,(2015)

2.4 Eddy Current Testing Probe

Explanation on designing probes for eddy current testing will be discussed in this section. By following the sub-topic included there are two main parts of discussions. The first part is about development probe by focusing the air coil probe and the second part is about Giant Magneto Resistance (GMR) probe development. Both sub-topics are included with the probe design and application of eddy current testing.

2.4.1 Air Coil Probe

Probe design can be improved and interpretation of the experimental signal can be easily understood by using dedicated numerical simulation tools provided they are computationally efficient and accurate, and it is simple enough to use at the end-user

level(Miorelli et al.,2013). ECT is the process of placing the excitation coil carries current near test samples to encourage the EC in it and use the sensing element to take a secondary magnetic field produced by the EC(Zeng et al., 2015). Figure 2.5(a) show ECT system framework dashed line represent the entire differential probe excitation.

The alternative magnetic field around the coil will be generated when an alternative sinusoidal voltage-controlled applied to the excitation coil, thus generate eddy currents in the specimen. The detection coil on the surface cause changes in the magnetic signal into a voltage signal and the changes can be affected by various factors, including the defects. After amplification is carried out, demodulation, filtering, and another signal conditioning measurement signal are converted by A/D according to data acquisition card into a digital signal and stored by the computer(Cao et al., 2013). Effective equipment is needed for probes tailored design, interpret measurements, and assessing the reliability test procedure.

Boundary Element Model (BEM) is suitable for eddy current inspection with affecting planar-stratified in several cracked smooth flow. Selected cracked can be very small and their orientation is either be parallel or octagon(Miorelli et al., 2012). Magnetic field and one error-free interconnect will be detected by sensor array planar coil using the ECT. This probe consists of a pair of the coil sensor planar array and Helmholtz coils. Planar coil sensor array is produced through flame retardant with a thickness of 1.6mm and the thickness of the copper plating used is a 32micro meter. The sensor is located at 1.6mm above the PCB and in between the pair of Helmholtz coils. The board and sensor that the tests separated by FR4 substrate shown in diagram Figure 2.5(b).

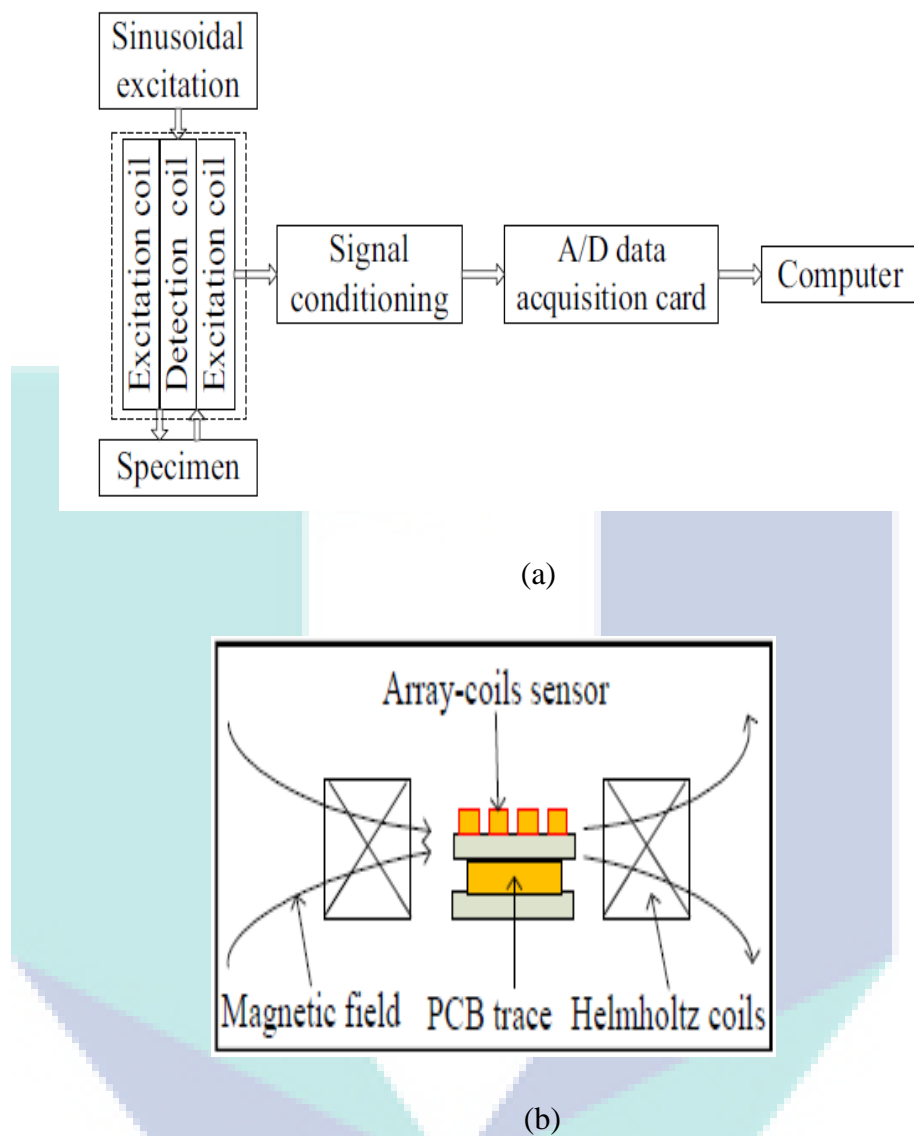


Figure 2.5 The block diagram of ECT excitation probe, a)ECT probe and PCB lines coil array sensor, b) The designed ECT probe in front view

Source: Miorelli et al., (2012)

The PEC probe consists of eight additional surface coils placed in arrays of four coils before and after the mid-coil drive. Preparation of the coil structured shown in Figure 2.6. The additional coil is 360 rounds of 42 American Wire Gauge (AWG) wires when the drive coil is 127 turns of 36 AWG wire (Buck et al.,2016)

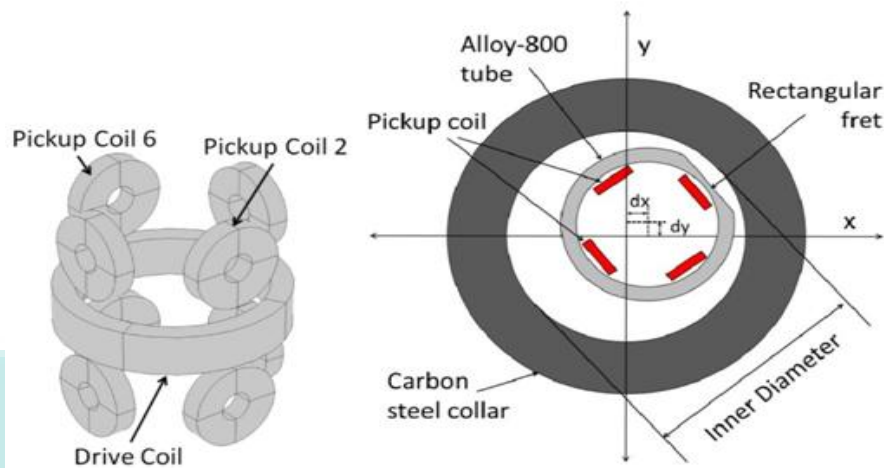


Figure 2.6 Coil arrangement and carbon steel collar

Source: Buck et al., (2016)

The development, characterization, and execution of an apply measuring system for NDT utilizing with dual new eddy current planar probe array, effective excitement driver traces also as multiple detection coils localized between the matrix configuration excitation traces (Tytko & Dzikowski, 2015). On sensing the equivalent inductances of 3 coils very regularly on the changing of crack raising guidance. Concurrently the standardized inductance is also affiliated the crack width and depth (Peng & Jun, 2013).

The crack width could be approximately supported the median value and variance of the standardized inductance variation. The crack depth could be gutted by analyzing the standardized inductance at the dissimilar exciting frequency. Low-frequency eddy current testing by predilections on the sensitivity of the 3 coils for inspecting wall-thinning of large pipes through experimental signals. One specimen was fabricated using carbon steel. Hollows with dissimilar depth were demonstrated on the bottom of the specimen. Three forms of coil's orientations shown in Figure 2.7(a) were discussed. Orientation 1 corresponds both axes of coils are basic to the surface of the plate. Orientation 2 constitutes both axes of coils are perpendicular to the surface of the plate. Orientation 3 corresponds one of the coils' axes is perpendicular to the surface of the plate but some other basic to surface of the plate.

Coil interval is normal as space between these 2 coils' center. Figure 2.7(b) presenting, the experimental setup of low-frequency eddy current testing (LFECT)

commonly admits a procedure synthesis, an oscilloscope, an isolation amplifier and a lock-in Amplifiers (Wang, J., et al.,2014.).

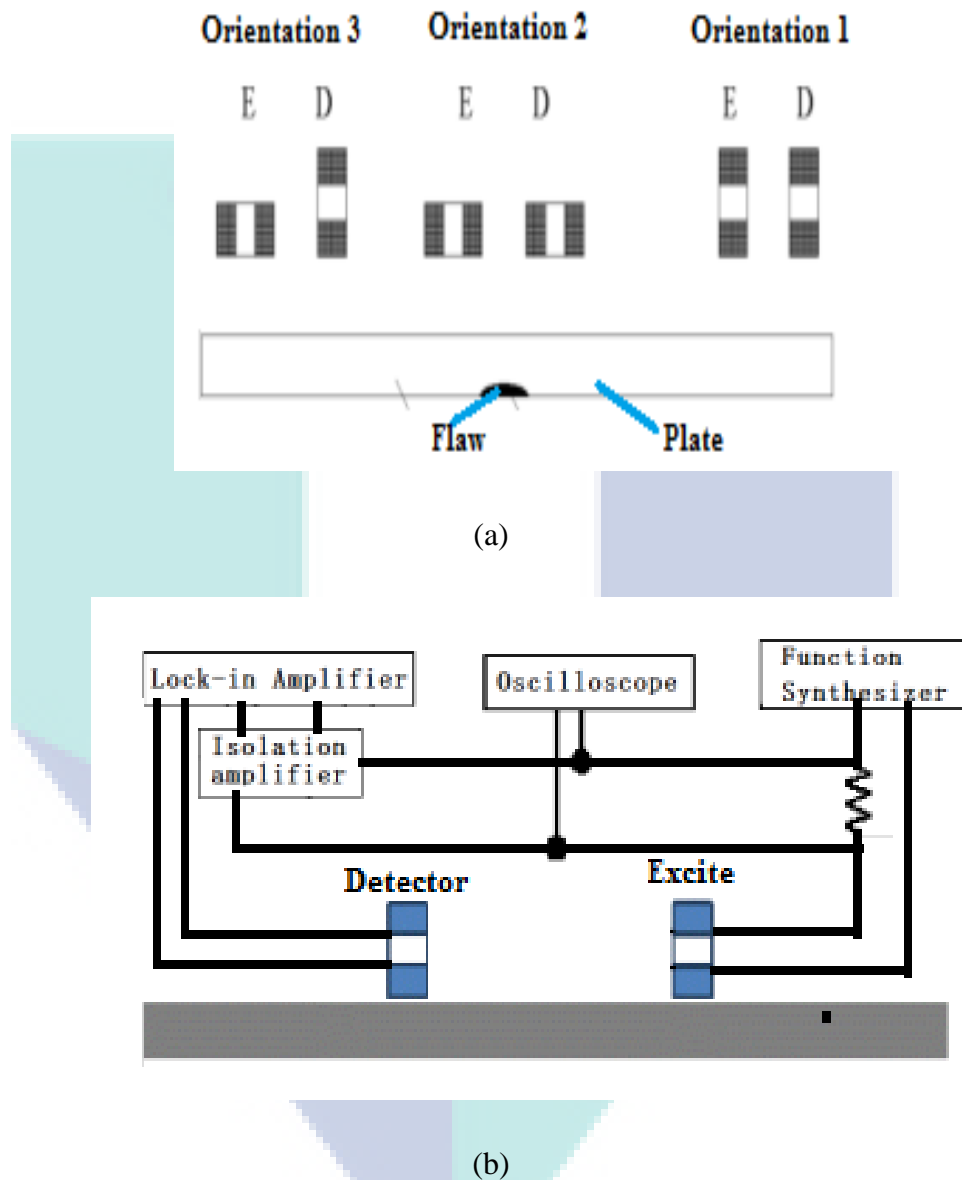


Figure 2.7 Specimen coil orientation and experiment setup, a) Coil's orientations, b) Experimental setup

Source: Wang, J., et al., (2011)

The send-receive coils probe has much more advantage than the absolute coil probe(Zhang et al., 2015). The probe coils are wound on the cylindrical frame due to the surface of inner conductive is a cylinder(Takahashi et al., 2015). Two types of probe

were being studied to optimize the types of probe geometry, first is a normal type and second is the diagonal type, as shown in Figure 2.8. One pair of probe coils is self-induction and one pair is the self-compensation type.

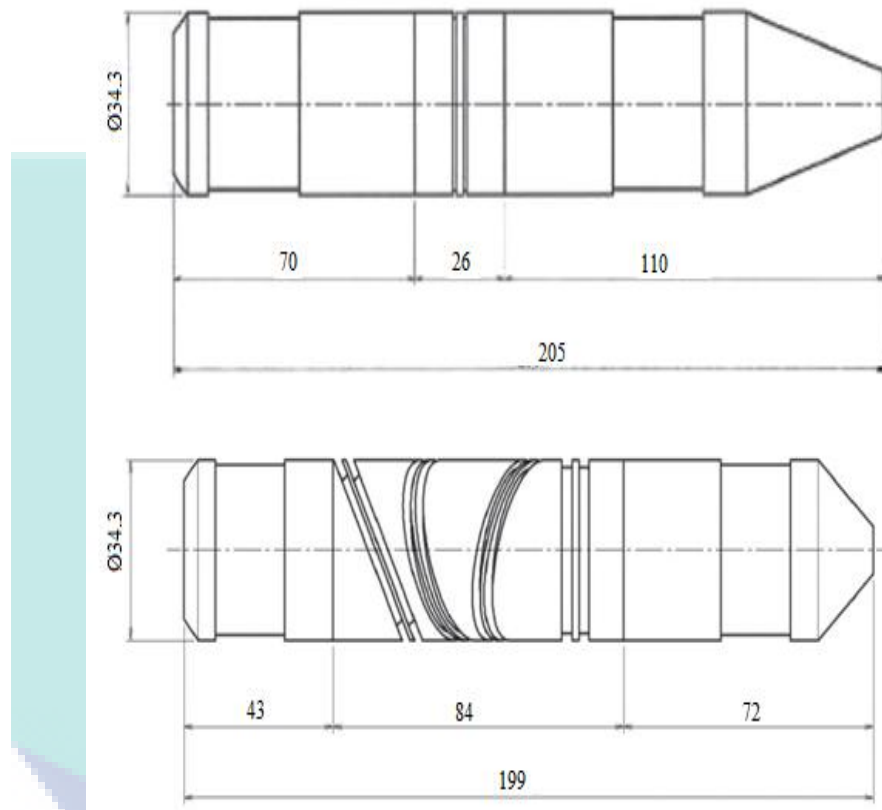


Figure 2.8 ECT Common type probe and Diagonal type probe
Source: Takahashi et al., (2015)

The averaging and riffle analysis / Faro shuffle (technique bandwidth and computation efficient) are accustomed de-noise the hall reaction signals. Along choosing peak amplitude and zero-crossing time of reception signal eventually domain as key boasts, faults in pored structures could be found effectively. In the class of probe rotating on its axis around the rivet, the hall reception signals of the differential probe are tested instantly. Concurrently, the peak amplitude aims of reception signals are extracted and connected to form peak waves (He et al., 2009).

2.4.2 GMR Probe

GMR-based ECT is a component as a sensor to detect small crack under the surface. The depth of optimization probe will increase based on high sensitive of the

crack detection. The size of the coil is selected as Coil2 in Table 2.2 (Wang chen et al.,n.d.). In order to create insensitive of the primary stronger excitation field, the GMR sensor measuring axis must be perpendicular to the excitation coil axis. On the other hand, to work in a linear portion of its characteristics, the GMR sensor must be polarized with a small permanent magnet whose position was conveniently adjusted to obtain a maximum dynamic range of operation. Figure 2.9(a) shows a block diagram of the measuring system(Rocha, T. J., et al., 2011).

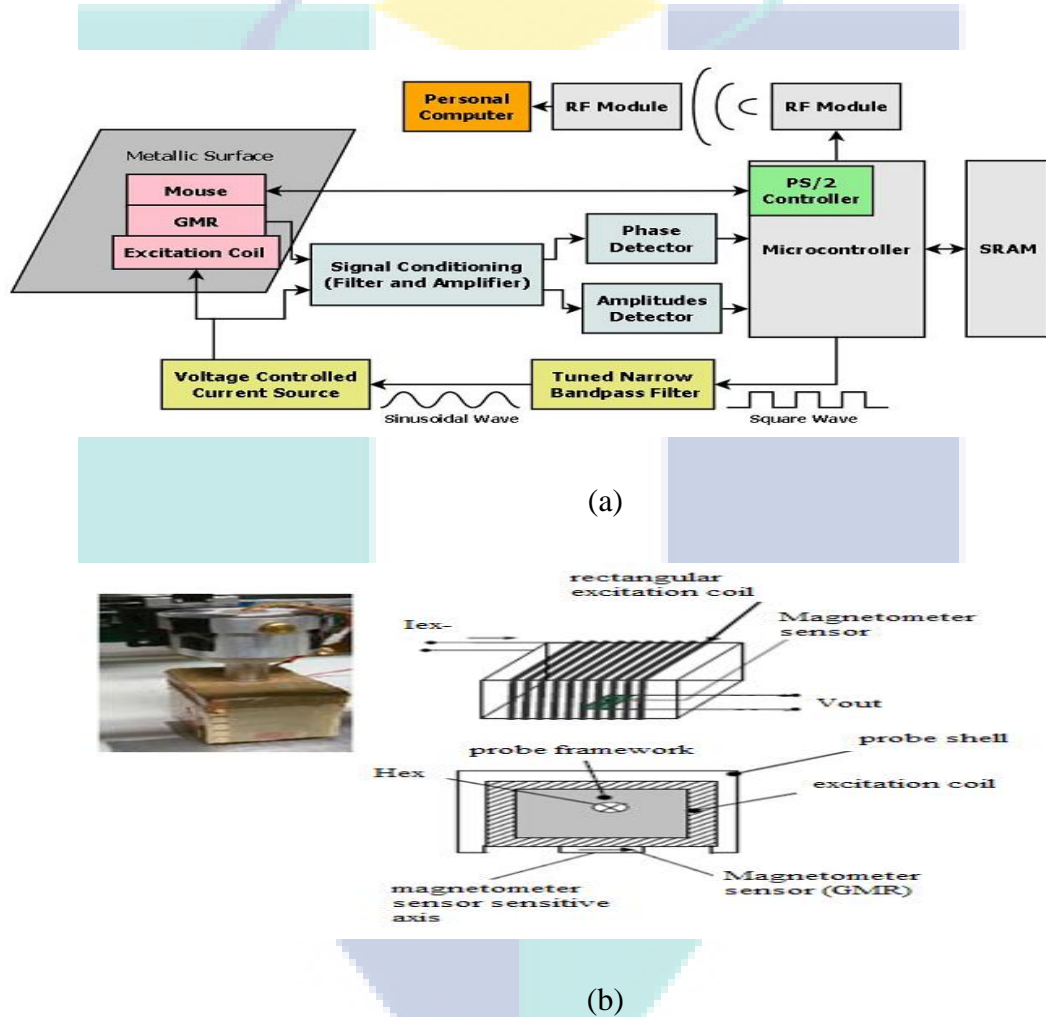


Figure 2.9 Block diagram of signal conditioning and eddy current ECP probe, a) Measuring system in Depicts block diagram, b) The architecture of 3D uniform eddy current ECP probe.

Source: Rocha, T. J., et.al., (2011)

The eddy current ECP probe has been designed along dissimilar architectures that combining unvarying magnetic field generation to a magnetometer sensor was applied and proved. The best metrological execution obtained delivered in Figure

2.9(b). Based on the figure, the probe shows a parallelepiped shape with a tangential excitation coil characterized by a rectangular section.

Table 2.2 Geometric parameters of the coils

Coil Type	Inside Radius (mm)	Outside Radius (mm)	Length of probe (mm)
Coil 1	5	6	30
Coil 2	4	7	15
Coil 3	2	8	4

Source: Wang chen, et.al., (2013)

The GMR sensor is an element that integrates an eddy current-based non-destructive testing due to high sensitive and signal to the noise in a large range of frequencies (from dc to hundreds of megahertz). A sensor was created in several magnetic tunnel junctions elements in series to reduce and included in a custom probe configuration for detection effect. Low frequency and high sensitivity (Wang, C., et.al., 2013) led to the GMR sensor successfully used in eddy current testing. EC smart probe, based on the GMR sensor and processing unit is an appropriate instrument(Giovanni Betta et.al., 2012). The ability to detect locates and characterizes flaws and sub-superficial thin superficial cracks are the main features of the instrument.

Four GMR elements are arranged in a Wheatstone bridge configuration is a key reference. A positive output regardless of the direction of the magnetic field so that the AC magnetic field will produce distortion effects on the output voltage, will appear as a full-wave rectified sinusoidal waveform as shown in Figure 2.10(a) is due to GMR sensor operates as omnipolar. Point magnet DC (after a dc operating point) at which the sensor function cause changes in this effect. Magnetic sensor bias is a method for creating a bipolar output. Detect defects in conductive materials typically includes a transmitter coil and a receiver coil or magneto-resistive (MR) sensor for the system using non-destructive testing (NDT) based on EC(Caetano et al., 2015). An arrangement sensor and the details of the excitation coil and permanent magnet is shown in Figure 2.10(b). Sensor GMR and two exciting coils disposed of orthogonally. An excited magnetic field direction and parallel to the other(Bernieri, A., et al., 2014) that cause each sensor are orthogonal.

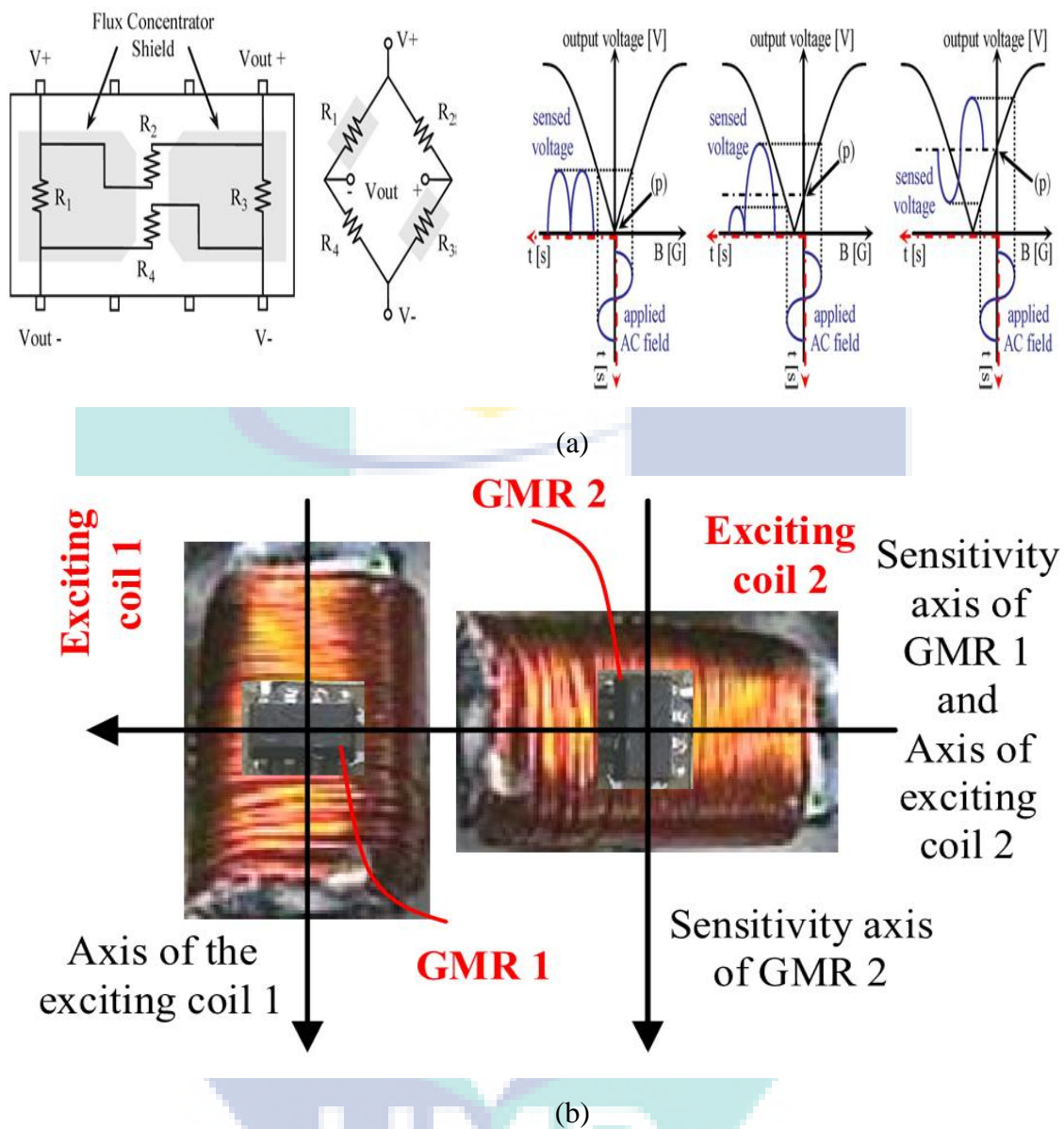


Figure 2.10 GMR-based ECT probe's schematic and configuration, a) Configuration of the sensor for GMR magnetometers are connected with Wheatstone bridge, b) The biaxial sensors arrangement and the permanent magnet and coil excitation.

Source: Bernieri, A., et al., (2014)

2.5 Crack Defect Classification

The crack defect classification often used in the design of electromagnetic problems where the goal is to find a topology change rather than to determine the surface shape. For example, in non-destructive testing applications, it is more important to know the number and location of all the flaws in the specimen than to find the right form cracked the only specimen. A numerical model was created in the magnet (Junjun

et al., 2011) with the same geometry as described in this TEAM problem. Reversal of the procedure starts with the assumption of no crack. The classification gradient is calculated and plotted in Figure 2.11(a). The highest gradient values topology (represented by the light areas) coincides with the position of the slot in the plate. The classification sensitivity analysis shows the topology changes in the domain of interest. Figure 2.11(b) shows the creation of the air in the slot early in the plate, where the border is dubious with five control points. The slot is then determined started from the right slot using sensitivity analysis design continuum (CDSA) form-based optimization. The Signal impedance changes are calculated from the reconstructed shape then compared with experimental results in Figure 2.11(c). Figure 2.11(d) shows changes in the value of the objective function during the procedure inversely proportionate to the reconstruction of the crack using topology optimization and shape optimization pure form.

The defects in the workpiece to modify the pattern in which EC caused by the probe during a given source. The source probes or the other probes have a variation of impedances that can be collected. The solution method of the defects classify from values of such impedances in almost real time can be created with enabling. A particle swarm algorithm is used for fast optimization can be replaced with a matching model with exact forward calculations(Douvenot et al., 2011).

PCA/ICA-based method is an obvious improvement. (Horan et al., 2014)PEC, engendered along a probe design that utilizes the ferric fastening as a flux conduit, are presented to bear potentiality of finding simulated cracks inside the spar with the wing skin demonstrate. Another joined pickup coils are accustomed sense differences in reception referable asymmetrical caused eddy current fields developing in the front of cracks.

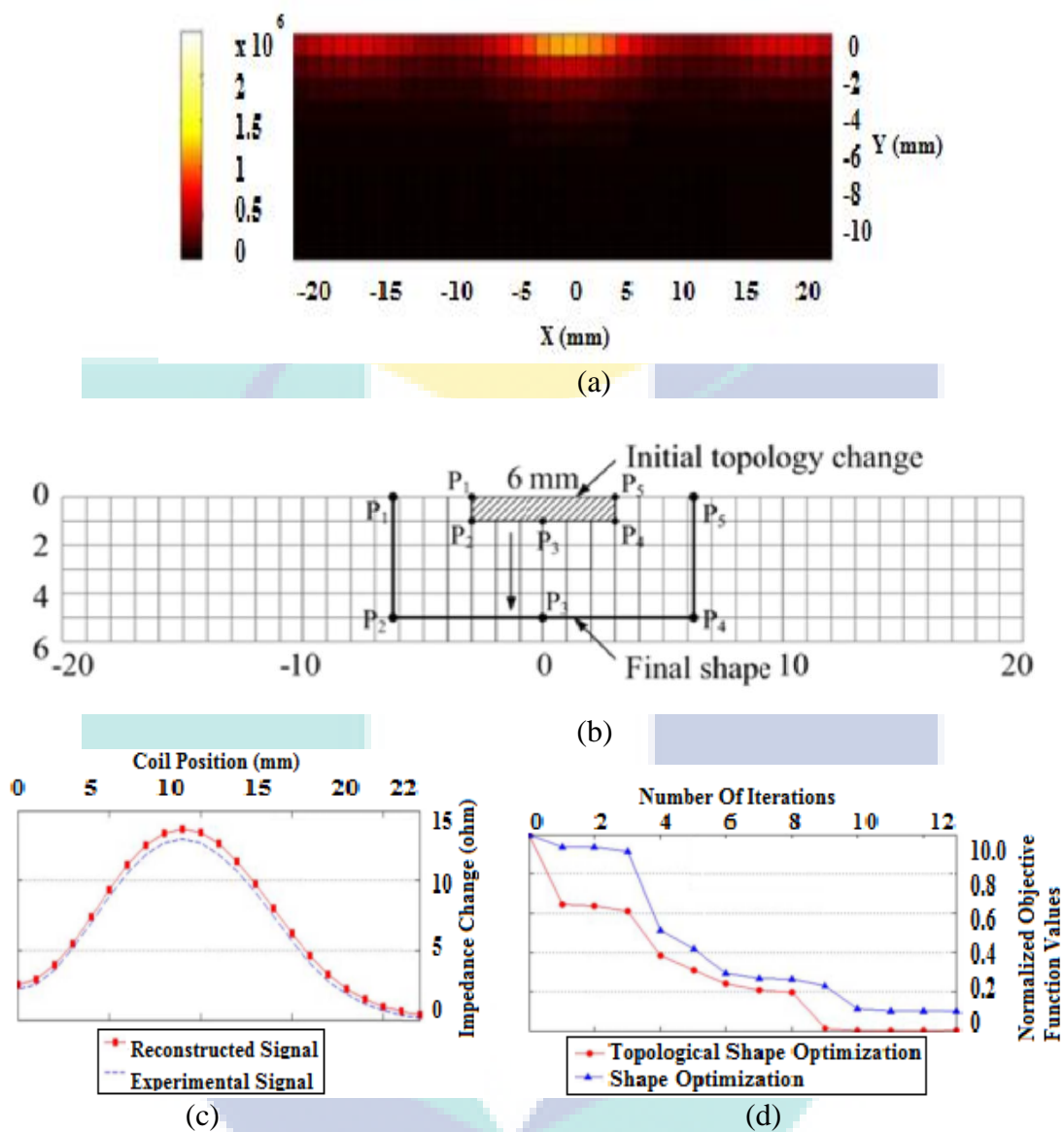


Figure 2.11 Topological gradient plot with reconstructed slot for performances of two optimization models, a) Rectangular slot in the topological gradient plot. b) Reconstructed slot for final shape. c) Reconstructed slot for impedance signal. d) Performances of two optimization models.

Source: Junjun et al., (2011)

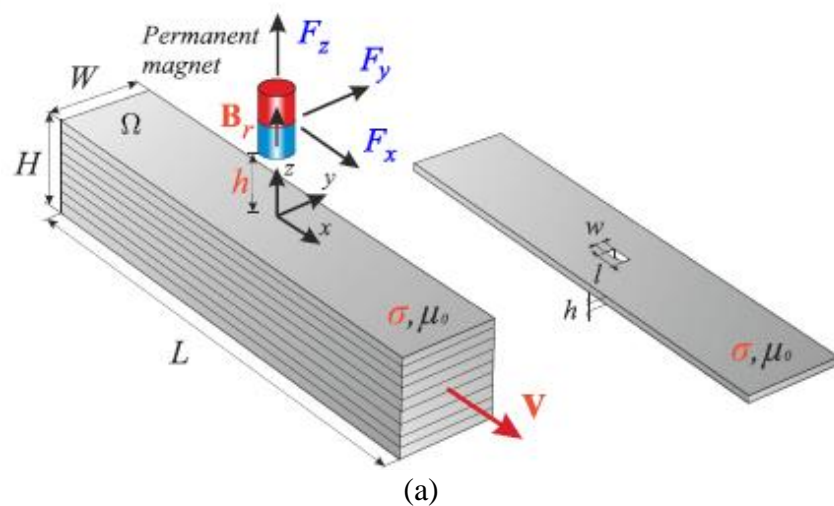
A characteristic descent process supported main component analysis for PEC NDT by encloses the application of main element analysis in reducing data from PEC reactions (Sophian.A.,et.al.,2003). The process reduces the size of the reaction signals and extracts applicable characteristics, which admit competent categorization of defects.

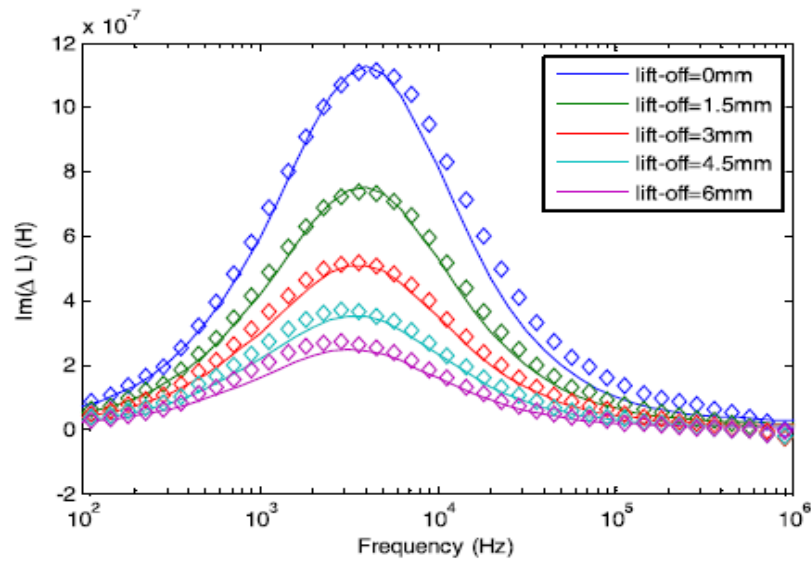
2.6 ECT Defect Measuring

On the last topic, the discussion is more about the defect measuring including the lift-off defect measuring in ECT and intelligent technique defect measuring.

2.6.1 Air-Coil for Lift-Off Measuring

The Eddy Current measurement of metallic plate thickness will cause an error of lift-off variation. The triple coil sensor was designed and operated as two pairs coil and make a research on multi-frequency mode. The difference of the peak frequencies found is directly series to the plate thickness but totally immune to reduce variations. Statistics velocity, specimen conductivity, magnetic resonance and the permanent magnet off distance are determined experimentally and β are modeled as a random variable uniformly distributed and circulated. Figure 2.12(a) illustrates the general principle of ECT. The test object and permanent magnet are based on the induction of eddy currents that cause relative movement between it. Lorentz force is functioning as on the magnet was measured and recorded to analyze the quality of the specimen in ECT(Weise et al., 2015). Sensor connection to a Solartron 1260 impedance analyzer is shown in Figure 2.12(b) (Yin & Xu, 2016). Based on the results showed, when high lift-off occurs from the cracks, the signal will be reduced, thus the lower lift-off will give the maximum measurable signal.





(b)

Figure 2.12 ECT principle in random variables output quantities and lift-offs simulation results, a) ECT Principle in random with (red) input variables and (blue) output quantities, b) The lift-offs simulation results

Source: Yin & Xu (2016)

2.6.2 Intelligent Technique in Defect Measuring

The fuzzy logic is very useful for achieving lift-off compensation. In addition, the use of the absolute and differential probe for compensation is also investigated. Based on AI technology, a lot of research has been done by many researchers with regard to eddy current compensation as shown in Table 2.3

Table 2.3 Intelligent Technique In Defect Measuring

Author	Research Area	Finding	Intelligent and Purpose	Criticizing Technique
(Rosado. L. S., et al., (2013))	Defect Characterization on ECT using Artificial Neural Networks	ANN was predicted deflect overfitting.	ANN to deal with complex data of the defect properties.	The use of nonlinear regressions and ANNs to estimate parameters of defects tested using an eddy current probe but the comparison between linear and nonlinear regressions not discussed.
(Betta. G., et al., (2015))	Image processing for Eddy-Current Testing for 2D crack	The width of the sensed defect, it is strongly determined along the skimming	Image processing technique in Fast reconstruction of	The digital filter to process the acquired image through deconvolution or correlation operations,

		resolving and dimension of the exciting coil.	defects geometry	the shape of the flaw that has generated the image can be retrieved. But the process only in offline processing
(Rosado. L. S.,et al., (2014))	Multi-Frequency for ECT Signals in RTP	Eddy currents testing signals for multi-frequency stimulus by using DSP	DSP purposes in FPGA	A real-time DSP-based processing architecture able to generate multifrequency stimulus and to process eddy currents testing signals was but lack in reduction of the peak value of the synthesized stimulus using optimization procedures on the different frequencies phases
(Dashtbani Moghari et al., (2015))	Pulse eddy current testing for stress accuracy measurement using ANN.	ANN improve the stress measurement accuracy	Neural network data fusion	Evaluation of stresses and residual stresses, which are key factors in mechanical component performance, has been a big challenge but the technique is used not applicable in measuring stress, even in aluminum.
(Guohou et al., (2011))	Multi-sensor Application for Data Fusion in Defects Evaluation	The defects parameters and conductive material is fined by using the D-S theory	Theory of Dempster–Shafer in fuzzy inference	The fuzzy set theory used calculating the BPA values in the D-S theory, and then the D-S rule of combination is applied to fuse the data from UT and ECT but the frequency used not discusses detail in this research.
(D’Angelo & Rampone, (2015))	NDT shape defect classification	Accuracy rate effectiveness of this approach.	Neural networks	The image through a feature vector composed of only three geometric parameters: length, width, and orientation angle of the shape but the comparison between the previous researcher and this author does not make for the efficient result.

Table 2.3 Continued

Author	Research Area	Finding	Intelligent and Purpose	Criticizing Technique
(Ahmed et al., (2013))	NDT sizing of defects for multidimensional learning	Multidimensional data used to improve the dimensional result	multidimensional in a neural network for Radial Basis Functions	Radial basis function (RBF) neural network with two novel modifications, which can be adapted for multidimensional learning but adaptation and comparison of other well-established algorithms such as support vector machine, neural networks, and ensemble learning for multidimensional learning not being discuss
(Shejuan et al., (2013))	Pulsed Eddy Current Testing Signals (PET) functioning in Sizing of Wall Thinning Defects	The combination CG methods and NN are effective by using PECT signals	ANN application in pulsed eddy current testing signals (PECT)	The normalized difference PEC response, as it significantly reduces the influence of variation of magnetic permeability but the microstructural investigation is needed to confirm this hypothesis.
(Buck et al., (2016))	Pulsed eddy current steam generator data in simultaneous measurement by using ANN	ANN model simplification for higher accuracy.	Investigated of the complex relation between inspection data and defect properties by using ANNs	PCA feature extraction and deterministic ANNs have been combined to estimate four separate experimental parameters but the comparing between PEC and coil probe not discuss in this researcher.
(He et al., (2013))	PEC defect automated classification in aircraft multi-ply structures with interlayer gaps and lift-offs	PEC technique for defect automated classification can effectively eliminate the air-gap and lift-off effect in multi-layer structures	PCA-based feature extraction methods (ANN)	Integrated in an instrument and PCA, ICA and SVM are used to conduct the classification of several kinds of defects in two-layer Al-Mn 3003 alloy specimens with different air gaps and lift-offs but

				the limitations of this work is more about the calculation time of the three optimised SVM methods has not been compared.
--	--	--	--	---

2.7 Summary

Various methods were used in ECT inspection process to obtain a good result in identifying the main fracture. The most common method used is based on the diversity of excitation input. As usual, there are 2 inputs used, input pulse excitation and signal ac excitation. The effect of the input pulse excitation signal is better than AC excitation signal due to traveling depth on the plate or pipe inspection besides of clarity output signal derived. There are two methods in ECT probe development, air coil probe, and GMR probe. Air coil probe is widely used in the inspection process than GMR probe. However, the stability and ability of air coil probe in measuring small cracks and defects of the pipe and plate are low. GMR probe can overcome the problems with high sensitivity on small defect and crack and low noise interference. In addition, an in-depth review has been made on ECT compensation techniques of air coil sensor and GMR sensor. Specifically, the review addressed the hardware and software compensation based on their main characteristics/structures, strength, and weakness. To eliminate the lift-off error, consideration of the methods has been analyzed from the hardware and software. Compared to the hardware compensation, software compensation is better and achieves higher accuracy.

CHAPTER 3

METHODOLOGY

3.1 Introduction

Therein chapter research process ECT error compensation is presented. The elaborate error compensation technique, particularly for ECT differential signal and absolute signal processing, specified probe shoe design, feature descent methodology and most especially the design of the fuzzy logic system are applied. The conception of the absolute probe, differential probe, examining samplings data and experimental results and conclusions will likewise be delivered consequently.

3.2 Proposed ECT Technique Using Fuzzy Logic

In methodology, the ECT proposed design is an important part of system development in ECECT system design. The architecture design is shown in Figure 3.1 where it dividing into five parts. First part is about the source supply. From here the AC excitation signals being chosen as source supply by using function generator. The second part is an input device. Two input device are used there are a differential probe and absolute probe. Both of two input device are used the same AC excitation signal source. The third part is about controlling or processing devices. ATMEGA 2560 is used as controlling devices and the system programming is embedded in this microcontroller. The fourth part is output devices where the LCD display and buzzer are used to display the actual depth of defect, differential probe sensor reading, absolute probe reading and percentage of error. The buzzer is functioning as an indicator where the defect over the normal defect reading then the buzzer will activate. Lastly, fifth part is simulating and processing devices. From here the PC is used to process the data from the microcontroller and showing in graph besides that the PC is used to simulating the

virtual signal from MATLAB/Simulink application, processing in FIS block and showing the resulting graph.

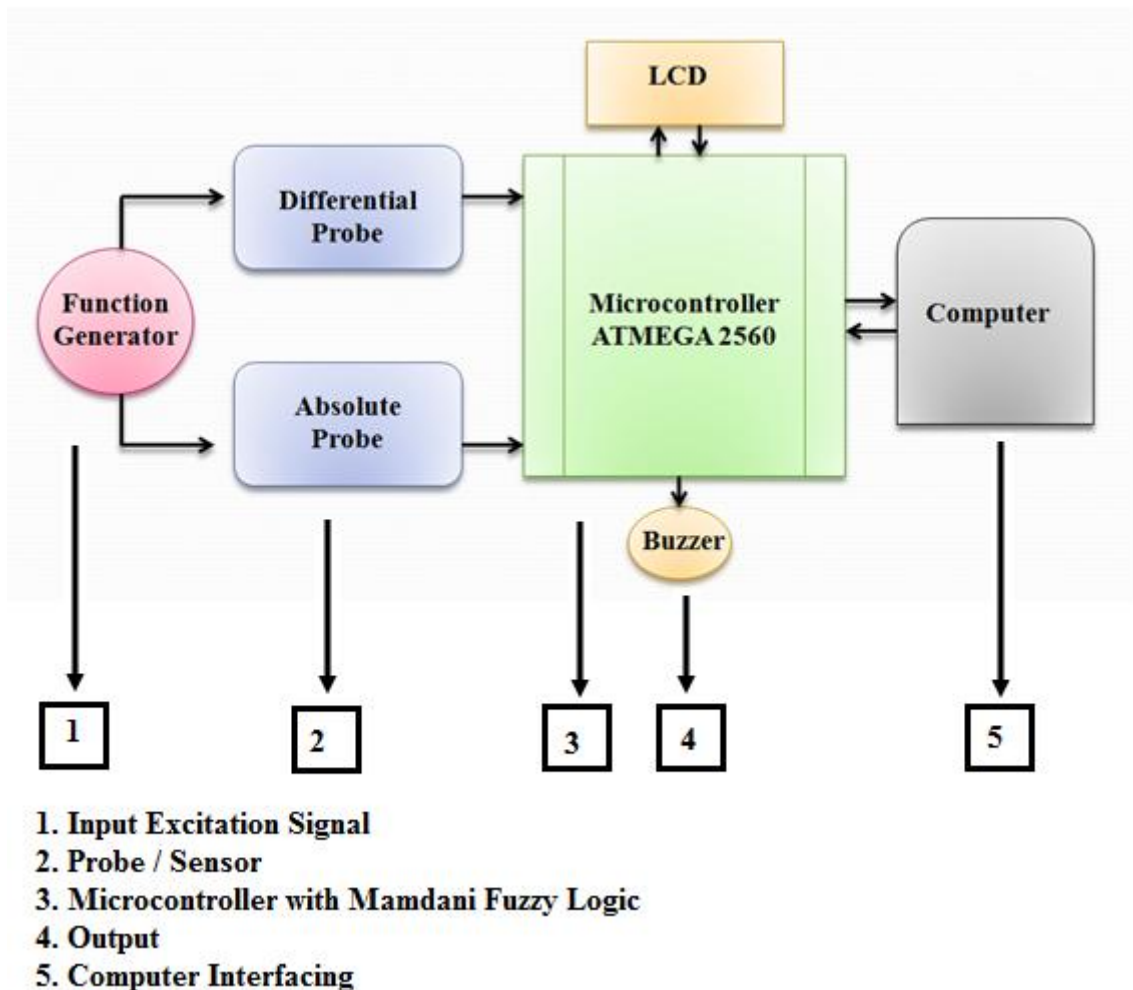


Figure 3.1 Proposed the Architecture of ECECT System.

Fuzzy logic therein analyze is applied since an administrator, to provide the crack data supported reduced features: amplitude, phase, and width. This fuzzy based deciding scheme contains system input, system output, membership functions (MF) and IF-THEN fuzzy rules. The inputs are the characteristics of crack specified amplitude, phase, and loop width. The output of the scheme is the real crack data specified depth, width, and shape. As shown in Figure 3.2, each input is associated one fuzzy set and each fuzzy set accepts its agreeing MF. The MF reacts to the degree of each fuzzy set as a member in the membership in the scale of 0 to 1. The fuzzification is executed appropriately to companion fuzzy set with MFs. Fuzzy rules are declared in IF- THEN lingual condemnations, which describe the relative between input and output for

example: IF the amplitude (input) is high THEN the crack depth is deep (output). Eventually, for more one fuzzy rule has constituted applied, and besides the execution result is lingual (deep), a defuzzification action is required to conveyance the lingual variables into mathematical crisp values.

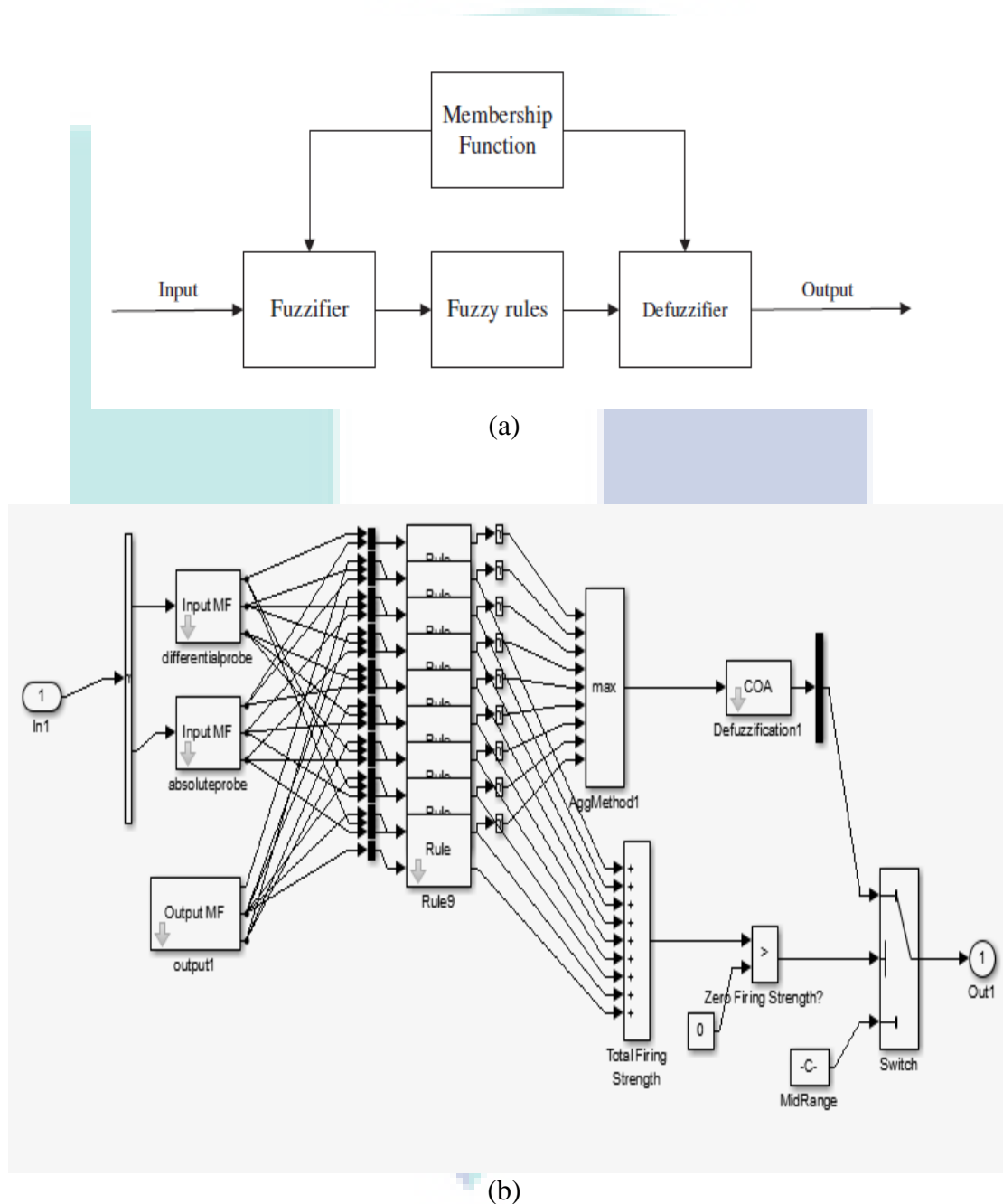


Figure 3.2 Flow chart of fuzzy logic (a) Basic block for Fuzzy Logic, (b) Internal block function in Fuzzy Logic.

In this research dissimilar frequencies are implemented to test the crack with dissimilar depths and shapes. For each MF, the numbers of MFs besides as the fuzzy

rules ought to be built up severally according to dissimilar characteristic groups. In that work, ANFIS in Matlab is applied as scheme acquiring technique to find fuzzy logic system. So these trained fuzzy logic engines are implemented to predict the crack data supported the extracted features or the combination of the characteristics.

3.3 Step of Development Fuzzy Logic

The Fuzzification method is used for this project is triangular membership functions. From here there are defined by a lower limit a , an upper limit b , and between of lower limit and upper limit value m , where $a < m < b$. By using the Matlab software the simulation and interfacing being make according to the step of fuzzy setting. Below are the steps of fuzzy setting on Matlab. The first step is setting block starting for Matlab by typing "fuzzy" on the command window. Figure 3.3 show the command window form for typing.

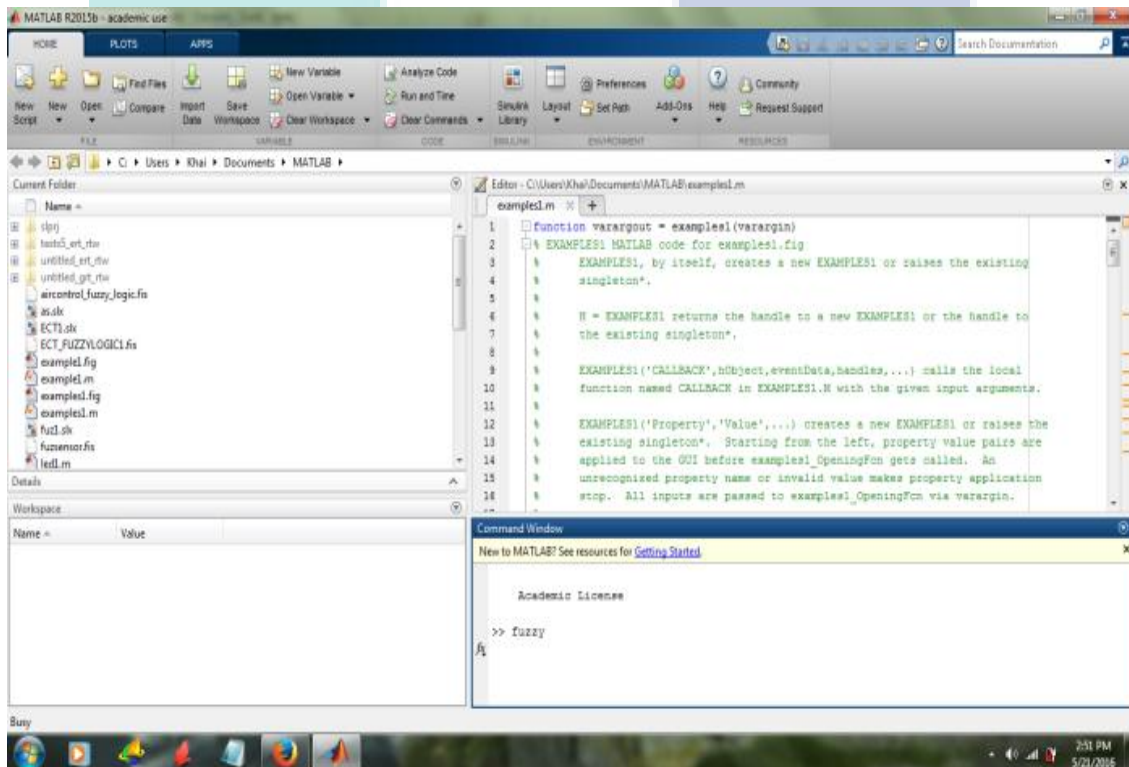


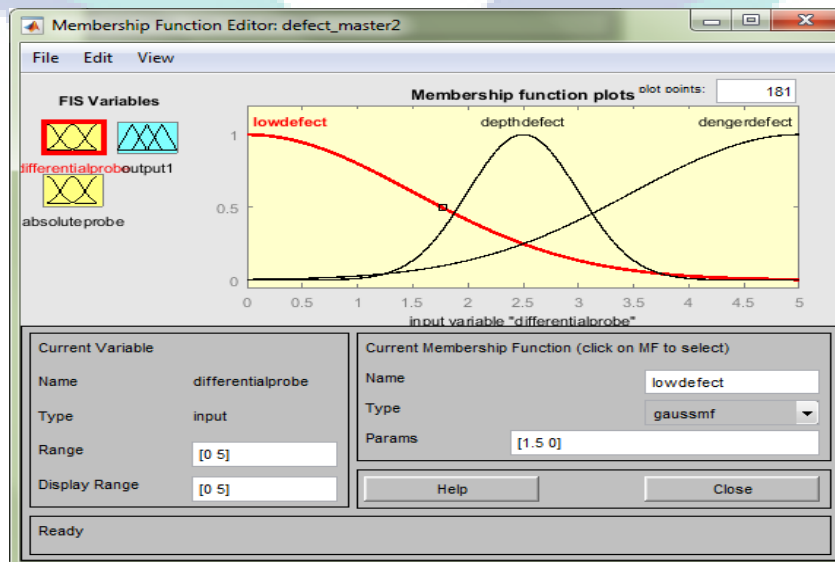
Figure 3.3 Command Window

After the fuzzy word is typing in the command window, the second step is Fuzzy logic design block (inference editor) setting and it will appear on the screen. From here the user could set the value of the input and the types of membership

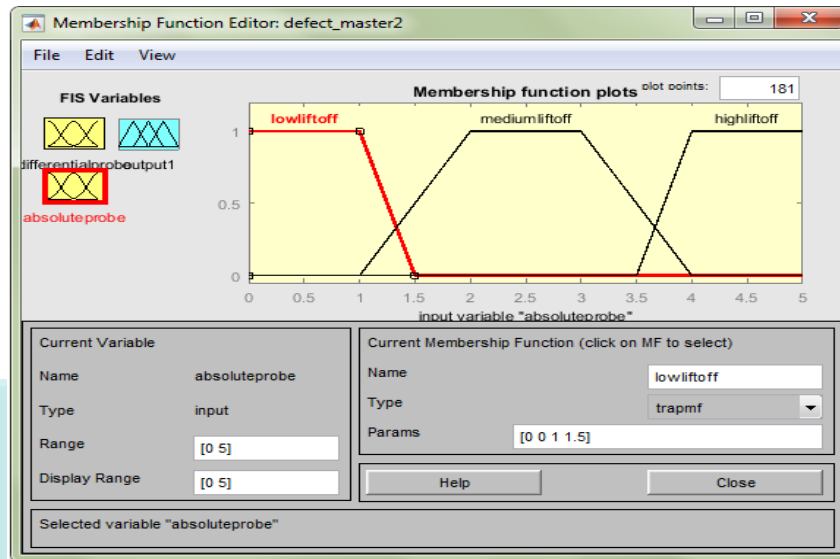
function want to use. On this research, the input selecting is two and the membership function used is triangular. The both of inputs and output name are lift-off for (absolute probe) and depth of crack (differential probe) and output (actual depth of crack).

The third step is setting the membership function for the absolute probe, differential probe, and the output. In each input and output then they have four number of membership function (MF) and the range from 0 to 4 according to the minimum and maximum depth of crack and lift-off that could be achieved of probes. For the absolute probe, the concept of the signal is inversely proportional to the thickness of coating or lift-off.

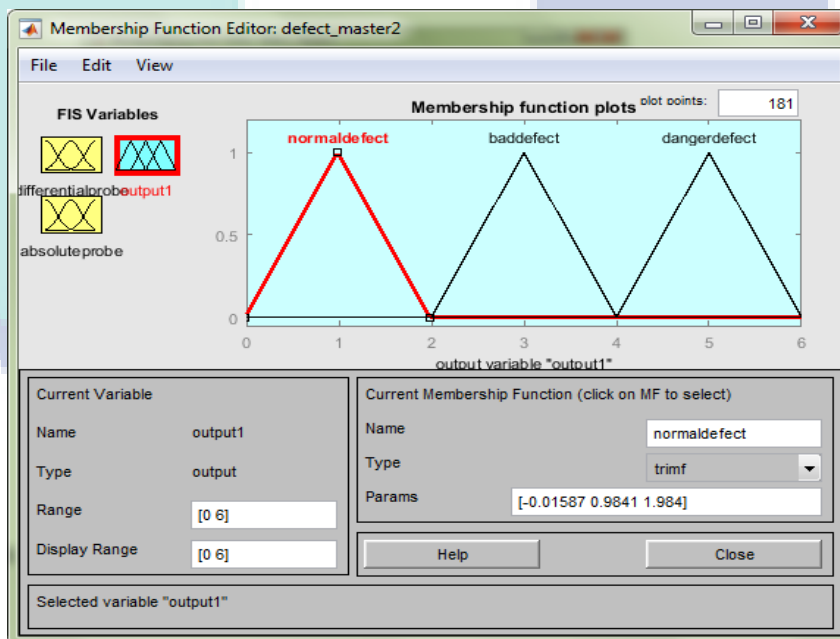
This means when the plate or pipe without the coating layer the signal are produced is high but when it be coated with coating the signal produces is decrease according to the thickness of the coating. It different with the differential probe. The differential probe functioning to measure the depth of defect on the plate or pipe. The concept of the differential probe is directly proportional with the signal produce of the probe. When the depth of crack is high then the signal generate is high and vice verse. Figure 3.4 show the membership function of absolute probe and differential probe and the output for fuzzy logic designed.



(a)



(b)



(c)

Figure 3.4 (a) MF Differential Probe, (b) MF Absolute Probe, (c) Output Actual Depth Defect.

3.3.1 Rules Of Fuzzy Logic

To complete the fuzzy logic block setting, the rule of the fuzzy block is setting according to rule editor for lift-off and depth measuring block. From here they have nine rule has been setting.

Fuzzy rule algorithm

If (differentialprobe is lowdefect) and (absoluteprobe is lowliftoff) then (output1 is normaldefect)

If (differentialprobe is depthdefect) and (absoluteprobe is lowliftoff) then (output1 is dangedefect)

If (differentialprobe is depthdefect) and (absoluteprobe is mediumliftoff) then (output1 is baddefect)

If (differentialprobe is depthdefect) and (absoluteprobe is highliftoff) then (output1 is baddefect)

If (differentialprobe is dangerdefect) and (absoluteprobe is lowliftoff) then (output1 is dangerdefect)

If (differentialprobe is dangerdefect) and (absoluteprobe is mediumliftoff) then (output1 is dangerdefect)

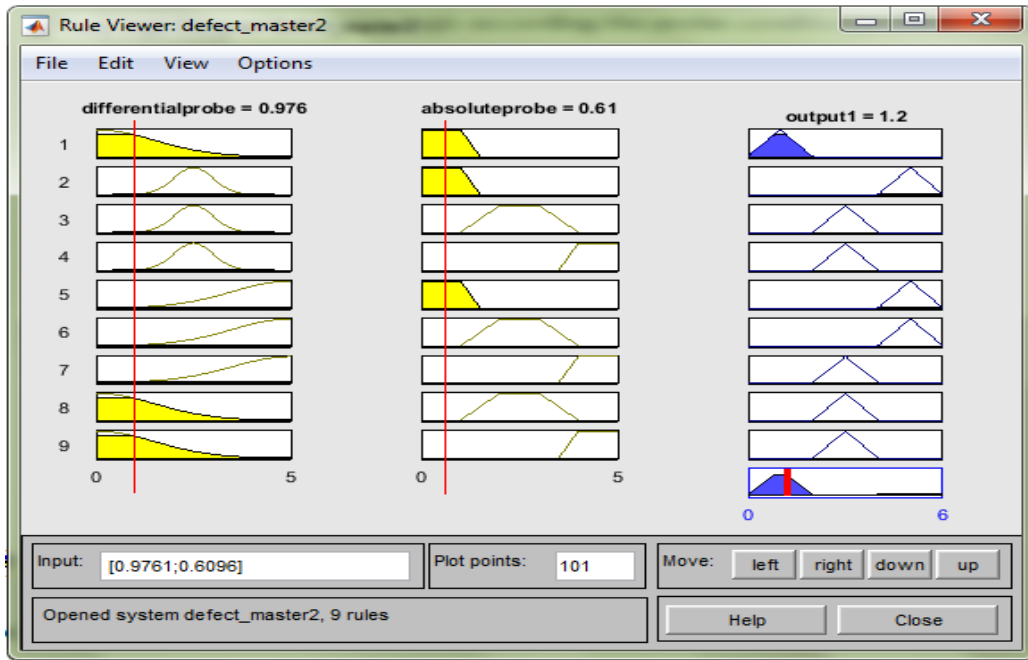
If (differentialprobe is dangerdefect) and (absoluteprobe is highliftoff) then (output1 is baddefect)

If (differentialprobe is lowdefect) and (absoluteprobe is mediumliftoff) then (output1 is baddefect)

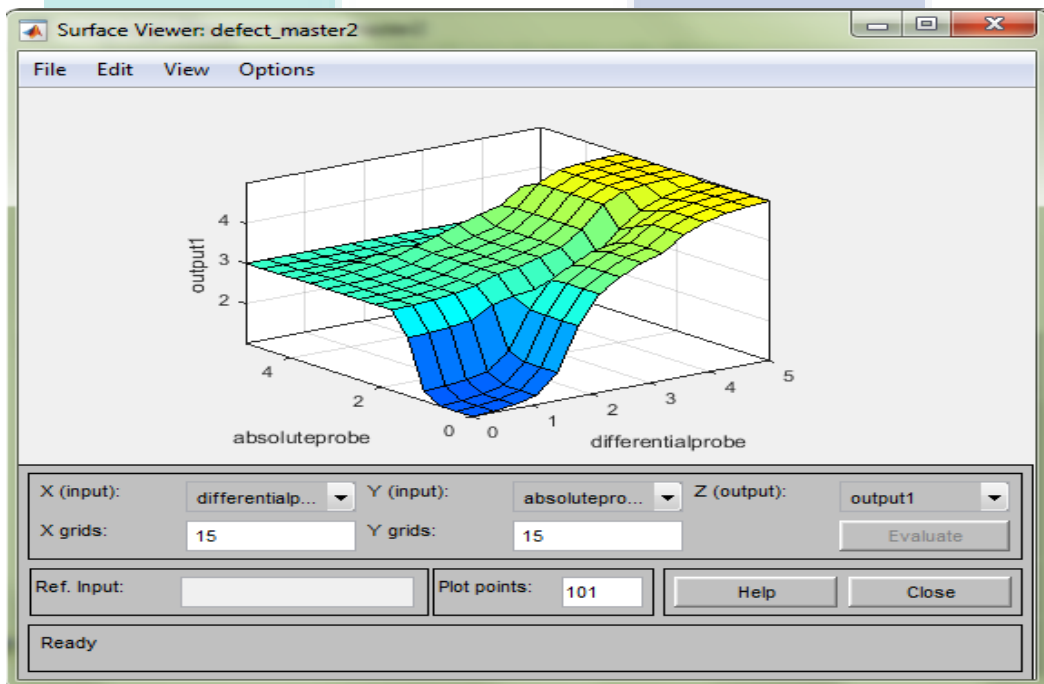
If (differentialprobe is lowdefect) and (absoluteprobe is highliftoff) then (output1 is baddefect)

3.3.2 Surface Viewer for Fuzzy Logic

The fifth step in the fuzzy logic setting is the result of fuzzy setting by looking on rule viewer and surface viewer. From here the user could look the input changes and effect the output for rule viewer and for the surface viewer it shows in the 3D graph. Figure 3.5 (a) show the rule viewer for lift-off and depth of a defect and (b) is surface viewer graph.



(a)



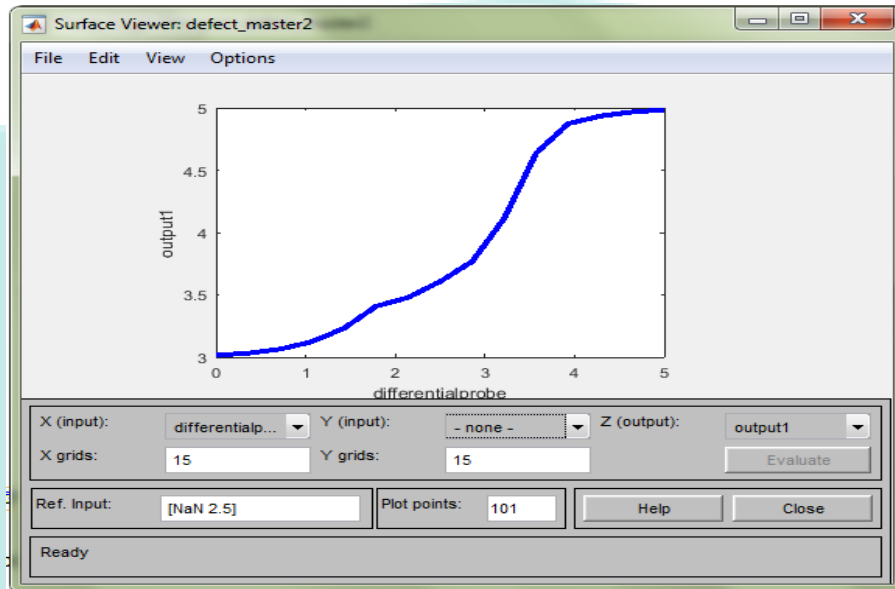
(b)

Figure 3.5 (a) Rule viewer, (b) Surface viewer

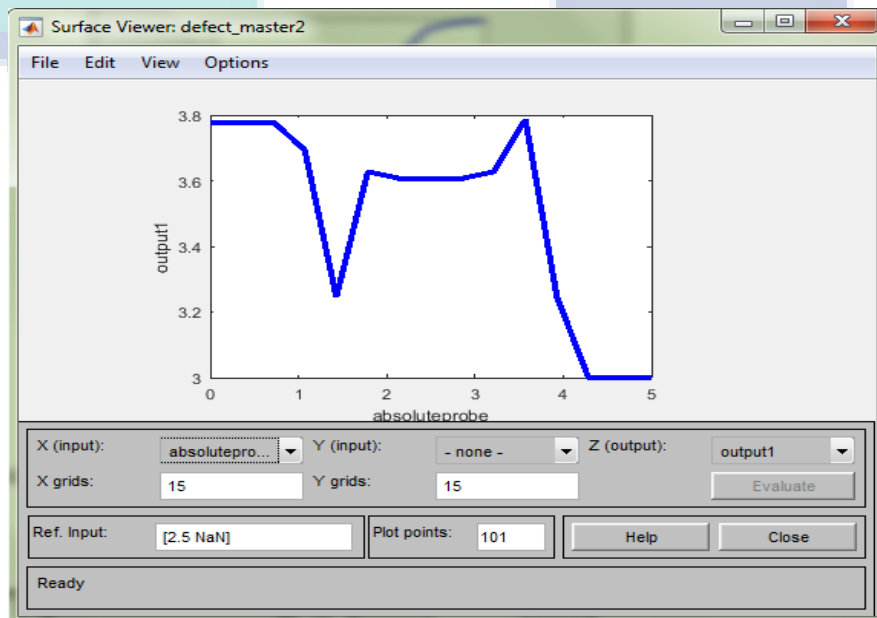
3.3.3 Graph Surface Viewer For Fuzzy Logic

In each of graph setting for differential and absolute probe, it could be shown in the 2D graph. By following the Figure 3.6 the differential probe graph and absolute

probe graph for the surface viewer are shown. The maximum value of differential probe graph is 5mm depth of defect for output at Y axis and 5Vp for signal measuring at X axis and for absolute probe the maximum output for coating thickness is 3.8mm at Y axis and for signal measuring is 5Vp at X axis



(a)



(b)

Figure 3.6 (a) Differential probe graph for surface viewer, (b) Absolute probe graph for surface viewer

3.4 Flow Chart

The main program than doing the correction based on the output result of Fuzzy Correction. The output voltage after compensated then is displayed on the LCD Display. The output has also been sent to buzzer as an indicator of the depth of defect. The flowchart for the measurement and FTCS process in Arduino Mega is shown in Figure 3.7.

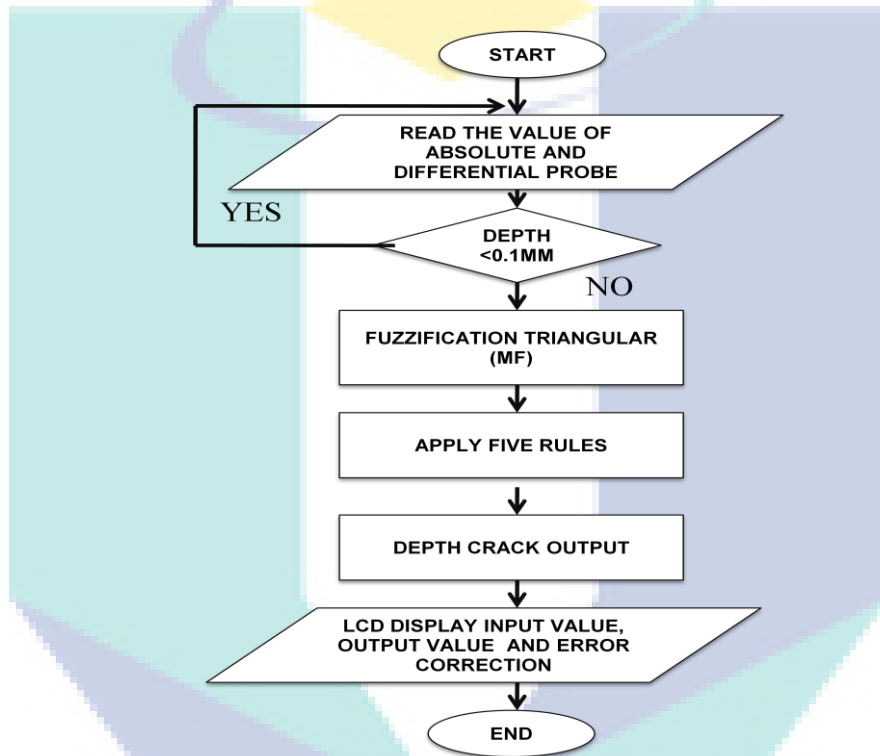


Figure 3.7 Flow Chart of Fuzzy ECT Compensation Scheme

3.5 Simulation Model of EECT system

In simulation process, the MATLAB/ Simulink is used to simulate the input and output result signal by following the AC excitation signal setting. According to the Figure, 3.8 simulation block diagram model for EECT there have four important part which in used for the fuzzy logic system. The first part is input source, second is conditioning process, the third is fuzzy logic process and feedback and lastly output display.

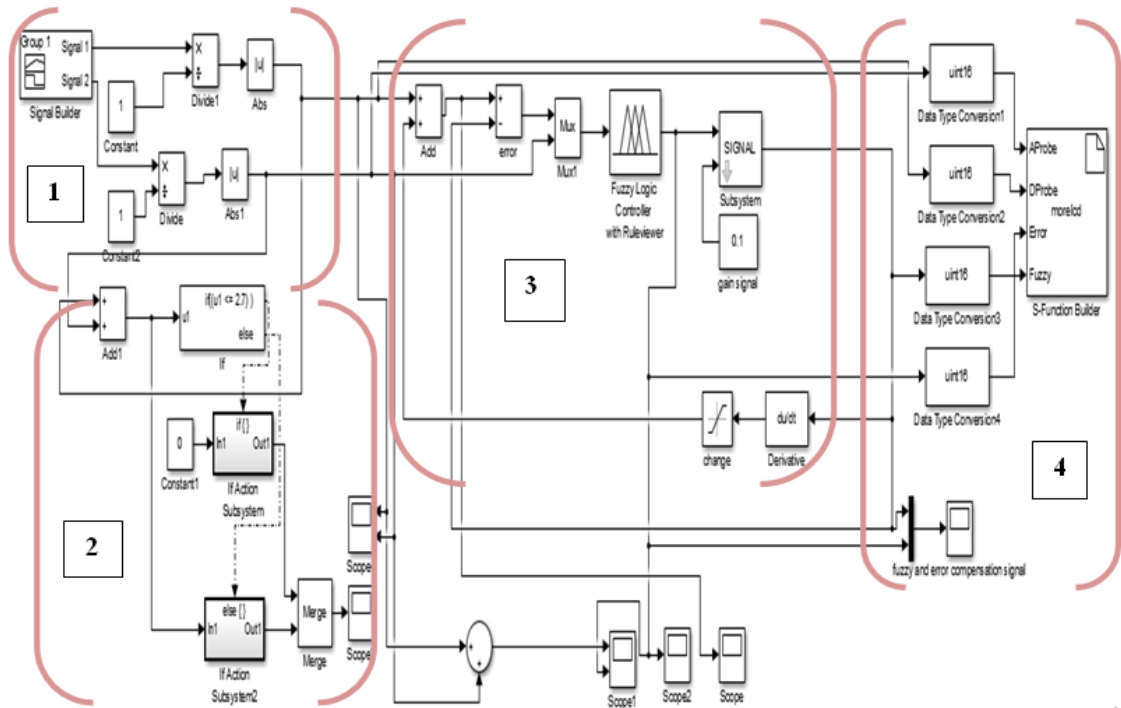


Figure 3.8 The Simulink Block Diagram Model for ECECT. 1) Input source, 2) Conditioning process, 3) Fuzzy logic process and feedback, 4) Output display

3.5.1 Input For Fuzzy Logic

In simulation process, the input used is an AC signal with the signal are setting according to the amplitude and the phase angle of the signal. Figure 3.9 show the input block diagram that has been converted to positive value waveform input by using absolute block and output will show on the scope.

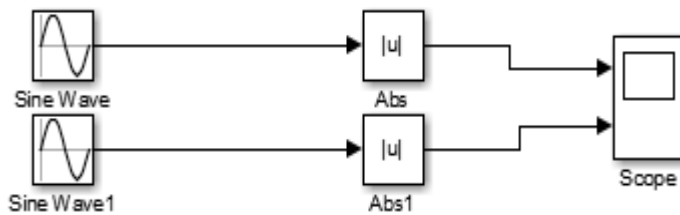


Figure 3.9 Input Block Diagram

3.5.2 Conditioning Function For Fuzzy Logic

The conditioning function is used in measuring the defect. From here when defect or signal is lower or equal than 2.7 then the signal will be low otherwise the

signal will be high according to the input probe signal after two input are mixed by using add block function. Figure 3.10 show the conditioning block is used in Simulink and the graph result from the conditional block will display on the scope.

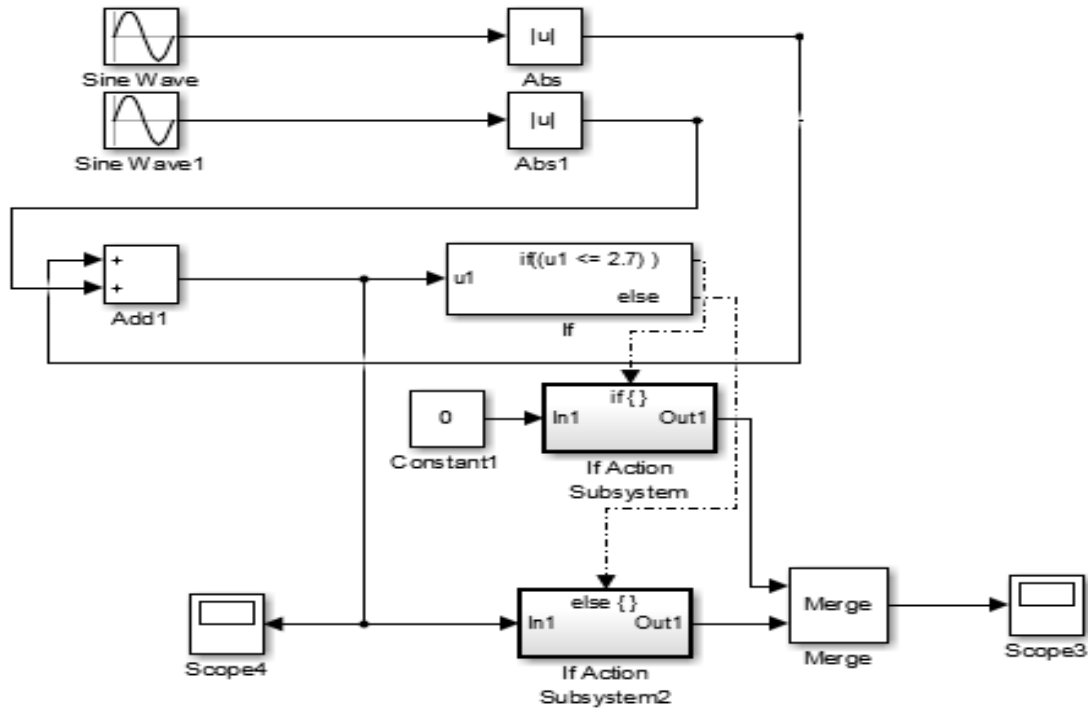


Figure 3.10 Conditioning Block Diagram

3.5.3 Fuzzy Logic Process and Feedback

The feedback and error compensation will be processed according to the output signal from fuzzy logic. From here the output signal from fuzzy will be through the error compensation equation in the signal block and it will feedback to error block. Figure 3.11 show the feedback block for error compensation and the output produced.

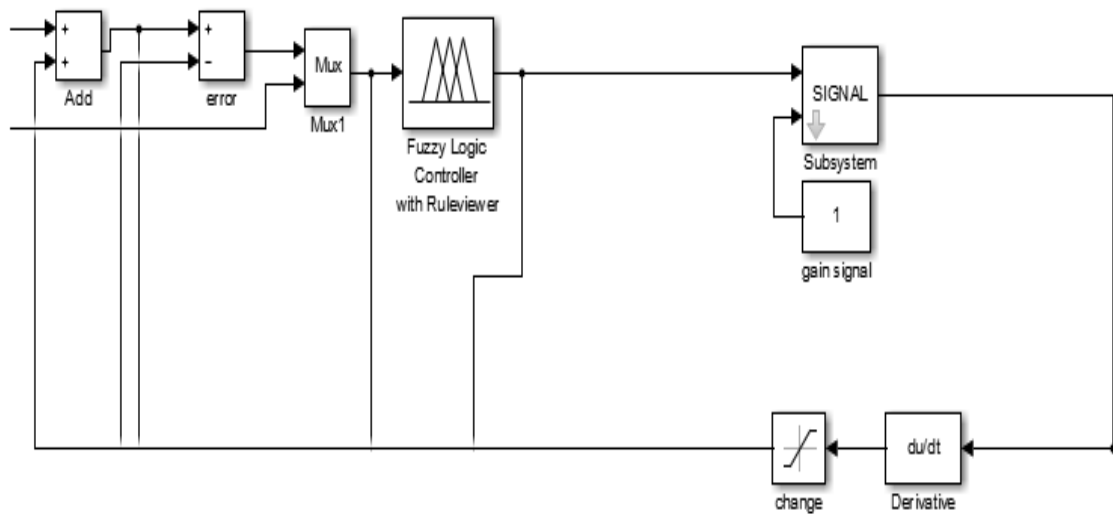


Figure 3.11 Error Compensation Feedback

3.6 Proposed Probe Design

The hardware designs are divided into two parts namely designing the probe shoes and lastly circuit development. The probe shoe design includes the probe design with 3D dimension and quadrant view and probe shoes. For the circuit, development designs it including the full schematic circuit and interconnecting with the computer.

3.6.1 3-D Probe Design

Probe size designing is very important to ensure that the probe shoe is appropriate with the sizing of the probe. From here the design of probe (differential probe and absolute probe) have the same size and diameter. The probes used are a commercial probe that being used for industrial in for inspection process. The designing of the probe are following the actual size of probe there are high is 84mm and the diameter 12mm. Figure 3.12 show the actual dimension value for the probe was used.

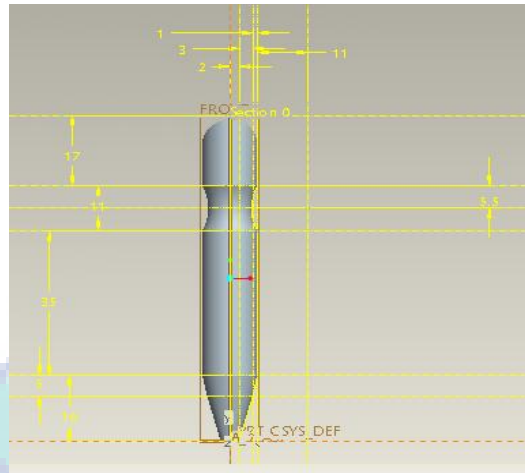


Figure 3.12 Dimensioning of Eddy Current Probe

According to the dimension of the probe, the direction view could be shown in four orientations; there are a front view, top view, side view and bottom view. From here the correct surface, different diameter, different curve and angle of the probe will be now actually. Figure 3.13 show the view of eddy current probe.

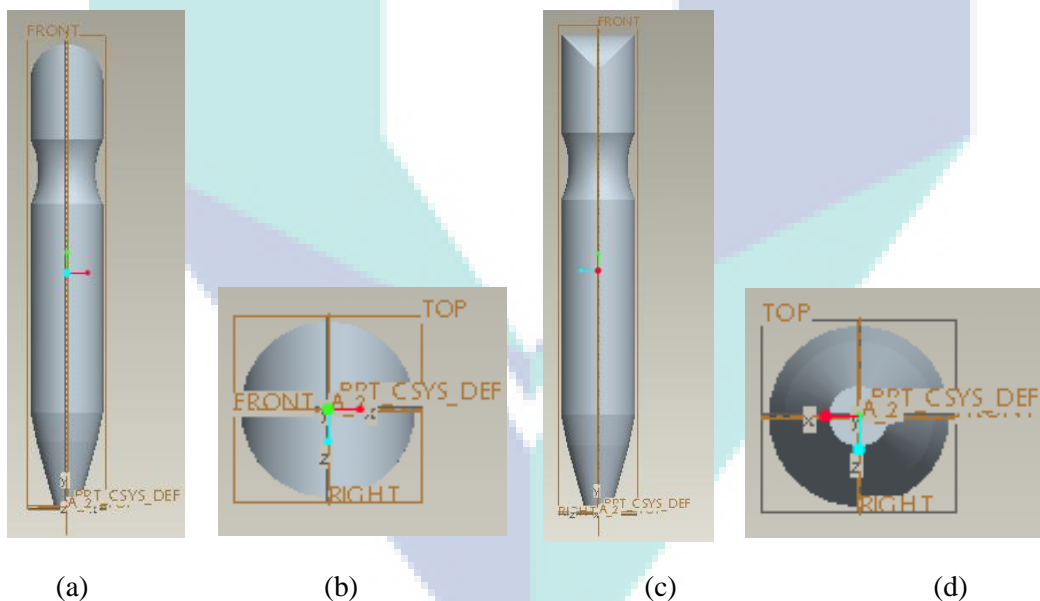


Figure 3.13 The view of Eddy Current Probe (a) Front View, (b) Top View, (c) Side View, (d) Bottom View

3.6.2 Design Probe Drive Circuit

In the schematic circuit, there are five important parts that should have in ensuring the system is properly functioning. The first part is AC supplies that functioning to supply the AC voltage for absolute probe and differential probes. In here

the function generator was used with according the frequency selecting and setting. The second part is probe application. The types of probes used are an absolute probe and differential probes. The concept probe is air-coil probe sensor that generates the magnetic field when the AC supply through it. Each defect especially the crack on the workpiece occurs then the signal reading show a different. The third part is output devices that function as an indicator and displaying the depth defect on the workpiece. From here the LCD and buzzer were used. Second last part is controller devices. In this system, the ATMEGA 2650 is used as a controller for the process the signal from the probe are used. Other than that it is used as data transmission device between controller and computer. The processing speed for the controller is 16 bit and it appropriate on this system. The last part is PC interfacing. From here the MATLAB 2015 is used as a signal analysis and intelligent application on this project. From here the filtering signal, fuzzy logic application and output waveform of each defect will be shown on the monitor. The connection between PC and microcontroller is using serial communication interfacing. Figure 3.14 shows the design of driver circuit for probes connection, microcontroller and PC interfacing.

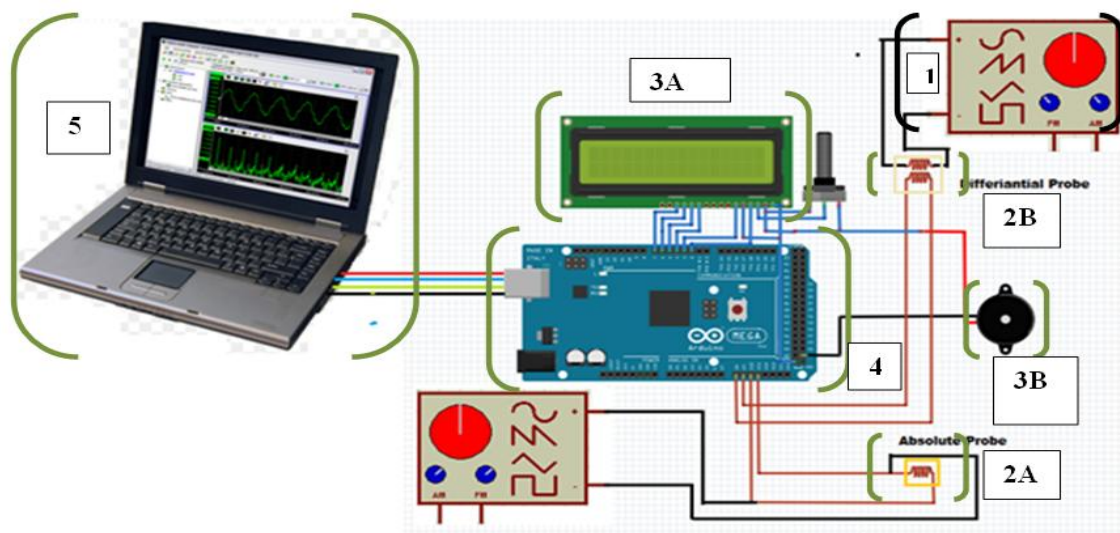


Figure 3.14 Designing of ECECT Drive Circuit. 1) AC signal, 2A) Absolute Probe, 2B) Differential Probe, 3A) LCD Display, 3B) Differential Probe, 4) ATMEGA 2560 microcontroller, 5) Computer.

3.7 Error Compensation Eddy Current Setup (ECECT)

In ECECT fully system devices development have six main part which is the first main part is Fuzzy Logic Interfacing System. In this part, the system of Fuzzy

Logic was developed by using MATLAB Simulink software. After the first part finishes, then the second part for interfacing being develop. From here the ARDUINO MEGA 2560 was used as a controller device in data input processing and output display. The third part is an input device. In here the absolute and differential probe being used as a sensor for measuring the defect. The output display for ECECT is LCD display. In here the depth of defect, the thickness of the coating, the percentage of error and fuzzy output value will display on LCD. The function generator is used as the supply or excitation signal for differential and absolute probe sensor and lastly the testing are doing by using the calibration block to ensure the depth of defect displayed are correct. Figure 3.15 show the ECECT system device setup for inspection testing.

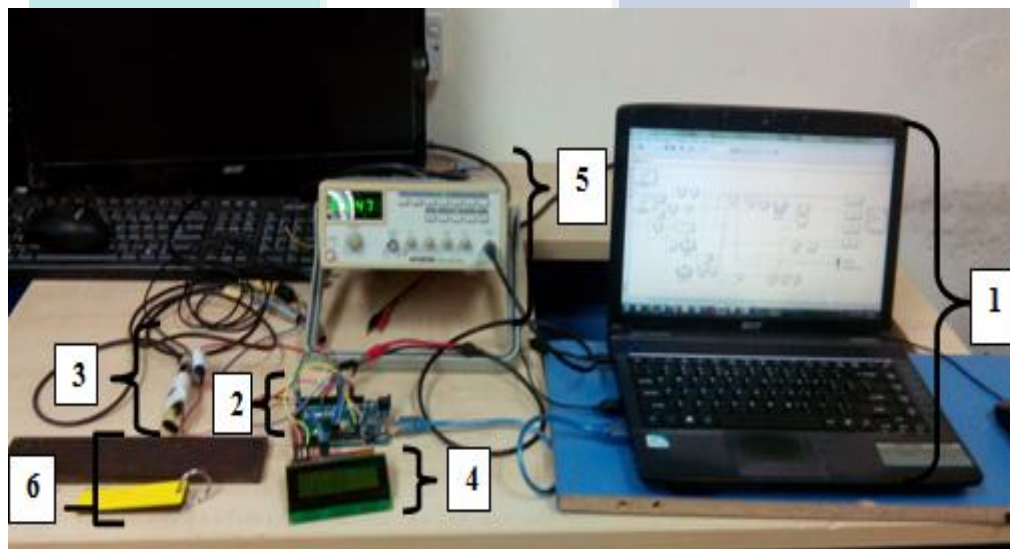


Figure 3.15 ECECT System Components Setup. 1) Computer, 2) ATMEGA 2560 microcontroller, 3) Absolute and Differential probe combining 4) LCD display, 5) Function generator, 6) Calibration block

3.8 Calibration Block Sample Testing

The eddy current tester is functioning to measure and finding the location of defect or discontinuities in metallic materials. Other than that it is functioning as assessing variations in magnetic and electrical material properties in order to determine material properties. From here the probe should be moved on the piping or surface plate for hole inspection. The measuring is including on non-ferrous metals conductivity and coating thickness. Figure 3.16 show the eddy current set unit.

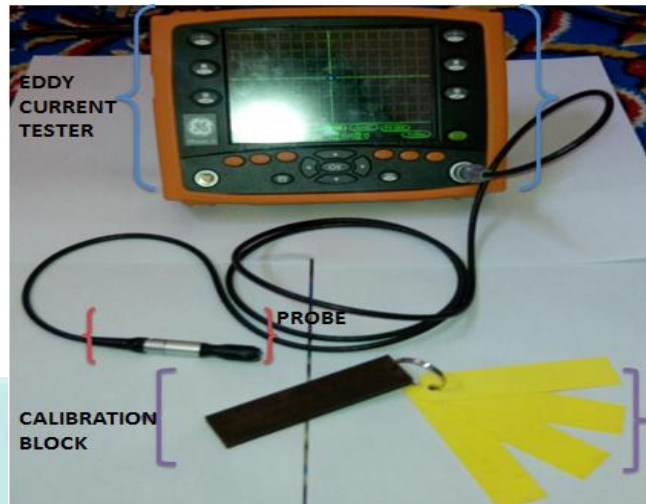


Figure 3.16 Eddy Current Set Unit.

Calibration block is functioning as the depth of defects reference. On calibration block, the depth of defect already identifies with a few different depths. As an example in Figure 3.17 show the calibration block with different depth there are 1mm, 2mm, and 3mm. The three different depths will give the difference of signal measuring.

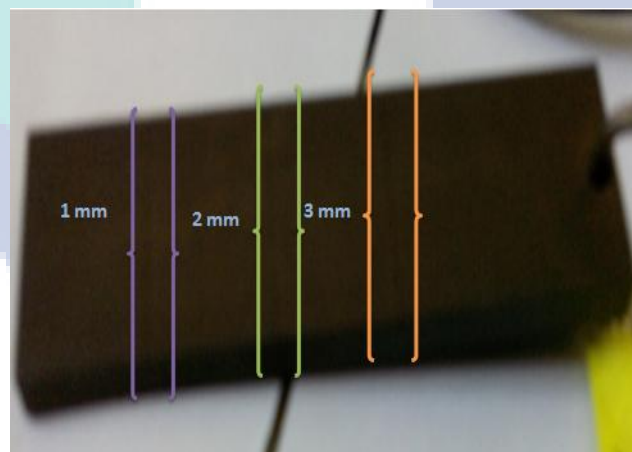


Figure 3.17 Calibration block with different depth

In coating thickness measurement a few guideline should be followed. The first step is in accuracy measuring of liftoff or coating thickness at the surface plate should be high until 0.01 mm probe measurement reading. From here the surface measured should be flat or of the same curvature as the calibration standards. Figure 3.18 show the sample of coating thickness shield.

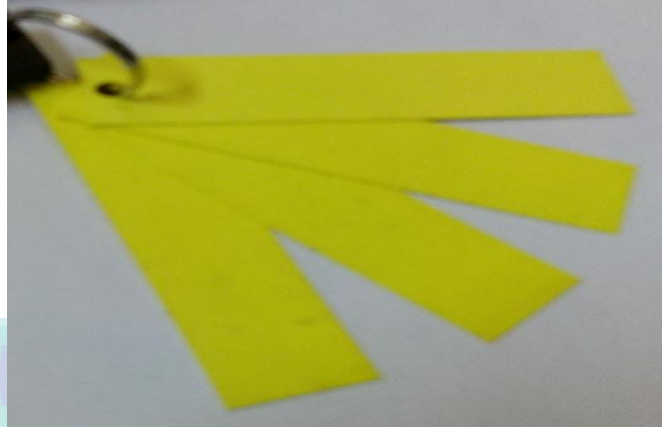


Figure 3.18 Coating thickness shield.

3.8.1 Sample Testing

The flat plate with the middle joint by welding is used as a sample for defect measuring. This plate calls it plate weld or A plate. Figure 3.19 show the A plate The dimension plate is 305mm x 150mm x 6mm.



Figure 3.19 A Plate Sample

CHAPTER 4

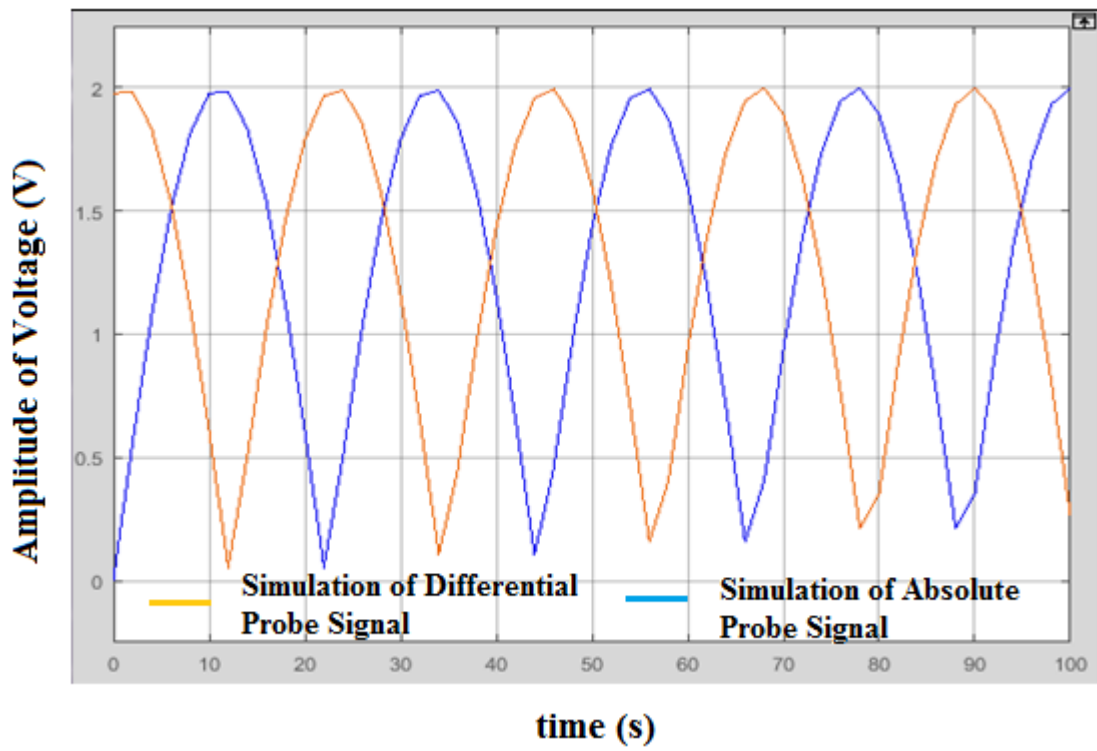
RESULTS AND DISCUSSION

4.1 Introduction

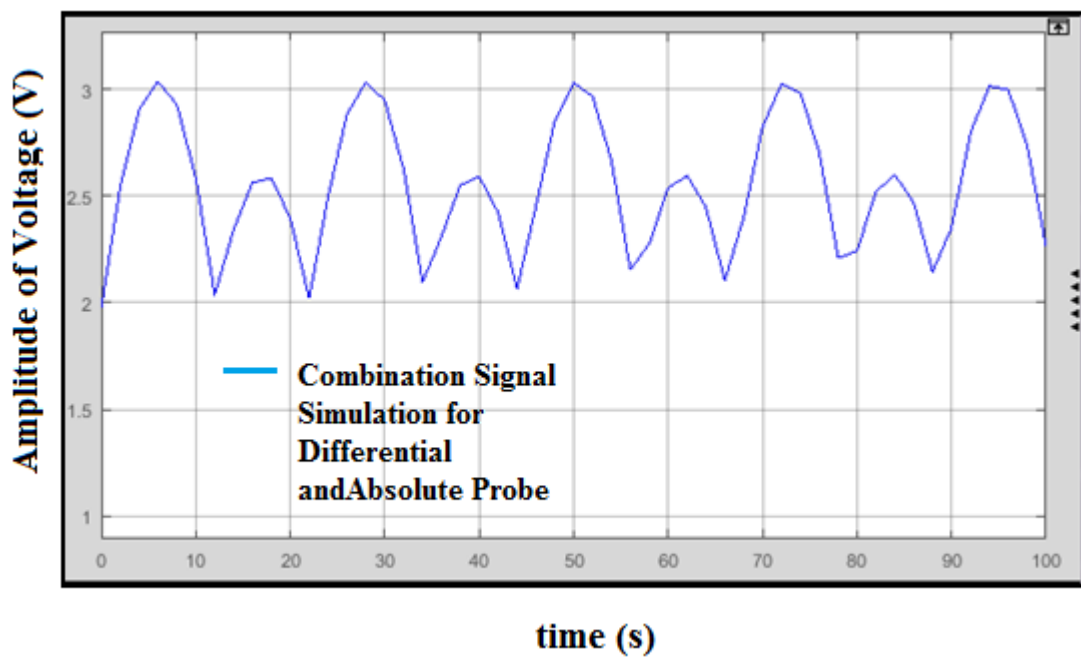
The simulation result of the Differential and Absolute Probe for fuzzy liftoff compensation scheme obtained by using Matlab/Simulink and hardware based real-time implementation will be presented in this chapter. This chapter also discussed the effectiveness of the proposed liftoff compensation method by comparing the error reduction for uncompensated and compensated measurement and discussing the percentage of error both in simulation and real implementation.

4.2 Simulation Result and Discussion

The simulation result of uncompensated (differential and absolute probe) output defect is as shown in Figure 4.1. According to Figure 4.1, it seems that the output voltage value of Differential and Absolute Probe is changing for the variation of depth of a defect and the thickness of the coating at the pipe surface. This condition is quite obvious for the defect and liftoff measuring in $\geq 1\text{mm}$ measuring defect. In simulation output setting based on the sine wave (AC) excitation signal with the amplitude 2, frequency 3 and phase angle zero for differential probe and for absolute probe the amplitude setting is 2, frequency 3 and phase angle 30 degree. This condition also demonstrated that the measurement accuracy of differential and the absolute probe is affected by variations of liftoff in range (1mm until 5mm) and need to be compensated. Based on that, ECECT has been proposed as in Chapter 3 was used in hardware and simulation models to validate the effectiveness of the proposed scheme. The simulation result for output voltage by using ECECT Compensation Scheme is shown in Figure 4.1



(a)



(b)

Figure 4.1 Simulation result for output voltage ECECT (a) Input Signal, (b) Output voltage value of Differential and Absolute Probe simulation

4.3 Experimental Conventional Probe Result

4.3.1 Differential Probe by Using ECECT

In ECECT system development the testing and verification are done by following the accuracy of defect measuring according to standard calibration block used. Figure 4.2 show the calibration block and the signal are produced by using the ECECT system. From here when the level of crack are increasing then the signal produced will increase. The time response for input port is set to 0.5 seconds.

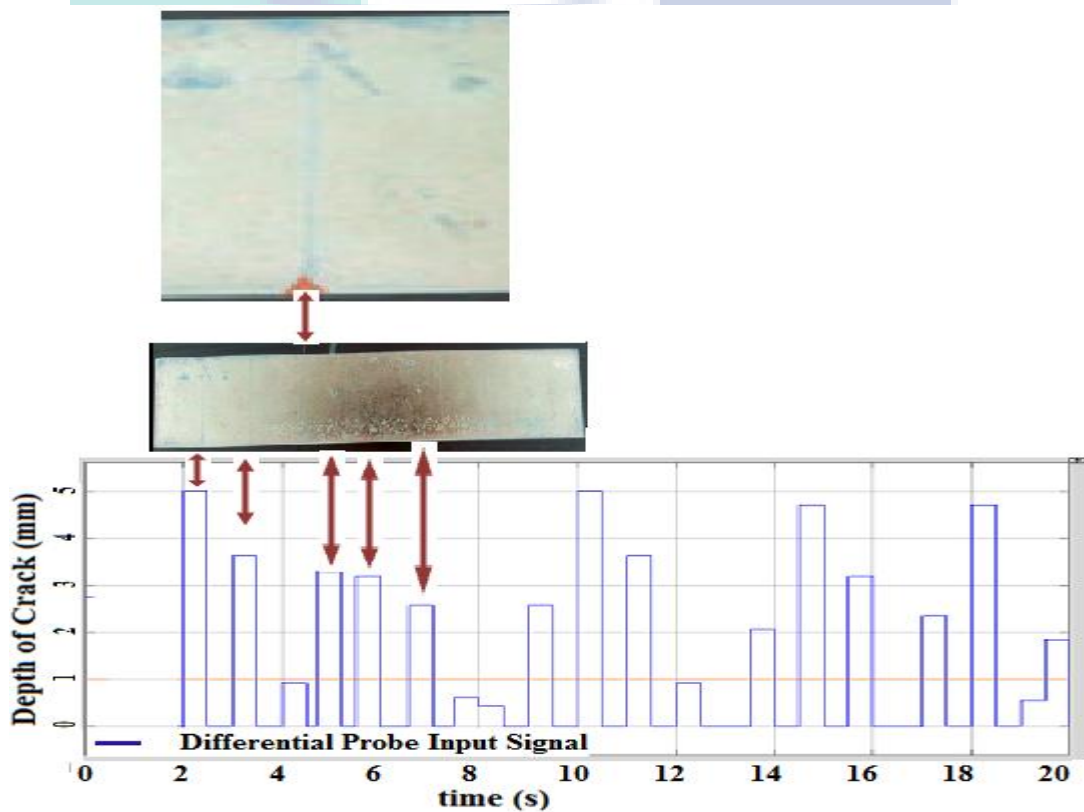


Figure 4.2 (a) Differential Probes Testing by Using Calibration Block, (b) The signal from the differential probe.

When the depth of defect at calibration block used is 5 mm, and then signally produces by following the conventional measurement will displaying 5mm. By following on this result below the accuracy of the conventional technique is lower than 70% because of the measurement on the lower depth especially for 2 mm is high (2mm actual crack = 3.2mm measuring).

4.3.2 Absolute Probe Signal Using ECECT

The absolute probe usually used for measuring the lift-off or coating thickness at the pipe surface and the plate. To ensure the reading of lift-off signal accurately the verification test is done by using the coating shield thickness. The coating shield thickness is started on 1mm until 4mm. The resulting measuring of lift-off or coating thickness is shown in Figure 4.3. The measuring tolerance on this system is +/-10% from actual thickness. From here when the thickness coating is high then the signal produces is increased. It will show on below when the coating shield thickness is 1mm then the conventional measurement by using absolute probe is 1.7mm and when the coating shield thickness achieves until 4mm then the measurement result show 4.1mm.

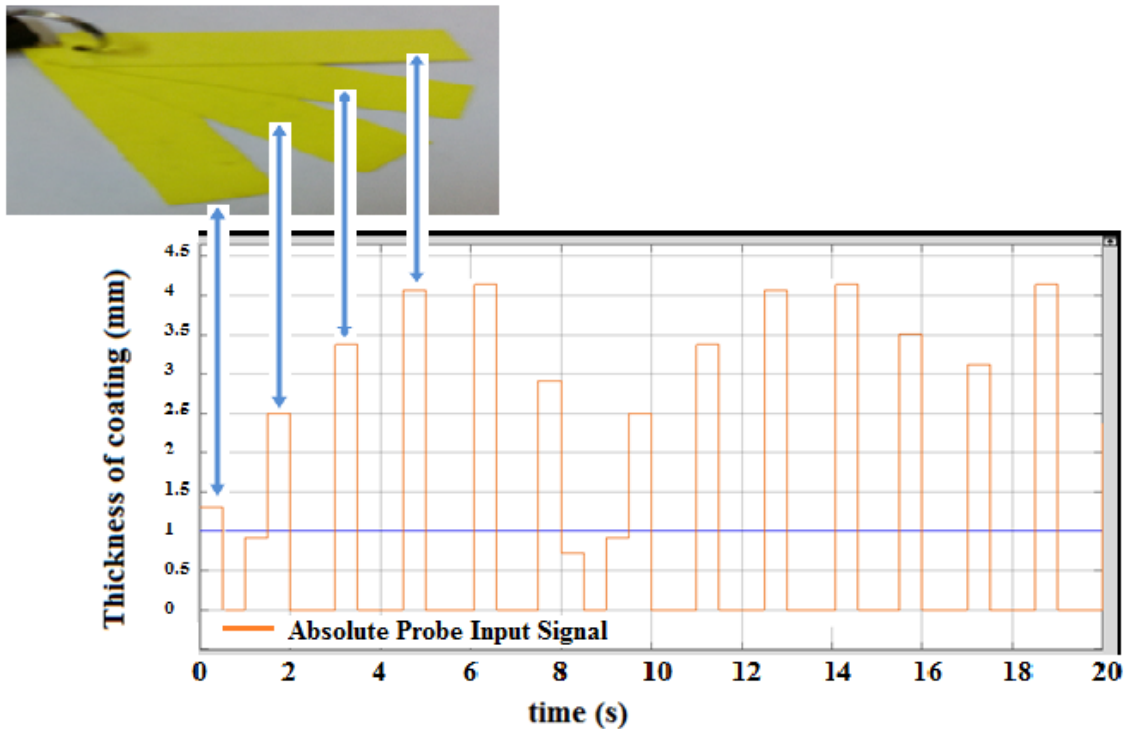


Figure 4.3 Absolute Probes Testing by Using Calibration Block

4.3.3 Differential / Absolute Probe without coating thickness

According to the Figure 4.4, the maximum signal is displayed is 5.3 mm which in less than 10% tolerance. From here the differential and absolute probe signal are integrated to get the right value of defect in the conventional technique. From the graph, the blue line is representing the differential probe signal and yellow is representing the absolute probe signal. In this testing, the coating shield not used but the lift-off still

occurs when the probe are lifted from sampling plate testing. This happened because of the resistance of plate and the surface plate not clearly flat. However, the minimum defect measuring is displaying is lower than 0.5 mm when no defect at the surface plate.

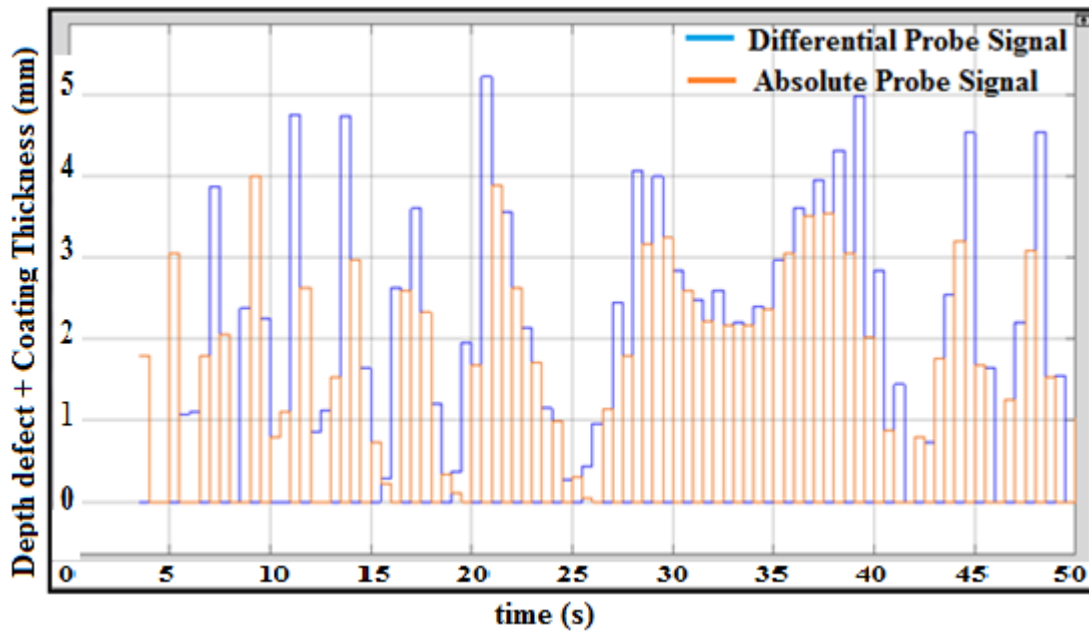


Figure 4.4 Integrated Probe Output without Coating Thickness

4.3.4 Differential / Absolute Probe with coating thickness

The pipe or plate with coating thickness will be the effect of the measuring of defect caused by the resistance of coating itself. The rate of frequency traveling at the plate or pipe will be reduced and the defect reading will be impaired. To reduce of coating resistance in measurement utilization of absolute probe are useful. Figure 4.5 show the graph of integrated between the absolute probe and differential probe in measuring the pipe or plate with coated by coating thickness. The maximum defect value is shown below is 4.7 mm. The blue signal is represented as coating thickness and orange for depth of defect. The thickness of the coating is not uniform at the whole surface are. From here the efficiency of the conventional technique is used can achieve until 94% and it effective with coating thickness plate by integrated of both probe.

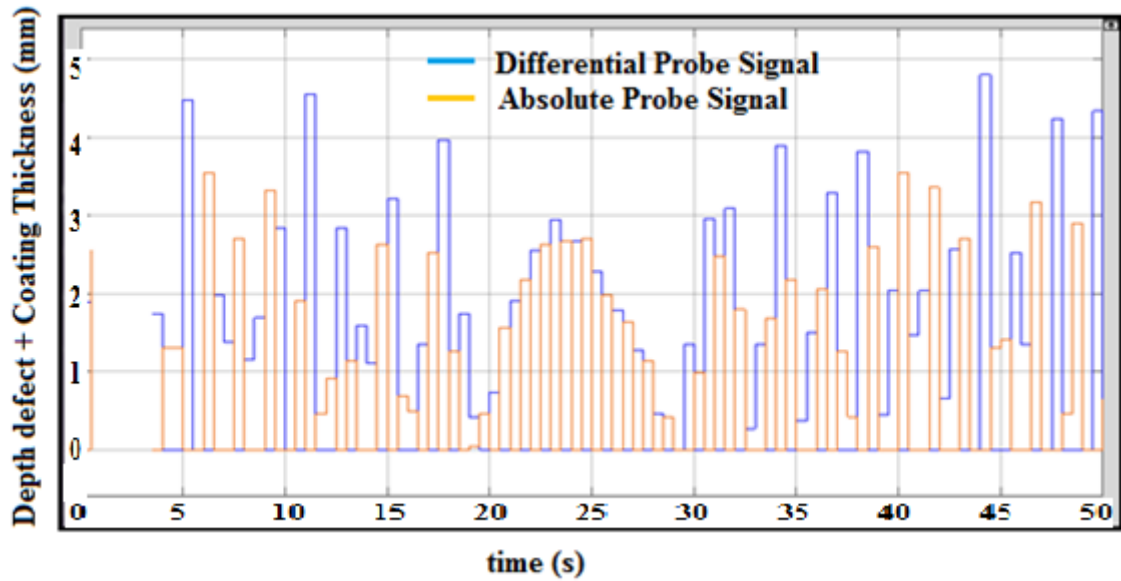


Figure 4.5 Integrated Probe Output with Coating Thickness

4.4 Comparison with Fuzzy Model

4.4.1 Differential Probe with Fuzzy Model

The triangle membership function is used for the Fuzzy Logic output in ECECT system. The amplitude of triangle will show the conditionings defects occur at pipe surface or plate. When the amplitude of triangle is high then the depth of defect is high otherwise the defect is low. The triangle output shape is selected because of higher pick defect at one point identify in measurements. In Figure 4.6 show the maximum amplitude of triangle is 5mm and minimum is 1mm. From here the blue line color for feedback or error compensation between the difference of actual defect and measuring defect. Other than that the yellow color represents the output of Mamdani fuzzy logic in ECECT system. The maximum depth of defect measuring can be achieved until 5mm by using a differential probe. The maximum limitation of depth defect is setting according to the limitation probe design.

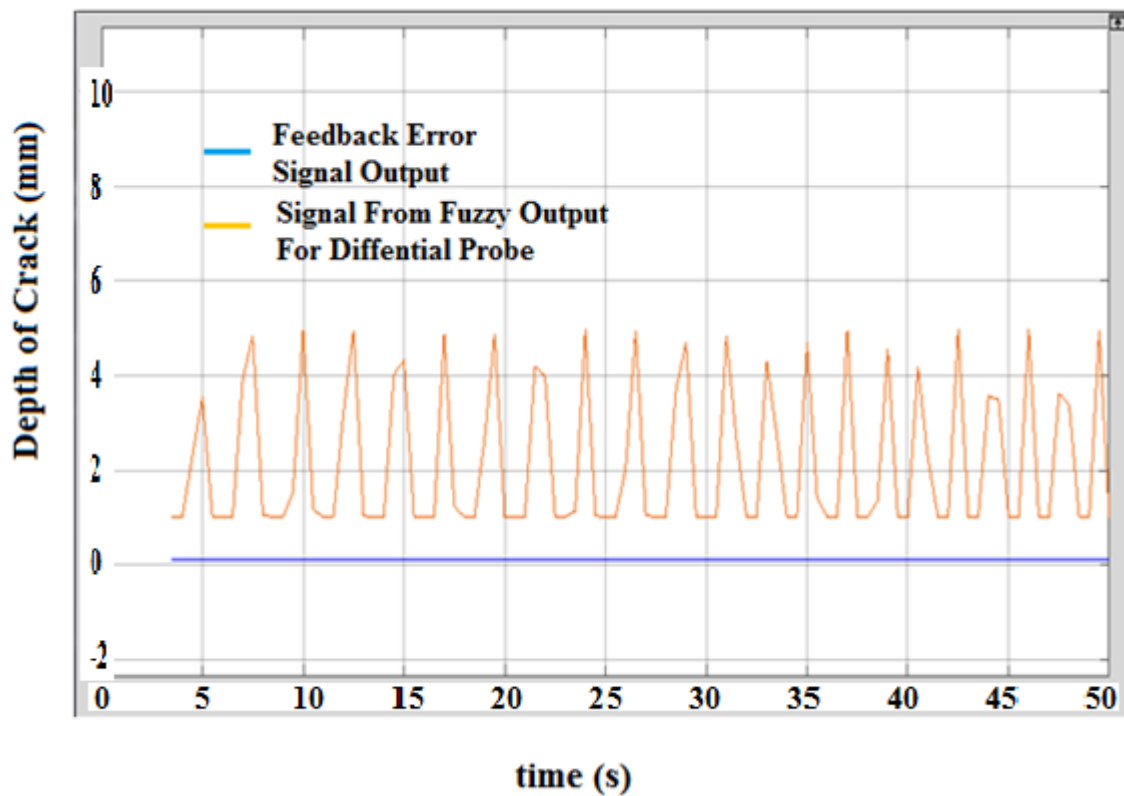


Figure 4.6 Output for Fuzzy Logic by using the Differential Probe

4.4.2 Absolute Probe with Fuzzy Model

By following the signal output from the Mamdani fuzzy logic system the maximum amplitude is produced is 3.5 mm by using the absolute probe and it still in the range of tolerances after considering of plate surface with not flatly clear. The measuring is testing at plated with coating thickness. From the graph below the minimum signals are displayed is 1.0 mm when the 1mm coating shield thickness is used. Figure 4.7 show the output of fuzzy logic by using an absolute probe.

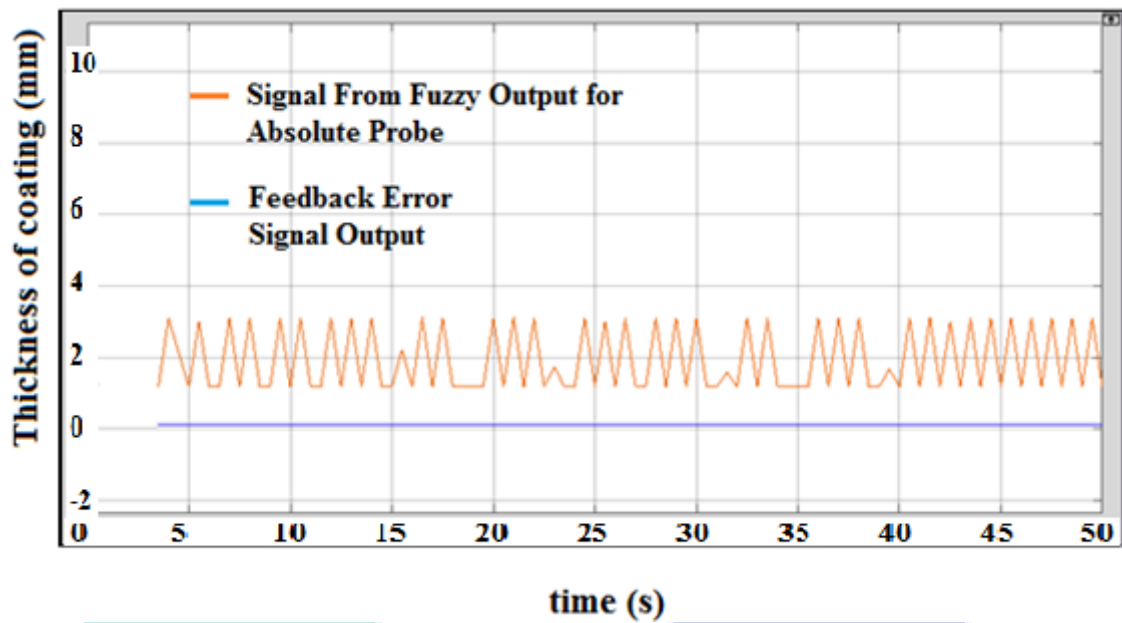


Figure 4.7 Output for Fuzzy Logic by using the Absolute Probe

4.4.3 Differential / Absolute Probe with Fuzzy Model

The intelligent for defect measuring was developed are purposely to measuring the error compensation. The liftoff compensation is frequently occurring in the measurement process. From here the right value of crack will be defined by considering the liftoff compensation. Figure 4.8 show the fuzzy logic for error compensation signal output without coating thickness/lift-off. The handling error is considering as liftoff in process inspection. The blue line graph is considering as conventional technique value and a yellow line graph is a fuzzy output after considering the liftoff for error compensation. The maximum signal for conventional value is 5.3 mm and the fuzzy value is 5 mm.

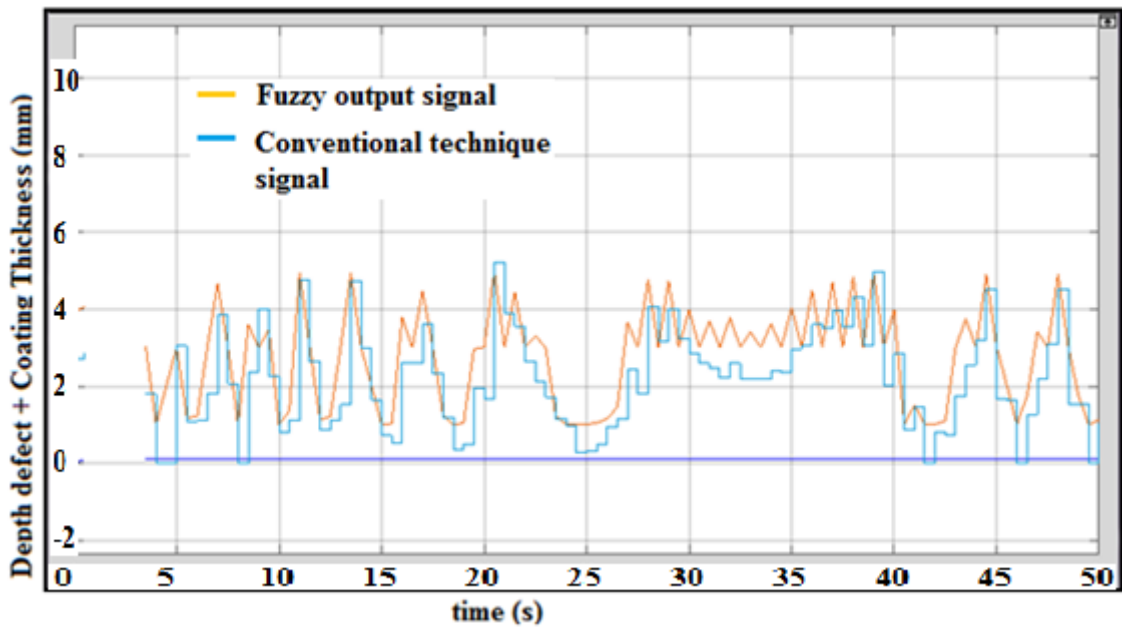


Figure 4.8 Fuzzy Logic for Error Compensation Signal Output without Coating Thickness

The different between coated plate and uncoated plate could look on according to the signal are produced when the inspection is run. The conventional technique signals are decreased slightly from the actual value of defect. The effect of coated plate is shown in Figure 4.9 as fuzzy logic for error compensation signal output with coating thickness (liftoff). The maximum defect value is measuring is low than 5mm according to the conventional result line and for fuzzy output, the value show approached 5mm. The average defect at the sample plate is in range 3.0 mm until 5.0 mm.

UMP

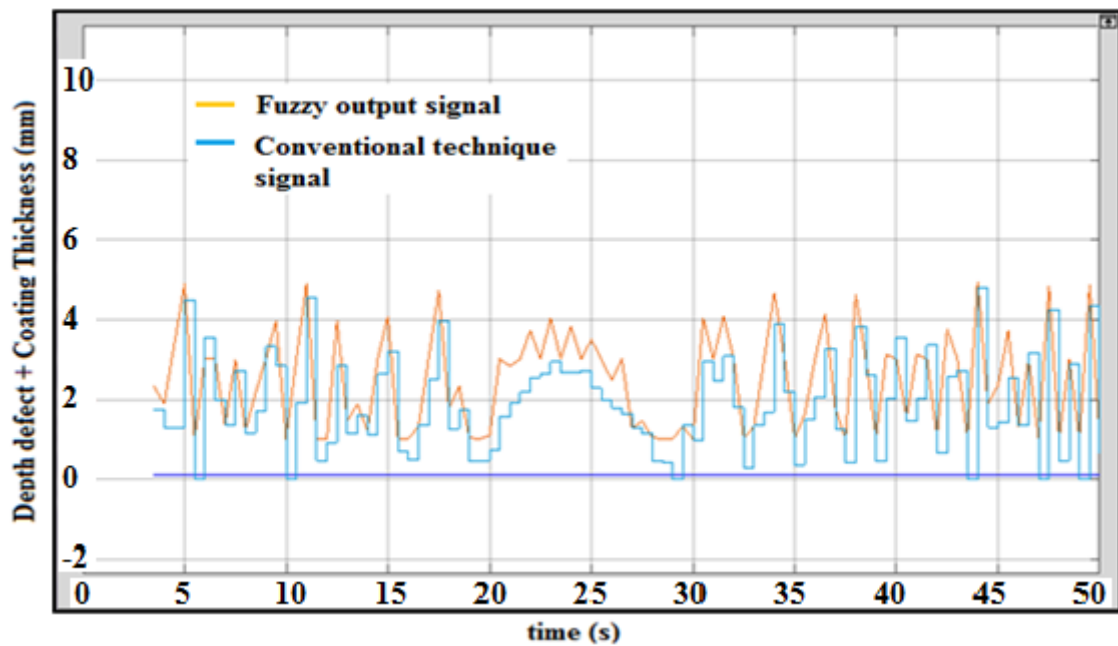


Figure 4.9 Fuzzy Logic for Error Compensation Signal Output with Coating Thickness

4.5 Comparisons with other technique

In this chapter, the simulation and hardware measuring for the ECECT lift-off Compensation Scheme have been done by using Matlab/Simulink to validate and compared the effectiveness of the proposed scheme. From here the comparison being made with (Yin & Xu, 2016) where the percentage of error as shown in Table 4.1. The error has obtained at zero mm liftoff of coating thickness was 0.23% and 0.1% for Yin&Xu 2016 and proposed methods respectively. The percentage of error can be calculated by following the equation 4.1.

$$\% \text{ of error} = \left(\frac{\text{Actual Depth Defect} - \text{Depth of Defect Measured}}{\text{Actual Depth Defect}} \right) \times 100\% \quad 4.1$$

Table 4.1 Comparison of liftoff with different coating thickness

Liftoff (mm)	Error from (Yin & Xu, 2016) (%)	Error from ECECT (%)
zero	0.23	0.10
1.5	0.64	0.50
3	1.36	0.40
4.5	1.63	0.87

4.6 ANOVA analysis

4.6.1 Data Testing ECECT

The two main parameters were affecting in defect measuring there are, frequency and liftoff. By following the ECECT system design two input parameter being considering in measurement. The result of a parameter affecting defect measuring is shown in Table 4.2. From the table below the comparing result was shown between actual defect data and measuring defect data by using ECECT system. From here the actual defect value is approximate with ECECT measuring value. By following the 3 kHz AC excitation signal supply, the minimum and maximum error are about 0 mm until 0.69mm or 0% until 13.8%. It different when used the 6kHz AC excitation signal supply the error measuring is a little bit high comparing 3kHz where the minimum and maximum error is 0.06mm until 0.94mm or 1.2% until 18.8%. But 9kHz AC excitation signal supply will give the high error which in 0.08mm until 1.07mm or 1.6% until 21.4%. From here it can conclude the 3kHz AC excitation signal supply will give the best result for defect measuring in ECECT system.

Table 4.2 Table of Parameter Effecting Defect Measuring

Frequency (kHz)	Depth Defect (mm)	Coating Thickness (mm)	Output Peak ECECT Technique (mm)
3	1	1	1.240
3	2	1	2.092
3	3	1	2.151
3	4	1	3.436
3	5	1	4.460
3	1	2	1.487
3	2	2	1.990
3	3	2	2.310
3	4	2	4.343
3	5	2	5.0166
3	1	3	1.562
3	2	3	2.590
3	3	3	3.240
3	4	3	3.50
3	5	3	5.024
3	1	4	2.642
3	2	4	3.801
3	3	4	3.960
3	4	4	4.030

Table 4.2 Continued

Frequency (kHz)	Depth Defect (mm)	Coating Thickness (mm)	Output Peak ECECT Technique (mm)
3	5	4	5.013
6	1	1	1.190
6	2	1	1.501
6	3	1	2.440
6	4	1	2.560
6	5	1	4.060
6	1	2	1.180
6	2	2	1.320
6	3	2	2.290
6	4	2	3.920
6	5	2	4.090
6	1	3	1.190
6	2	3	2.660
6	3	3	3.680
6	4	3	3.950
6	5	3	4.410
6	1	4	2.310
6	2	4	2.720
6	3	4	3.460
6	4	4	3.650
6	5	4	4.160
9	1	1	1.390
9	2	1	1.920
9	3	1	1.790
9	4	1	2.070
9	5	1	3.820
9	1	2	1.040
9	2	2	1.210
9	3	2	2.090
9	4	2	3.020
9	5	2	4.680
9	1	3	1.180
9	2	3	1.750
9	3	3	3.090
9	4	3	4.010
9	5	3	4.660
9	1	4	1.210
9	2	4	1.980
9	3	4	3.250
9	4	4	4.380
9	5	4	4.450

4.6.2 Comparing Output Peak Effecting by Coating Thickness in ECECT Technique

Figure 4.10 show the effect of depth defect at frequency and coating thickness. The red bar color representing the output peak and blue for coating thickness. According to the bar graph below the very accurate depth of defect shown when the defect plate is 5mm and the output produced is 5mm at coating thickness 2mm, 3mm, and 4mm (at testing sampling 10, 15 and 20). The efficiency of the result by using 3kHz frequency can achieve more than 91% according to testing are done. This is because of the frequency are used can traveling deeply in the surface plate defect and the feedback from the signal is more clearly and accurate.

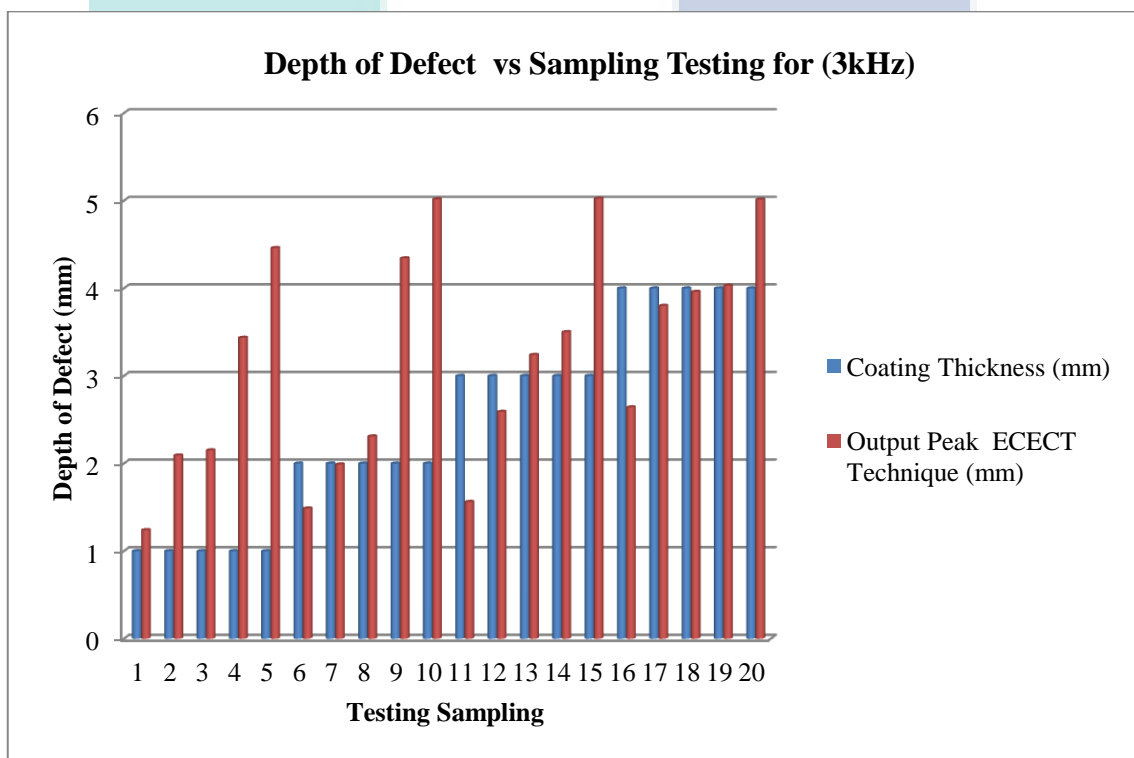


Figure 4.10 Depth Of Defect (mm) vs Testing Sampling By Using 3khz Frequency

On second testing the 6kHz frequency is used at the plate and from here the Figure 4.11 show the result below. From here the blue bar represents the coating thickness and red bar for output peak for ECECT. The accuracy of the result below is lower compared to result in Figure 4.10 by using 3kHz frequency. From here the accuracy result is more than 80%. By based on sampling testing at 5, 10, 15 and 20 the plate defect is choose in the inspection is the 5mm depth of defect. From here the

measuring displays only 4.1mm until 4.4mm. This is because of the frequency traveling in plate testing is lower and the feedback or effect of the signal are produced is lower too.

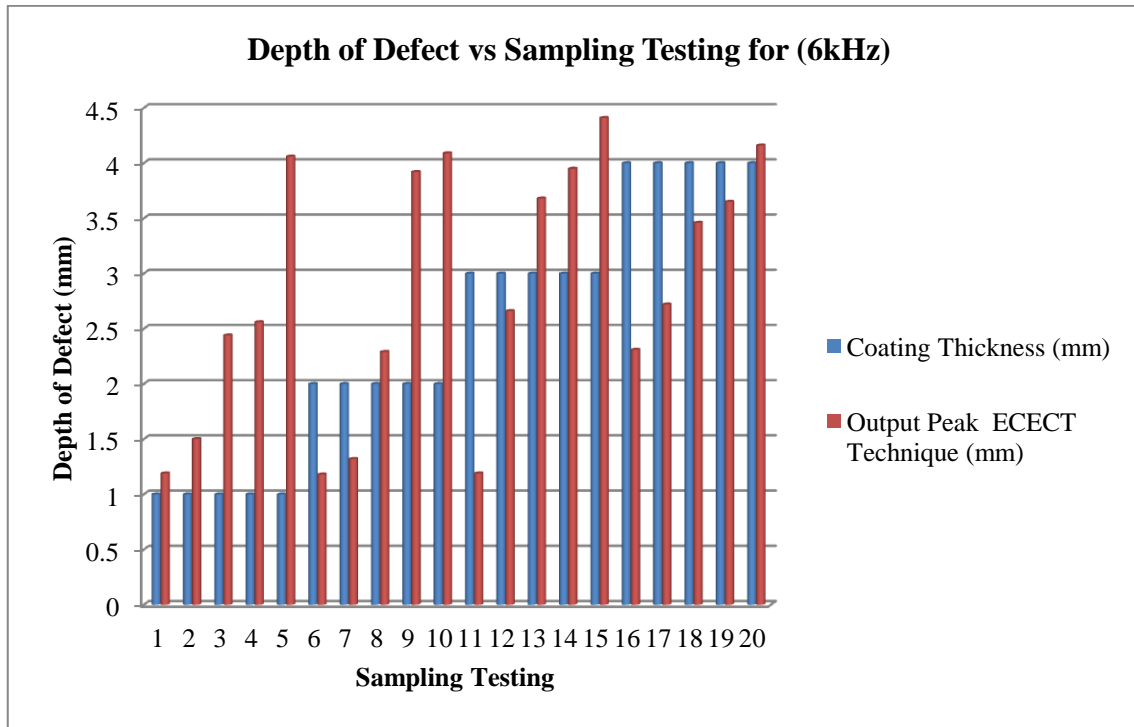


Figure 4.11 Depth Of Defect (mm) vs Testing Sampling By Using 6khz Frequency

Lastly, the testing is done by using 9kHz frequency. Figure 4.12 show the bar graph for depth of a defect and sampling testing. According to the result below show the accuracy of measuring is reduced to 74% and above. It can look on the sampling testing at 5,10, 15 and 20 where the lift-off respectively is 1mm, 2mm, 3mm, and 4mm. The depths of defect plate choose is 5mm. From here the output measuring are 4.1mm, 4.1mm, 4.4mm, and 4.2mm.

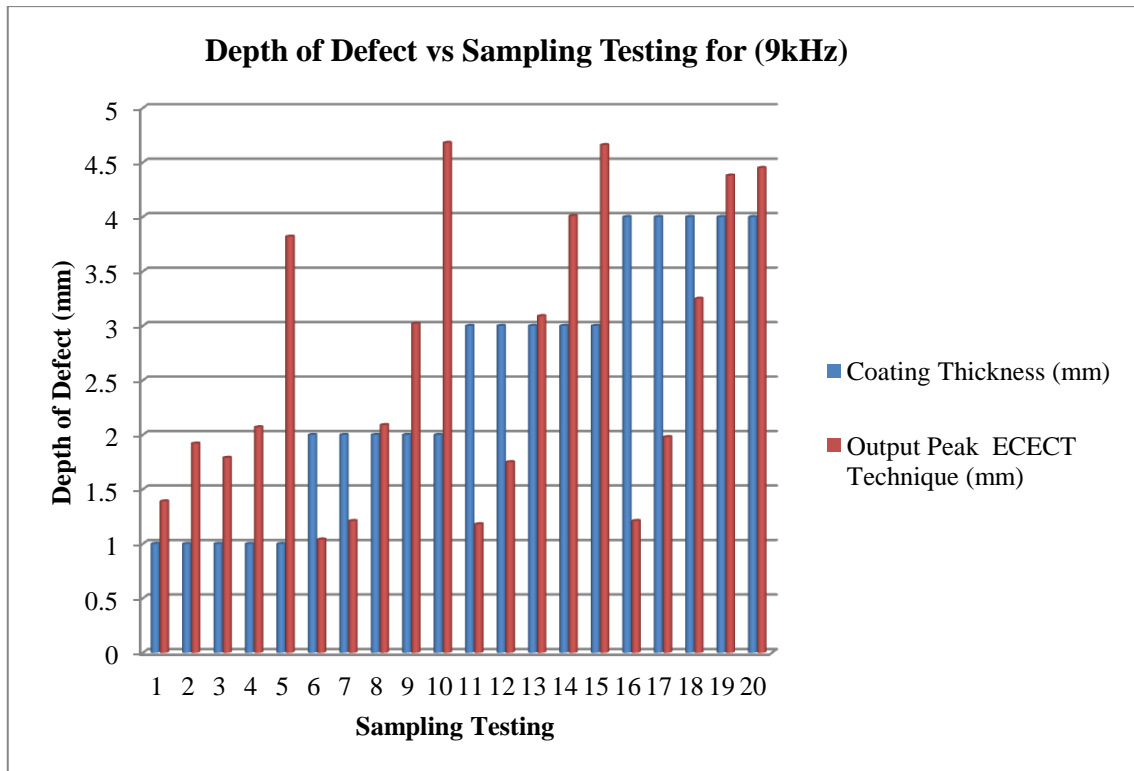


Figure 4.12 Depth Of Defect (mm) vs Testing Sampling By Using 9khz Frequency

Based on Figure 4.10 until 4.12 the 3Khz input excitation signal gives the best result in normal measuring. From here the 1mm coating thickness and 1mm output peak giving the same result in both three frequencies (3kHz, 6kHz, and 9kHz) which in normal measuring are 1.24mm, 1.19mm, and 1.39mm but the higher gap result could look on 4mm coating thickness in 2mm output peak for both three frequency there are 3.8mm, 2.27mm and 1.98mm.

4.6.3 Response Surface Linear Model

The scientific analysis was done meaning use of the design expert software. Five parameters have being analyzed including model, frequency, depth of defect, coating thickness and residuals. This analysis is based on the three frequency used for inspection including 3kHz, 6kHz, and 9kHz. Besides that, the coating thickness on the sample is measuring in range 1mm until 4mm. The depth of crack at the coating plate is 1mm until 5mm. Table 4.3 show the response output peak result was getting from design expert software simulation.

Table 4.3 Response Output Peak

Source	Sum of Squares	df	Mean Square	F Value	p-value Prob > F
Model	78.81	3	26.27	146.08	< 0.0001
<i>A-Frequency</i>	2.88	1	2.88	16.01	0.0002
<i>B-Depth Defect</i>	67.17	1	67.17	373.51	< 0.0001
<i>C-Coating Thickness</i>	8.76	1	8.76	48.72	< 0.0001
Residual	10.07	56	0.18		
Cor Total	88.88	59			

4.6.4 Final Equation in Terms of Actual Factors

$$\text{Output Peak} = (+0.32833 - 0.089417) * (\text{Frequency} + 0.74817) * (\text{Depth Defect} + 0.34180) * (\text{Coating Thickness}) \quad 4.2$$

Y₁: Output Peak

X₁: Frequency

X₂: Depth Defect

X₃: Coating Thickness

$$Y_1 = +0.32833 - 0.089417 * X_1 + 0.74817 * X_2 + 0.34180 * X_3 \quad 4.3$$

The higher output signals are obtained at the maximum predicted value which is 5.17 where the residuals value is negative 0.5. The maximum output peak is in range 4.03 until 5.17 for predicted line and 1.50 until -0.5 in residuals area. The lower output peak will show on at the point 0.16 of the predicted line and 2.00 for residuals area. The medium output peak mostly in range 1.75 until 4.03 in predicted area and -1.50 until 2.00 in the residual area. The range of residual point is set from -3.00 until 3.00 and maximum output peak is 5 and lower is 1.04. Figure 4.11 show the residuals value vs. predicted

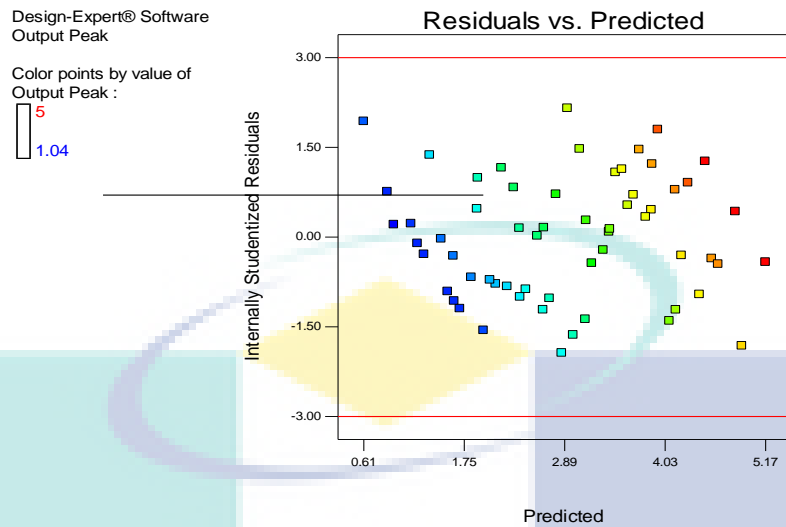


Figure 4.13 Residuals vs Predicted

By looking at the Figure 4.12 the frequency of probes will be effect at the signal traveling on the plate testing. The maximum output results are 5.2mm with the frequency used is 3kHz with the depth of defect point at 5.0mm. From here the lower value of output peak can be finding at frequency 9kHz at depth defect at point 1.00mm and the output is 1.2mm. The maximum output peak can be finding in range 4.00 to 5.00 for depth defect with frequency 3to 6kHz. Otherwise, the lower output peak can be defined at range 1.00 until 2.50 of depth defect with frequency 7.5 until 9kHz.

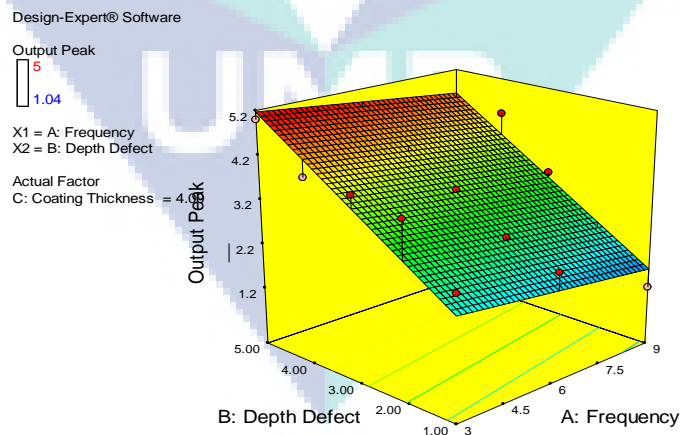


Figure 4.14 Relations between Depth of Defect, Frequency and Output Peak

The main factor is affected of output peak is coating thickness and depth of defect. By refer to Figure 4.13, the mostly defect on output peak are in range 3.15 until

4.5 and depth defect starts on 2.50 until 4.00 within the green color in the graph below. From this graph, the dangerous situation or maximum crack (red color) was measured in 4.00 to 5.00 in depth defect and the coating thickness is 2.50 until 4.00. The lower output measuring is in range 1.00 to 2.00 in depth defect with coating thickness in 1.00 until 2.50.

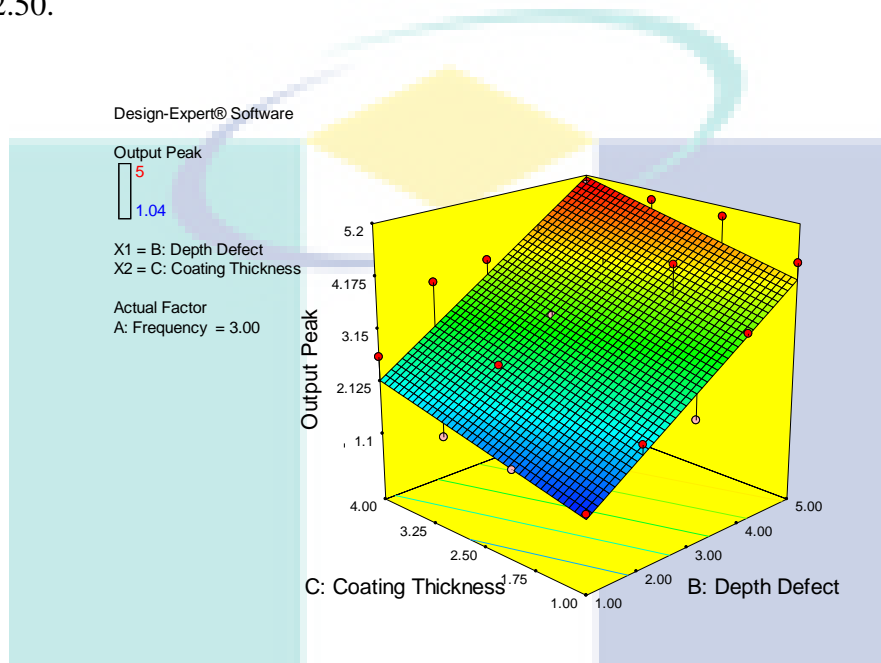


Figure 4.15 Relations between Depth of Defect, Coating Thickness, and Output Peak

Lastly the major of higher output peak was obtained according to the Figure 4.14. From here the range of coating thickness is 2.50 until 4.00 and the frequency at 3.00 to 6.00 kHz. The major red color is that area. The lower output peak being simulating at point 7.50 to 9.00 for frequency and 1.00 to 1.75 for coating thickness.

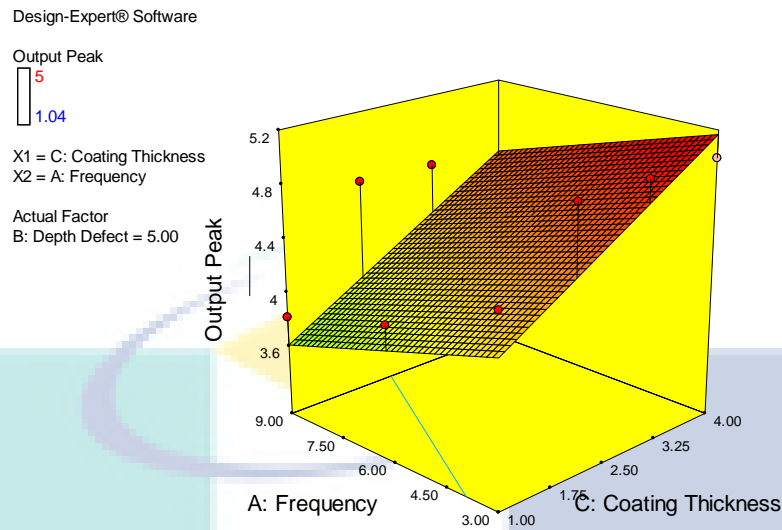
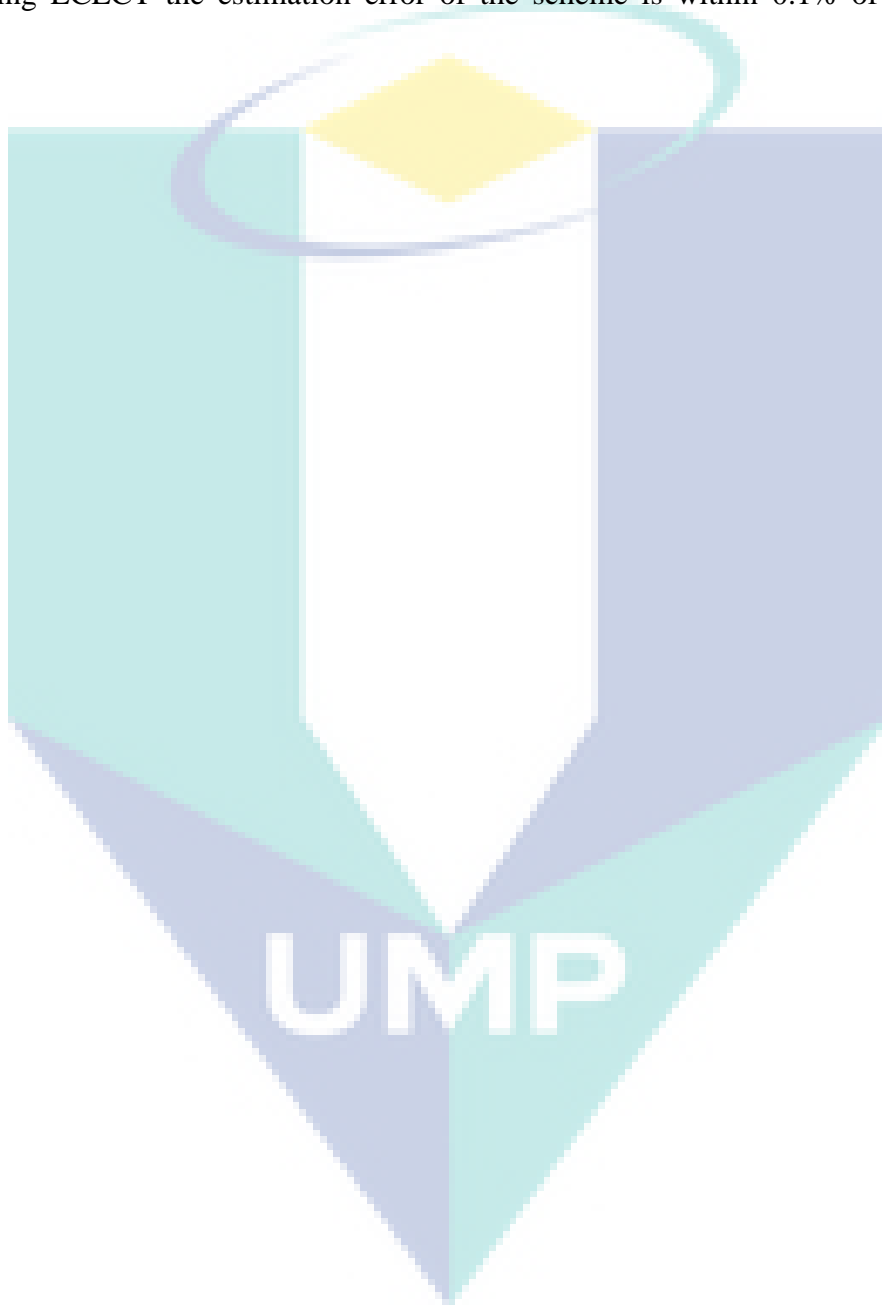


Figure 4.16 Relations between Frequency, Coating Thickness, and Output Peak

4.7 Summary

The ECECT was first simulated in Simulink for testing as well as tuning the fuzzy logic controller. The fuzzy logic toolbox that was available was used. Initially, the fuzzy logic controller was built using the fuzzy logic toolbox, taking advantage of its graphical interface. As in Chapter 3, the Mamdani-Type Fuzzy Inference system was used as the fuzzy inference engine. For the fuzzification, the triangle MF was used according to the conveniently used in Programming C Language in ATMEGA 2560 for real-time implementation. In the fuzzy logic toolbox, the rules developed also can be changed, and the effect observed easily. The defuzzification of the Mamdani output MF is either linear or constant fluctuated. Lift-off Compensation model with the offset defect due to its variation of ambient crack from the reference defect will be minimized. Based on the simulation result, the scheme has been utilized to compensate the effect of depth of crack on the sensor characteristics over defect range from 1mm to 5mm. It is shown that the excellent estimation error of the scheme is within 0.1% of its full-scale value comparing the (C. Huang and Wu, 2014) Signal EC highly effective in reducing the lift-off to 2.16% based on the thickness of the plate. The hardware for real-time implementation of the scheme using the ATMEGA 2560 also presented. The ECECT is embedded in an ATMEGA 2560 chip by using C Programming Language. The software description for algorithm codified using Programming C Language also been described in Appendix A. The main hardware used for real-time implementation and

publication will be detailed described including the specification, connection diagram and features in Appendix B. In order to evaluate and validate the proposed ECECT in hardware based real-time implementation, the experiment was conducted as the measurement setup in Chapter 3. The output liftoff is achieved desired value which is by using ECECT the estimation error of the scheme is within 0.1% of its full-scale value.



CHAPTER 5

CONCLUSIONS AND FUTURE WORK

5.1 Conclusions

In this research, an ECECT has been developed for solving the measurement error of depth of defect caused by liftoff variations. An extensive literature review has been conducted in the early stage to reveal the liftoff of error compensation method of differential and absolute probe. From there, it is found that the liftoff for error compensation method has been given high attention due to its ability to improve the measurement accuracy of the sensor. The temperature compensation method is divided into two types of compensation which is hardware compensation and software compensation. In this research, the both compensation method is used.

In order to demonstrate the measurement error of the sensor under study caused by the lift-off variations, an experimental setup for data collection have been conducted. The inaccuracy and error analysis have been done and a liftoff for error compensation method has been proposed by using Mamdani-Type Fuzzy Inference System. The input MF was chosen according to the simplicity of the coding algorithm for hardware based real-time implementation. Rules have been developed based on expert knowledge.

The input for the defuzzification process is a fuzzy set, which is the combined output of each rule, and the output is the weighted average of all rule outputs single number which is a non-fuzzy crisp value. Upon determining the effectiveness of the Fuzzy Liftoff Compensation Scheme, the simulation studies have been done using Matlab/Simulink Toolbox. In order to compare the performance and validity of ECECT testing, the other hardware for eddy current tester also been proposed using the Eddy Current Tester for liftoff Compensation Scheme. The simulation and hardware results

obtained were encouraging and they confirm the performance of ECECT compared with Eddy Current Tester Compensation Scheme in the following areas:

The ECECT gives optimal correction for the liftoff which the reducing percentage error is only within 0.1% of its full-scale value. The ECECT is appropriate for measurement liftoff in around 1mm until 5mm.

Based on the simulation result, the ECECT has implemented in hardware based real-time implementation by embedded in ATMEGA 2560 microcontroller with C Programming Language. The ATMEGA 2560 is used because it has larger RAM and higher speed of instruction execution compared to PIC. The ECECT performance validation has been done by using real-time measurement and the output value after compensation that displayed using LCD confirmed the performance of ECECT for differential and absolute probe in real time. According to the simulation and real-time implementation result, the ECECT have been successfully implemented.

5.2 Future Work

In future, differential and absolute probe for liftoff compensation's research could be extended into other intelligent technique areas in order to increase its applicability. For example, for the hardware for eddy current for error compensation, the Particle Swarm Optimization (PSO) method can be used to identify and optimized the parameters involve in absolute and differential probe. Instead of that, software compensation also could use another intelligent method such as Genetic Algorithm (GA) or Ant Colony.

REFERENCES

- Abbas, S., Ali, T., Gilani, U., Ahmed, S., Sajid, I., Amir, F., & Khan, T. M. (2015). PC based Eddy Current Non-Destructive Testing (NDT) System. *IEEE International Instrumentation and Measurement Technology Conference*, 165-170.
- Abbas, S., Gillani, U., Ahmed, S., Javed, S. B., & Sajid, I. (2014). Constant Current AC Source using Improved Howland Pump for Exciting Eddy Current Testing (ECT) Probe. *IEEE 17th International Multi-Topic Conference (INMIC)*,508-513.
- Abbas, S., Khan, T. M., Javaid, S. B., Ahmed, S. A., Haider, S. S., & Rajar, Z. (2016). Low Cost Embedded Hardware based Multi- Frequency Eddy Current Testing System Depth of Penetration. *International Conference on Intelligent Systems Engineering (ICISE), 2016*. 135–140.
- Aguiam, D. E., Rosado, L. S., Ramos, P. M., & Piedade, M. (2014). Portable instrument for eddy currents Non-Destructive Testing based on heterodyning techniques. *IEEE Instrumentation and Measurement Technology Conference*, 1368–1372.
- Ahmed, S. S., Chandra Rao, B. P., & Jayakumar, T. (2013). Radial basis functions for multidimensional learning with an application to nondestructive sizing of defects. *IEEE Symposium on Foundations of Computational Intelligence, IEEE Symposium Series on Computational Intelligence*, 38–43.
- Barbato, L., Poulakis, N., Tamburrino, A., Theodoulidis, T., & Ventre, S. (2015). Solution and Extension of a New Benchmark Problem for Eddy-Current Nondestructive Testing. *IEEE Transactions on Magnetics*, 51(7):1–7.
- Båvall, L. (2007). Determination of thickness of silver coatings on brass by measuring the impedance of a thin elliptic coil. *IEEE Transactions on Instrumentation and Measurement*, 56(3): 790–799.
- Bernieri, a., Betta, G., & Ferrigno, L. (2001). Improving non-destructive testing probe performance by digital processing techniques. *IEEE Instrumentation and Measurement Technology Conference. Rediscovering Measurement in the Age of Informatics*, 2:1291–1295.
- Bernieri, A., Betta, G., Ferrigno, L., Laracca, M., & Mastrostefano, S. (2014). Multifrequency excitation and support vector machine regressor for ECT defect characterization. *IEEE Transactions on Instrumentation and Measurement*, 63(5):1272–1280.
- Bernieri, A., Betta, G., & Ieee, M. (2000). Metrological Characterization of an Eddy-Current-Based System, *The 17th IEEE Instrumentation and Measurement Technology Conference*, 3:1608-1611.

- Betta, G., Ferrigno, L., & Laracca, M. (2012). GMR-based ECT instrument for detection and characterization of crack on a planar specimen: A hand-held solution. *IEEE Transactions on Instrumentation and Measurement*, 61(2): 505–512.
- Betta, G., Ferrigno, L., Laracca, M., Burrascano, P., & Ricci, M. (2014). Optimized complex signals for Eddy Current Testing. *IEEE Instrumentation and Measurement Technology Conference*, 1120–1125.
- Betta, G., Ferrigno, L., Laracca, M., Ramos, H. G., Ricci, M., Ribeiro, A. L., & Silipigni, G. (2015). Fast 2D crack profile reconstruction by image processing for Eddy-Current Testing. *2nd IEEE International Workshop on Metrology for Aerospace, MetroAeroSpace*, 341–345.
- Bowler, N. C. H. and J. R. (1992). Eddy-Current Imaging of Buried Cracks by Inverting Field Data. *IEEE transactions on magnetics*, 28(2), 1336-1339.
- Brauer, H., Ziolkowski, M., & Toepfer, H. (2014). Defect detection in conducting materials using eddy current testing techniques. *Serbian Journal of Electrical Engineering*, 11(4): 535–549.
- Buck, J. A., Underhill, P. R., Morelli, J. E., & Krause, T. W. (2016). Simultaneous Multiparameter Measurement in Pulsed Eddy Current Steam Generator Data Using Artificial Neural Networks. *IEEE Transactions on Instrumentation and Measurement*, 65(3): 672–679.
- Cap C., T. R. and M. L., & 1. (2015). Efficient Model Choice and parameter estimation by using Using Nested Sampling applied In Eddy-Current Testing. *IEEE ICASSP*, 4165–4169.
- Caetano, D. M., Piedade, M., Graca, J., Fernandes, J., Rosado, L., & Costa, T. (2015). Live demonstration: A CMOS ASIC for precise reading of a Magnetoresistive sensor array for NDT. *IEEE International Symposium on Circuits and Systems*, 1906.
- Cai, X. (2001). Iterative blind deconvolution and its application in characterization of eddy current NDE signals.
- Cao, M., Zhang, W., Zeng, W., & Chen, C. (2013). Research on the device of differential excitation type eddy current testing for metal defect detection. *FENDT 2013 - Proceedings of 2013 Far East Forum on Nondestructive Evaluation/Testing: New Technology and Application*, 155–158.
- Center, N. R. (2016). A Web Resource. Retrieved from www.ndt-ed.org/EducationResources/CommunityCollege/EddyCurrents/cc_ec_index.htm,2016
- Chady, T., Kowalczyk, J., & Psuj, G. (2011). Eddy current transducer for evaluation of inhomogeneity in titanium billets. *IEEE Transactions on Magnetics*, 47(10): 3967–3970.

- Chady, T., Psuj, G., Kowalczyk, J., & Spsychalski, I. (2013). Electromagnetic system for nondestructive evaluation of train hollow axles. *FENDT - Far East Forum on Nondestructive Evaluation/Testing: New Technology and Application*, 29–34.
- Chelabi, M., Hacib, T., & Bihan, Y. Le. (2013). Identification of default from Eddy Current Testing Signals using multi output support vector Machine. *International Conference on Systems and Control (ICSC)*, 183-186.
- Chudacik, V., Janousek, L., & Smetana, M. (2015). Evaluation of Spatial Components on Eddy Current Testing Response Signals of Selected Defect Parameters. *Acta Tehnica Corviniensis - Bulletin of Engineering*, VIII(1): 35–38.
- Coil, H. T. S., Sasayama, T., Ishida, T., Matsuo, M., & Enpuku, K. (2016). Thickness Measurement of an Iron Plate Using Low-Frequency Eddy Current Testing. *IEEE Transactions on Applied Superconductivity*, 26(5):1-5.
- D'Angelo, G., & Rampone, S. (2015). Shape-based defect classification for non destructive testing. *2nd IEEE International Workshop on Metrology for Aerospace, MetroAeroSpace*, 406–410.
- Dashtbani Moghari, M., Safizadeh, M. S., Habibalahi, A., Samadian, K., & Mousavi, S. S. (2015). Improving pulse eddy current and ultrasonic testing stress measurement accuracy using neural network data fusion. *IET Science, Measurement & Technology*, 9: 514–521.
- Douvenot, R., Lambert, M., & Lesselier, D. (2011). Adaptive metamodells for crack characterization in eddy-current testing. *IEEE Transactions on Magnetics*, 47(4), 746–755.
- Duca, A., Rebican, M., Duca, L., Janousek, L., & Altinoz, T. (2015). Advanced PSO algorithms and local search strategies for NDT-ECT inverse problems. *2014 International Symposium on Fundamentals of Electrical Engineering*, 3–7.
- Dziczkowski, L. (2013). Elimination of coil liftoff from eddy current measurements of conductivity. *IEEE Transactions on Instrumentation and Measurement*, 62(12):3301–3307.
- Enokizono, M., Tsuchida, Y., & Chady, T. (1998). Crack Size and Shape Determine by Moving Magnetic Field Type Sensor, *IEEE transactions on Magnetics*, 34(4), 1252-1254.
- Forster, F. (1952). Theoretical and Experimental Bases of Non-Destructive Material Testing-Using Eddy Current Method. *International Journal of Materials Research*, 43(5):163 – 171.
- François Caire1, Denis Prémel1, and G. G. (2015). Fast computation of the fields diffracted by a multi-layered conductor with non-parallel rough interfaces. Application to eddy-current non-destructive testing simulation. *IEEE Transactions on Magnetics*, 51(3):1-4.

- Goldshstein, A. E., Bulgakov, V. F., Kroning, H. M. V. A., Kalganov, S. A., & Belyankov, V. Y. (2012). A method of eddy-current testing of bars and tubes based on the eddy currents with different frequencies of circular and longitudinal directions excitation. *7th International Forum on Strategic Technology*, 1–4.
- Gulbahce, M. O., Nak, H., & Kocabas, D. A. (2013). A new approach for temperature rising test of an induction motor loaded by a current controlled eddy current brake. *3rd International Conference on Electric Power and Energy Conversion Systems*, 8–13.
- Guohou, L., Pingjie, H., Peihua, C., Dibo, H., Guangxin, Z., & Zekui, Z. (2011). Application of multi-sensor data fusion in defects evaluation based on Dempster-Shafer theory. *IEEE Instrumentation and Measurement Technology Conference*, 53–57.
- Gyimóthy, S. (2015). Optimal sampling for fast eddy current testing inversion by utilising sensitivity data. *IET Science, Measurement & Technology*, 9(3): 235–240.
- He, Y., Luo, F., Pan, M., Hu, X., Gao, J., & Liu, B. (2010). Defect classification based on rectangular pulsed eddy current sensor in different directions. *Sensors and Actuators, A: Physical*, 157(1): 26–31.
- He, Y., Member, S., Tian, G., Member, S., Zhang, H., Member, S., Jackson, P. (2012). Steel Corrosion Characterization Using Pulsed Eddy Current Systems, *IEEE Sensors Journal*, 12(6), 2113-2120.
- He, Y., Pan, M., Chen, D., & Luo, F. (2013). PEC defect automated classification in aircraft multi-ply structures with interlayer gaps and lift-offs. *NDT and E International*, 53(2013):39–46.
- He, Y., Pan, M., Luo, F., Chen, D., & Hu, X. (2013). Support vector machine and optimised feature extraction in integrated eddy current instrument. *Measurement: Journal of the International Measurement Confederation*, 46(1): 764–774.
- He, Y., Tian, G., Pan, M., & Chen, D. (n.d.). Composites : Part B Non-destructive testing of low-energy impact in CFRP laminates and interior defects in honeycomb sandwich using scanning pulsed eddy current. *Composites Part B*, 59(2014): 196–203.
- Homberg, C., Henneron, T., Clénet, S., Arts, P., & Xiv, B. L. (2011). Stochastic model in eddy current non destructive testing Keywords Numerical model for eddy current non destructive testing. *14th European Conference on Power Electronics and Applications*, 1-7.
- Horan, P., Underhil, R., & Krause, T. W. (2014). Pulsed eddy current detection of cracks in F/A-18 inner wing spar at large lift-off using modified principal component analysis. *International Journal of Applied Electromagnetics and Mechanics*, 45(1-4): 287–292.

- Hsu, W., Miao, H., & Liu, J. (2011). A Study on the Electric Property of Buckypaper by Eddy Current Testing, In *Nanotechnology Materials and Devices Conference (NMDC)*, 137-140.
- Huang, C., & Wu, X. (2014). Probe lift-off compensation method for pulsed eddy current thickness measurement. *Proceedings of 3rd Asia-Pacific Conference on Antennas and Propagation*, 937–939.
- Huang, L., He, R., & Zeng, Z. (2012). An extended iterative finite element model for simulating eddy current testing of aircraft skin structure. *IEEE Transactions on Magnetics*, 48(7): 2161–2165.
- Ida, N. (2014). Eddy current nondestructive evaluation - The challenge of accurate modeling. *2014 International Conference on Development and Application Systems*, 97–102.
- Janousek, L., & Smetana, M. (2014). Advanced Procedure for Non-destructive Diagnosis of Real Cracks from Eddy Current Testing Signals. In *ELEKTRO*, 567–570.
- Junjun, X., Naiguang, L., Udpa, L., & Udpa, S. S. (2011). Nondestructive Inspection Using Rotating Magnetic Field Eddy-Current Probe. *Magnetics, IEEE Transactions on*, 47(5), 1070–1073.
- Koliskina, V., & Kolyshkin, A. (2015, June). Mathematical model for eddy current testing of metal plates with two cylindrical flaws. In *Environment and Electrical Engineering (EEEIC)*, 2015 IEEE 15th International Conference on (pp. 374-377).
- Krause, H. J., Panaitov, G. I., & Zhang, Y. (2003). Conductivity tomography for non-destructive evaluation using pulsed eddy current with HTS SQUID magnetometer. *IEEE Transactions on Applied Superconductivity*, 13(21), 215–218.
- Lambert, M., Nougier, F., & Zorgati, R. (2011). Eddy-current modeling of a continuous conductivity profile resulting from a diffusion process. *IEEE Transactions on Magnetics*, 47(8): 2093–2099.
- Lee, K. H., Baek, M. K., & Park, I. H. (2012). Estimation of deep defect in ferromagnetic material by low frequency eddy current method. *IEEE Transactions on Magnetics*, 48(11), 3965–3968.
- Li, M., & Lowther, D. A. (2011). Topological Sensitivity Analysis for Steady State Eddy Current Problems With an Application to Nondestructive Testing, *IEEE Transactions on Magnetics*, 47(5): 1294–1297.
- Li, Y., & Chen, Z. (2012). Pulsed Eddy Current Testing Based on Gradient Magnetic Field Measurement. *2012 Sixth International Conference on Electromagnetic Field Problems and Applications*, 1-4.

- Liu, X., Wu, Y., Chen, Z., & Zhao, H. (2014). Eddy Current Test Research for Eccentricity of International Thermonuclear Experimental Reactor (ITER) in-vessel coils (IVCs) conductor. In *IEEE Far East Forum on Nondestructive Evaluation/Testing (FENDT)*, pp. 186-189.
- Liu, Y., Cheng, N., & Liu, W. (2015). Feeding Devices of Eddy Current Testing on Titanium Alloy Tube . In *IEEE International Conference on Information and Automation*, 89–93.
- McKeehan, L. W. (1930). Electrical resistance of nickel and permalloy wires as affected by longitudinal magnetization and tension. *Physical Review*, 36(5), 948.
- Mengelkamp, J., Lattner, D., Haueisen, J., Carlstedt, M., Weise, K., Brauer, H., & Eichardt, R. (2016). Lorentz Force Evaluation With Differential Evolution. *IEEE Transactions on Magnetics*, 52(5), 1-10.
- Miorelli, R., Reboud, C., Lesselier, D., & Theodoulidis, T. (2012). Eddy current modeling of narrow cracks in planar-layered metal structures. *IEEE Transactions on Magnetics*, 48(10): 2551–2559.
- Miorelli, R., Reboud, C., Theodoulidis, T., Poulakis, N., & Lesselier, D. (2013). Efficient modeling of ECT signals for realistic cracks in layered half-space. *IEEE Transactions on Magnetics*, 49(6): 2886–2892.
- Moore P O, M. P. (eds) and S. R. K. (technical ed). (2009). Nondestructive Testing Handbook: Visual Testing. In P. O. Moore (Ed.), *Nondestructive Testing Handbook*, 9:157–178.
- Morozov, M., Yun, G., & Withers, P. J. (2010). The pulsed eddy current response to applied loading of various aluminium alloys. *NDT and E International*, 43(6): 493–500.
- Nelligan, T., & Calderwood, C. (2014). Introduction to eddy current testing. *Olympus IMS*.
- Pasadas, Ramos, H. G., & Alegria, F. (2011). Handheld instrument to detect defects in conductive plates with a planar probe. *IEEE Instrumentation and Measurement Technology Conference*, 144–149.
- Pasadas, D., Ribeiro, A. L., Ramos, H., & Rocha, T. (2015). ECT image analysis applying an inverse problem algorithm with Tikhonov/TV Regularization. *IEEE Instrumentation and Measurement Technology Conference*, 940–944.
- Pasadas, D., Rocha, T., Ramos, H., & Ribeiro, A. L. (2011). Portable eddy current NDT instrument using two different implementations. *International Conference on Computer as a Tool - Joint with Confitele 2011*.

- Peng, X., & Jun, H. (2013). A new eddy current sensor composed of three circumferential gradient winding coils. *Proceedings of the International Conference on Sensing Technology, ICST*, 912–915.
- Pipis, K., Skarlatos, A., Theodoulidis, T., & Lesselier, D. (2016). ECT-Signal Calculation of Cracks Near Fastener Holes Using an Integral Equation Formalism With Dedicated Green's Kernel. *IEEE Transactions on Magnetics*, 52(4):1-8.
- Postolache, O., Ribeiro, A. L., & Ramos, H. (2011). A novel uniform eddy current probe with GMR for non destructive testing applications. *International Conference on Computer as a Tool - Joint with Conftel*.
- Ramos, H. G., Rocha, T., Ribeiro, A. L., & Pasadas, D. (2014). GMR versus differential coils in velocity induced eddy current testing. *IEEE Instrumentation and Measurement Technology Conference*, (1): 915–918.
- Ribeiro, A. L., Ramos, H. G., Pasadas, D. J., & Rocha, T. J. (2012). Current around a crack in an aluminum plate under nondestructive evaluation inspection. *IEEE I2MTC - International Instrumentation and Measurement Technology Conference*, 1635–1639.
- Rifai, D., Abdalla, A. N., Ali, K., & Razali, R. (2016). Giant magnetoresistance sensors: A review on structures and non-destructive eddy current testing applications. *Sensors*, 16(3):298.
- Rifai, D., Abdalla, A. N., Khamsah, N., & Aizat, M. (2016). Subsurface Defects Evaluation using Eddy Current Testing. *Indian Journal of Science and Technology*, 9(9):17485.
- Rocha, T. J., Ribeiro, A. L., & Ramos, H. M. G. (2011). Low-cost stand-alone system for eddy current testing of metallic non-ferromagnetic plates. *IEEE Instrumentation and Measurement Technology Conference*, 225–230.
- Rocha, T., Pasadas, D., Ribeiro, A. L., & Ramos, H. M. (2012). Characterization of defects on rivets using a eddy current technique with GMRs. *IEEE I2MTC - International Instrumentation and Measurement Technology Conference, Proceedings*, 1640–1644.
- Rocha, T., Ramos, H., Ribeiro, A. L., & Pasadas, D. (2015). Sub-surface defect detection with motion induced eddy currents in aluminium. *IEEE Instrumentation and Measurement Technology Conference*, 930–934.
- Rosado, L., Ramos, P. M., Janeiro, F. M., & Piedade, M. (2012). Eddy currents testing defect characterization based on non-linear regressions and artificial neural networks. *IEEE I2MTC - International Instrumentation and Measurement Technology Conference*, 2419–2424.

- Rosado, L. S., Janeiro, F. M., Ramos, P. M., & Piedade, M. (2013). Defect characterization with eddy current testing using nonlinear-regression feature extraction and artificial neural networks. *IEEE Transactions on Instrumentation and Measurement*, 62(5):1207–1214.
- Rosado, L. S., Ramos, P. M., & Piedade, M. (2014). Real-time processing of multifrequency eddy currents testing signals: Design, implementation, and evaluation. *IEEE Transactions on Instrumentation and Measurement*, 63(5):1262–1271.
- Salucci, M., Ahmed, S., & Massa, A. (2016). An Adaptive Learning-by-Examples Strategy for Efficient Eddy Current Testing of Conductive Structures. *European Conference on Antennas and Propagation*, (1): 1–4.
- Schroeder, M. R. (1970). Synthesis of Low-Peak-Factor Signals and Binary Sequences with Low Autocorrelation. *IEEE Transactions on Information Theory*, 16(1), 85–89.
- Shejuan Xie , Zhenmao Chen , Hong-En Chen , XiaoweiWang , Toshiyuki Takagi, and T. U. (2013). Sizing of Wall Thinning Defects Using Pulsed Eddy Current Testing Signals Based on a Hybrid Inverse Analysis Method, 49(5), 1653–1656.
- Shin, H. J., Choi, J. Y., Cho, H. W., & Jang, S. M. (2013). Analytical torque calculations and experimental testing of permanent magnet axial eddy current brake. *IEEE Transactions on Magnetics*, 49(7):4152–4155.
- Sophian A., Tian G. Y., Taylor D., and R. J. (2003). A feature extraction technique based on principal component analysis for pulsed Eddy current NDT. *Journal of Chemical Information and Modeling*, 36(1): 37–41.
- Sophian, G. Y. T. and A. (2005). Reduction of lift-off effects for pulsed eddy current NDT. *NDT&E Int*, 38(4):319–324.
- Stubendekova, A., Smetana, M., & Janousek, L. (2014). Non-destructive Testing of Artificial Knee Joint by Eddy Current Method precise control of the probe movement . *The measurement*, 630–633.
- Takahashi, Y., Suwa, T., Nabara, Y., Ozeki, H., Hemmi, T., Nunoya, Y., Sekiguchi, N. (2015). Non-destructive examination of jacket sections for ITER central solenoid conductors. *IEEE Transactions on Applied Superconductivity*, 25(3):3–6.
- Thess, A., & Boeck, T. (2013). Electromagnetic drag on a magnetic dipole interacting with a moving electrically conducting sphere. *IEEE Transactions on Magnetics*, 49(6):2847–2857.
- Tian, G. Y., Li, Y., & Mandache, C. (2009). Study of lift-off invariance for pulsed eddy-current signals. *IEEE Transactions on Magnetics*, 45(1):184–191.

- Tian, G. Y., Morozov, M., & Takahashi, S. (2013). Pulsed eddy current testing of thermally aged and cold-rolled fe-cu alloys. *IEEE Transactions on Magnetics*, 49(1):517–523.
- Tytko, G., & Dzikowski, L. (2015). E-Cored Coil With a Circular Air Gap Inside the Core Column Used in Eddy Current Testing. *IEEE Transactions on Magnetics*, 51(9): 1-4.
- Vijayashree, R., Veeraswamy, R., Nashine, B. K., Dash, S. K., Sharma, P., Rajan, K. K., Kalyanasundaram, P. (2011). Testing of inductively coupled Eddy current position sensor of diverse safety rod in sodium. *2nd International Conference on Advancements in Nuclear Instrumentation, Measurement Methods and Their Applications*.
- Voulgaraki, C., Poulakis, N., & Theodoulidis, T. (2013). Theoretical simulations and quantitative magnetic field measurements for eddy-current testing with an HTS SQUID system. *IEEE Transactions on Applied Superconductivity*, 23(4):1603012-1603012.
- Wang chen, Zhao yulu¹, Fan jingjing, Z. xiaojuan¹. (n.d.). Giant Magneto Resistance Based Eddy-Current testing system, 2–5.
- Wang, C., Zhi, Y., & Gao, P. (2013). GMR based eddy current system for defect detection. *Proceedings of 2013 IEEE 11th International Conference on Electronic Measurement and Instruments*, 2:1052–1056.
- Wang, J., Yusa, N., Fukutomi, H., & Hashizume, H. (2014). Low Frequency Eddy Current Inspection of Wall- thinning of Large Pipes by Bobbin Coils. *Far East Forum on Nondestructive Evaluation/Testing*, 4–7.
- Wang, J., Yusa, N., & Hashizume, H. (2012). Discussion on Distributed Conductivity for Modeling Stress Corrosion Crack in Eddy Current Testing. *Sixth International Conference on Electromagnetic Field Problems and Applications (ICEF)*, 1–4.
- Wang, L., Xie, S., Chen, Z., Wang, X., & Takagi, T. (2013). Reconstruction of Deep Stress Corrosion Cracks Using Signals of the Pulsed Eddy Current Testing. *Nondestructive Testing and Evaluation*, 28(2), 145-154.
- Weise, K., Carlstedt, M., Ziolkowski, M., & Brauer, H. (2015). Uncertainty Analysis in Lorentz Force Eddy Current Testing. *IEEE Transactions on Magnetics*, 52(4):1–1.
- Wu, J., Zhou, D., Wang, J., Guo, X., You, L., An, W., & Zhang, H. (2014). Surface crack detection for carbon fiber reinforced plastic (CFRP) materials using pulsed eddy current testing. *IEEE Far East Forum on Nondestructive Evaluation/Testing*, 181–185.

- Xiao-lei CHEN, X. W. (2008). The design of testing system based on eddy current technology. *Anesthesia & Analgesia*, 107(3):1040.
- Xie, S., Chen, Z., Takagi, T., & Uchimoto, T. (2011). Efficient numerical solver for simulation of pulsed eddy-current testing signals. *IEEE Transactions on Magnetics*, 47(11):4582–4591.
- Yamazaki, K., Fukuoka, T., Akatsu, K., Nakao, N., & Ruderman, A. (2012). Investigation of locked rotor test for estimation of magnet PWM carrier eddy current loss in synchronous machines. *IEEE Transactions on Magnetics*, 48(11):3327–3330.
- Yin, W., & Xu, K. (2016). A novel triple-coil electromagnetic sensor for thickness measurement immune to lift-off variations. *IEEE Transactions on Instrumentation and Measurement*, 65(1):164–169.
- Yu, Y., Zou, Y., Jiang, M., & Zhang, D. (2015). Investigation on conductivity invariance in eddy current NDT and its application on magnetic permeability measurement / Coil. In *IEEE Far East NDT New Technology & Application Forum (FENDT)*, 257–262.
- Zec, M., Uhlig, R., Ziolkowski, M., & Brauer, H. (2013). Finite Element Analysis of Non Destructive Testing Eddy Current Problems with Moving Parts. *IEEE Transactions on Magnetics*, 49(8):4785–4794.
- Zeng, Z., Wang, T., Sun, L., He, R., & Chen, J. (2015). A Domain Decomposition Finite-Element Method for Eddy-Current Testing Simulation. *IEEE Transactions on Magnetics*, 51(10):6202009.
- Zhang, S., Liu, Y., Yin, C., & Qi, C. (2014). Imperialist Competitive Algorithm for Natural Crack Shape Reconstruction from ECT Signals. *11th World Congress on Intelligent Control and Automation (WCICA)*, 4912–4917.
- Zhang, S., Tang, J., Wu, W., & Model, A. A. (2015). Calculation Model for the Induced Voltage of Pick-up Coil Excited by Rectangular Coil above Conductive Plate. *IEEE International Conference on Mechatronics and Automation (ICMA)*, 2(6), 1805–1810.
- Zhu, P., Bai, L., Cheng, Y., & Yin, C. (2015). Selection of significant independent components in eddy current pulsed thermography non-destructive testing. *IEEE International Instrumentation and Measurement Technology Conference*, 853–857.

APPENDIX A C PROGRAMMING CODE

C1. LCD display programming

```
/*
 * Include Files
 *
 */
#if defined(MATLAB_MEX_FILE)
#include "tmwtypes.h"
#include "simstruc_types.h"
#else
#include "rtwtypes.h"
#endif

/* %%-SFUNWIZ_wrapper_includes_Changes_BEGIN --- EDIT HERE TO _END */
#include <math.h>
#ifndef MATLAB_MEX_FILE
#include "LiquidCrystal.h"
#include "LiquidCrystal.cpp"

LiquidCrystal lcd(12, 11, 5, 4, 3, 2);
#endif
/* %%-SFUNWIZ_wrapper_includes_Changes_END --- EDIT HERE TO _BEGIN */
#define u_width 1
/*
 * Create external references here.
 *
 */
/* %%-SFUNWIZ_wrapper_externs_Changes_BEGIN --- EDIT HERE TO _END */
/* extern double func(double a); */
/* %%-SFUNWIZ_wrapper_externs_Changes_END --- EDIT HERE TO _BEGIN */

/*
 * Output functions
 *
 */
extern "C" void morelcd_Outputs_wrapper(const uint16_T *AProbe,
                                       const uint16_T *DProbe,
                                       const uint16_T *Error,
                                       const uint16_T *Fuzzy,
                                       const real_T *xD)
{
/* %%-SFUNWIZ_wrapper_Outputs_Changes_BEGIN --- EDIT HERE TO _END */
/* This sample sets the output equal to the input
   y0[0] = u0[0];
   For complex signals use: y0[0].re = u0[0].re;
   y0[0].im = u0[0].im;
   y1[0].re = u1[0].re;
   y1[0].im = u1[0].im;
*/
if(xD[0] == 1)
{
    #ifndef MATLAB_MEX_FILE
    lcd.setCursor(0,0);

```

```

    lcd.print("AProbe: ");
    lcd.print(AProbe[0]);
    lcd.print((char)223);
    lcd.print("mm");
    lcd.setCursor(0,1);
    lcd.print("DProbe: ");
    lcd.print(DProbe[0]);
    lcd.print((char)223);
    lcd.print("mm");
    lcd.setCursor(0,2);
    lcd.print("Error : ");
    lcd.print(Error[0]);
    lcd.print((char)223);
    lcd.print("mm");
    lcd.setCursor(0,3);
    lcd.print("Fuzzy : ");
    lcd.print(Fuzzy[0]);
    lcd.print((char)223);
    lcd.print("mm");
    #endif
}
/* %%-SFUNWIZ_wrapper_Outputs_Changes_END --- EDIT HERE TO _BEGIN */
}

/*
 * Updates function
 *
 */
extern "C" void morelcd_Update_wrapper(const uint16_T *AProbe,
    const uint16_T *DProbe,
    const uint16_T *Error,
    const uint16_T *Fuzzy,
    real_T *xD)
{
    /* %%-SFUNWIZ_wrapper_Update_Changes_BEGIN --- EDIT HERE TO _END */
    /*
    * Code example
    *   xD[0] = u0[0];
    */
    if(xD[0] !=1)
    {
        #ifndef MATLAB_MEX_FILE
        lcd.begin(20,4);
        // lcd.print("DProb");
        #endif
        xD[0] = 1;
    }
    /* %%-SFUNWIZ_wrapper_Update_Changes_END --- EDIT HERE TO _BEGIN */
}

```

C2. Fuzzy Logic Rules Setting

```

[System]
Name='defect_master2'
Type='mamdani'
Version=2.0
NumInputs=2
NumOutputs=1

```

```

NumRules=9
AndMethod='min'
OrMethod='max'
ImpMethod='min'
AggMethod='max'
DefuzzMethod='centroid'

[Input1]
Name='differentialprobe'
Range=[0 5]
NumMFs=3
MF1='lowdefect':'gaussmf',[1.5 0]
MF2='depthdefect':'gaussmf',[0.5 2.5]
MF3='dengerdefect':'gaussmf',[1.5 5]

[Input2]
Name='absoluteprobe'
Range=[0 5]
NumMFs=3
MF1='lowliftoff':'trapmf',[0 0 1 1.5]
MF2='mediumliftoff':'trapmf',[1 2 3 4]
MF3='highliftoff':'trapmf',[3.5 4 5 5]

[Output1]
Name='output1'
Range=[0 6]
NumMFs=3
MF1='normaldefect':'trimf',[-0.0158730158730158 0.984126984126984
1.98412698412698]
MF2='baddefect':'trimf',[2 3 4]
MF3='dangerdefect':'trimf',[4 5 6]

[Rules]
1 1, 1 (1) : 1
2 1, 3 (1) : 1
2 2, 2 (1) : 1
2 3, 2 (1) : 1
3 1, 3 (1) : 1
3 2, 3 (1) : 1
3 3, 2 (1) : 1
1 2, 2 (1) : 1
1 3, 2 (1) : 1

//

```

APPENDIX B HARDWARE SYSTEM SPECIFICATION

B1. Fuzzy Simulink System

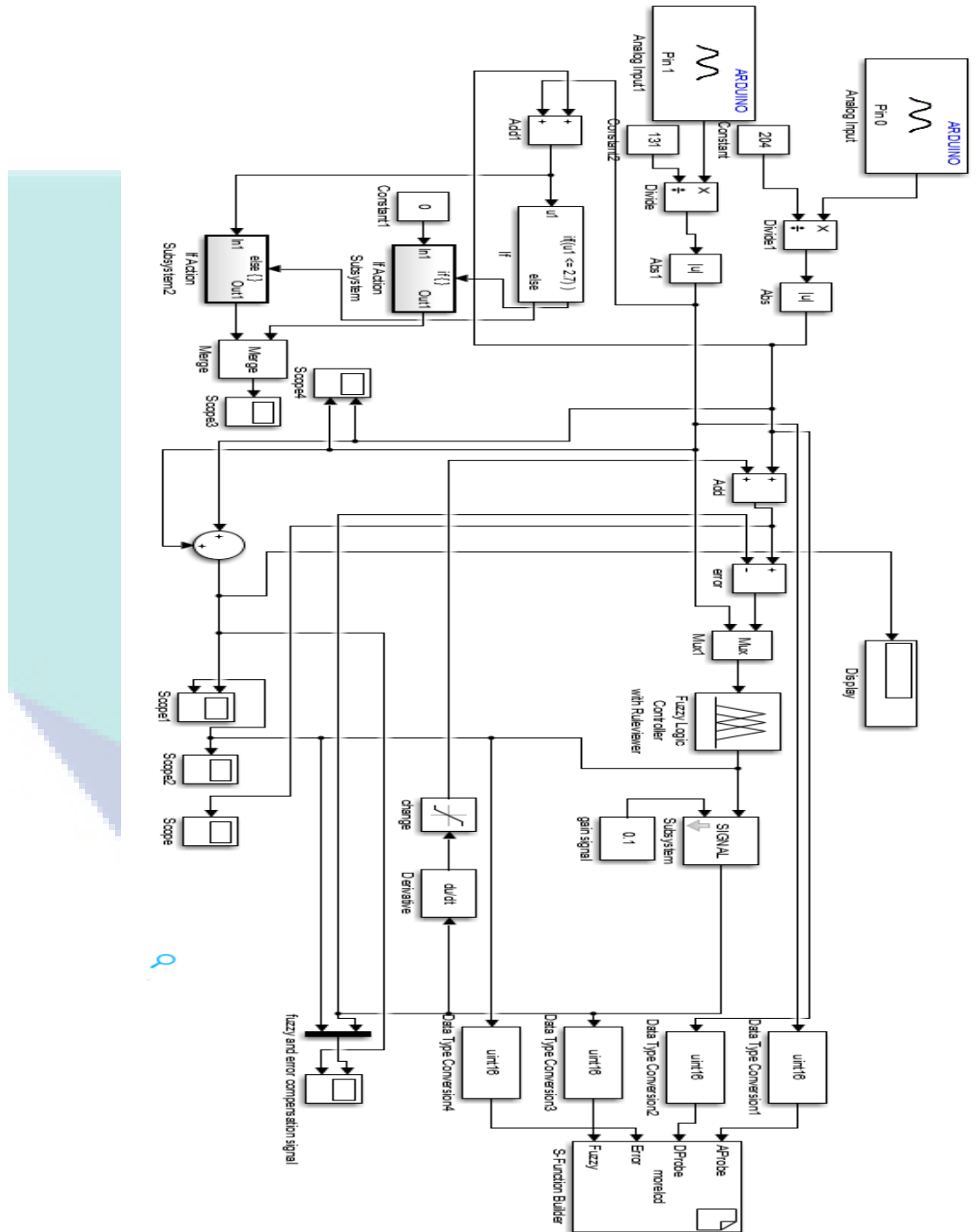


Figure B1 Complete system for ECECT

B2. Design Brass Calibration Block

The design is very important in the development of calibration block. The desired shape for calibration block is drawn by using AUTOCAD software. The design in 2D and 3D is useful in identifying the actual size of calibration block beside the depth of defect are required. Figure B25 shows the top view, front view and 3D design for calibration block with including the depth of the defect within 0.5mm and 2mm.

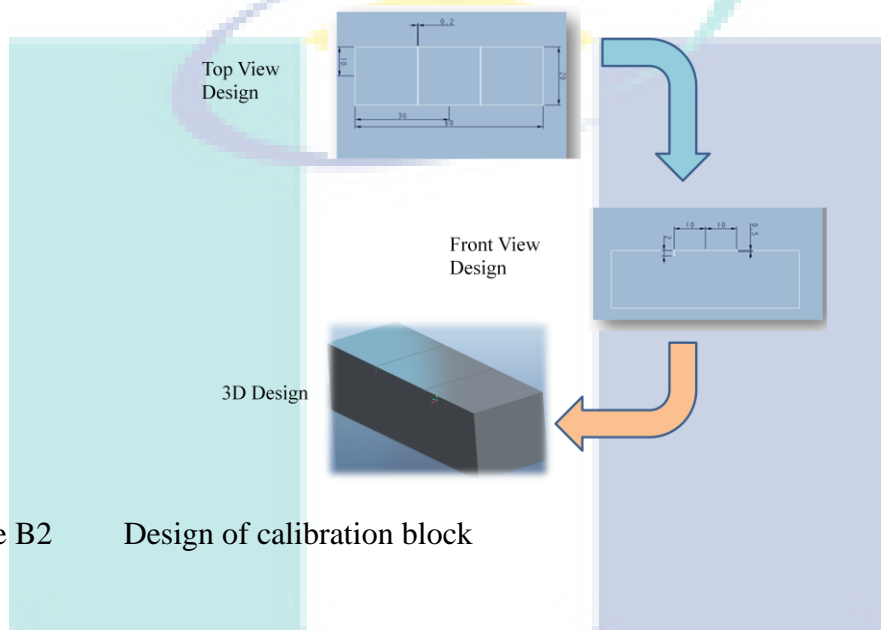


Figure B2 Design of calibration block

B3. Hardware Fabrication

The process for fabrication of the Brass Calibration block should thoroughly three main steps there is surface grinding, wire cutting and lastly heat treatment. Surface grinding is the most common of the grinding operations. It is a finishing process that uses a rotating abrasive wheel to smooth the flat surface of metallic or non-metallic materials to give them a more refined look or to attain the desired surface for a functional purpose.

Wire Electrical Discharge Machine (EDM) is used to make manufactured 3 blocks with the dimension of 60mm (length) \times 20mm (width) \times 20mm (height). In the top view of the block, there will be 2 slots surface defect. Each slot has a different depth from the top surface. The first slot which starts At the most left side of the block, have a slot depth of 0.5mm and the second slot depth is 2.0mm. The block is troubleshooting for accuracy and precision and any discontinuities will be rejected and brings it to the starting point of reproduction.

The Annealing machines or heat treatment machine is used to heat the brass material. This heat treatment machine need to set up early before makes the heat treatment process on the brass material. The heat treatment machine is set up using the information from the brass material for the time taken to make the heat treatment process and the heating temperature of the brass material. Figure B26 shows the step of fabricating the Brass calibration block.

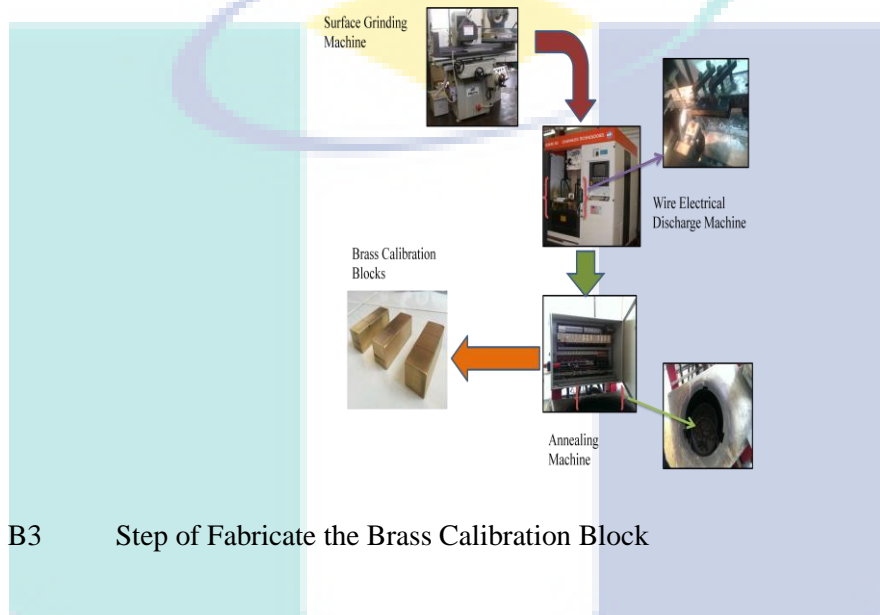


Figure B3 Step of Fabricate the Brass Calibration Block

B4. Sample Testing

The flat plate with the middle joint by welding is used as sample for defect measuring. This plate is call it plate weld or A plate. Figure B27 show the A plate The dimension plate is 305mm x 150mm x 6mm.



Figure B4 A Plate Sample

B5. Differential Probe Measuring

Penetration depth (more normally called skin depth) is greater at LF, conduction, and permeability. Skin depth drop-offs as these values increase. Since don't bear any control across conduction or permeability, frequency is best ally. Thus, contingent the type of defect are anticipating, but more significantly where these defects are located in the material decide a frequency that will give and an decent eddy current penetration. The guideline is for defects to be inside one to two skin depths from the surface to acquire good far-side indication detection.

The effect of frequency could be show on Figure 4.10 with 4KHz frequency. The angle and size of signal was show is not high though the depths of defect are 1mm, 2mm and 3mm. From Figure B28 the angle of signal are 1° , 2° and 3° with the wide of signal are a quarter, half and a block signal.

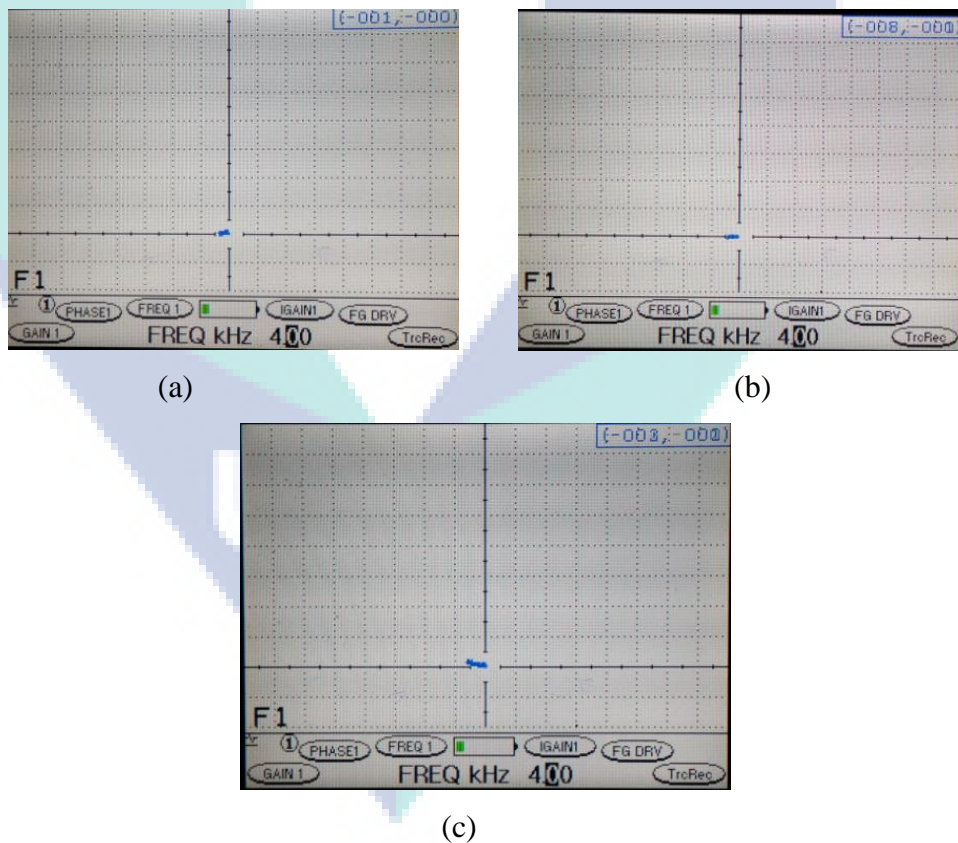


Figure B5 Signal with 4KHz (a) 1mm, (b) 2mm, (c) 3mm

From 10KHz frequency, the signal produce is clear and higher the 4 KHz. In 1mm, 2mm and 3mm depth the angle and wide of signal are 3° with 1.5 blocks, 25°

with 2 blocks and 45° with 3 blocks signal. Figure B29 show the 10KHz frequency signal and angle.

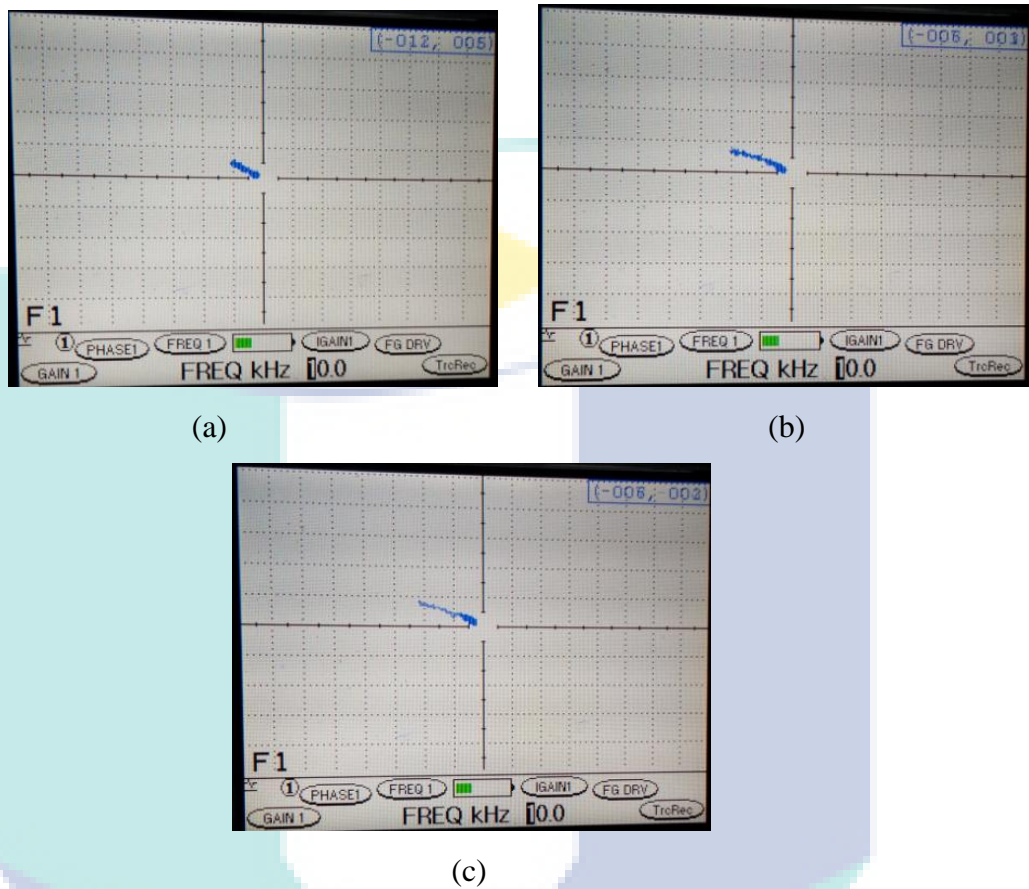
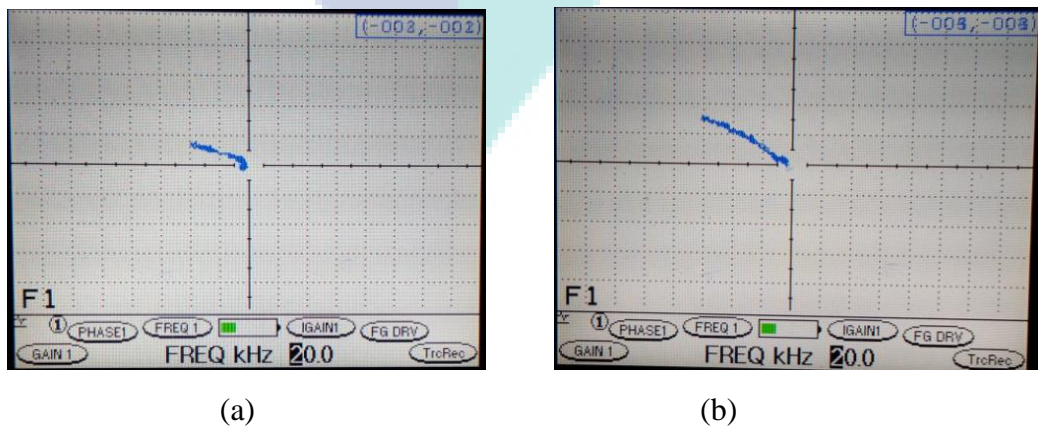
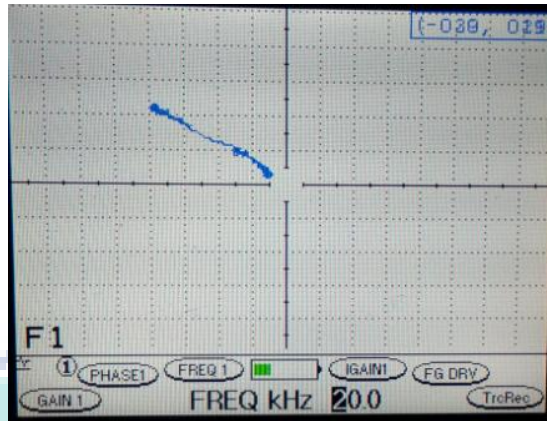


Figure B6 Signal with 10KHz (a) 1mm, (b) 2mm, (c) 3mm

Lastly when the frequencies are setting at 20 KHz, the depths of defect are very clearly. If frequency setting is more than that, the signal shows will over than block signal. From frequency 20KHz, the angle and block signal was produced are 3 blocks with 30° , 3.5 blocks with 45° and 4 blocks with 50° . Figure B30 shows the block signal and angle signal by using 20KHz





(c)

Figure B7 Signal with 20KHz (a) 1mm, (b) 2mm, (c) 3mm

B6. Absolute Probe Measuring

A few testing have being making in order to getting the appropriate frequency for absolute probe. In here the three frequencies are selecting on this testing. There are 4 KHz, 10 KHz and 20 KHz. Figure B31 shows the measuring of thickness of coating layer by using 4 KHz frequency. The signal levels are decrees when the layers of coating are high. From here (a) is signal of absolute probe without the coating layer, (b) is signal with the 0.5mm coating layer depth, (c) is signal with the 1.0mm coating layer depth, (d) is signal with the 1.5mm coating layer depth and lastly (e) signal with the 0.5mm coating layer depth.



(a)



(b)

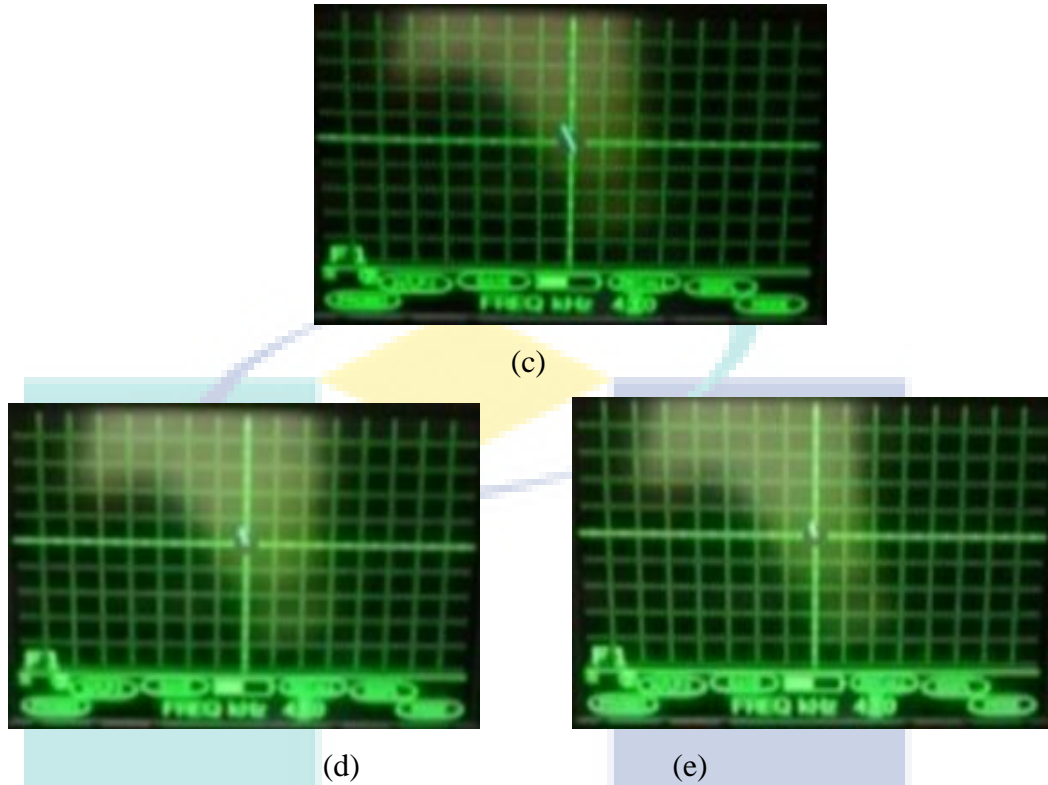
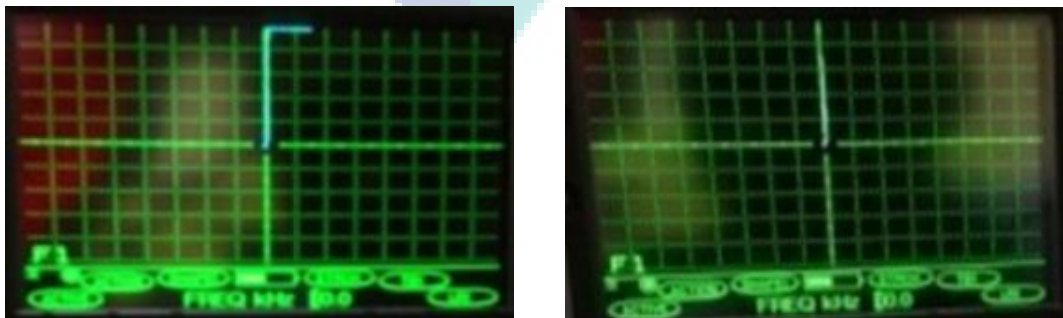


Figure B8 Signal with 4 KHz (a) Without coating layer, (b) With 0.5 mm depth coating layer, (c) With 1.0 mm depth coating layer, (d) With 1.5mm depth coating layer and (e) With 2.0 mm depth coating layer.

The length of signal is quietly clear on 10 KHz frequency with 2.0mm coating layer thickness compare of 4 KHz frequency. From here the length of non coating thickness is higher compare 4 KHz frequency. Figure B32 show the signal of 10 KHz frequency within (a) is signal of absolute probe without the coating layer, (b) is signal with the 0.5 mm coating layer depth, (c) is signal with the 1.0mm coating layer depth, (d) is signal with the 1.5mm coating layer depth and lastly (e) signal with the 2.0mm coating layer depth.



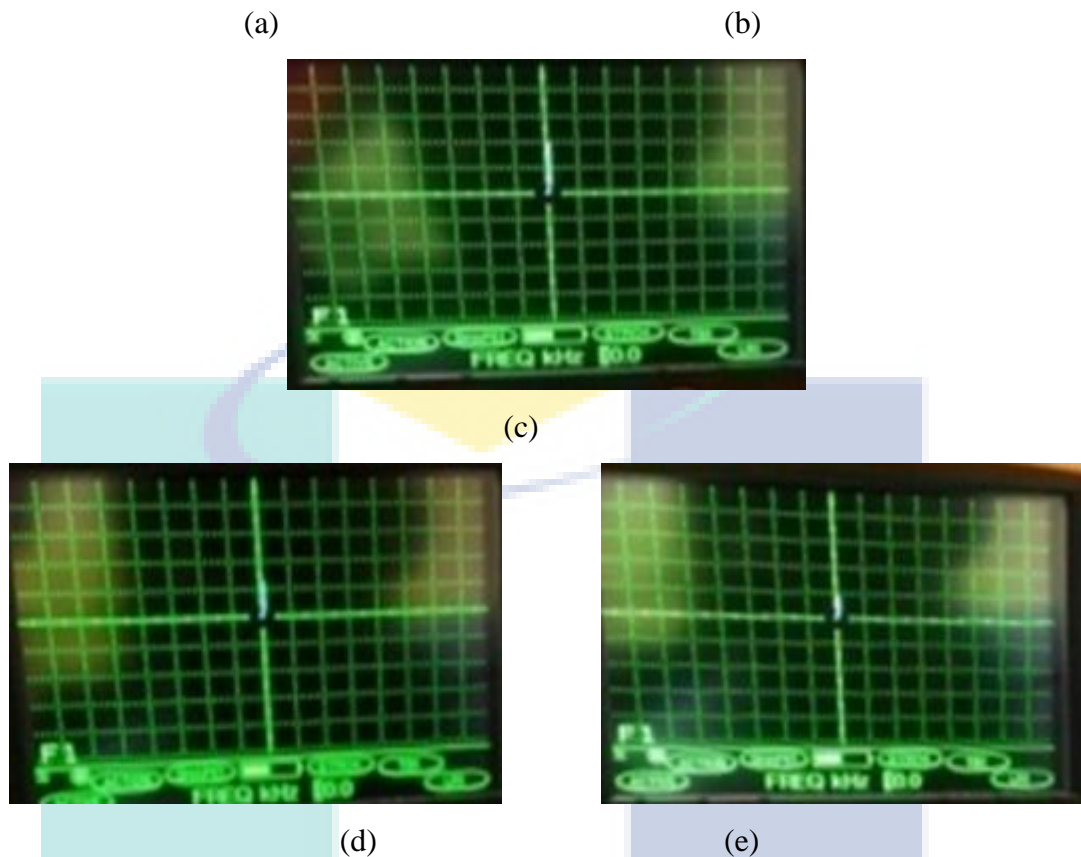


Figure B9 Signal with 10 KHz (a) Without coating layer, (b) With 0.5mm depth coating layer, (c) With 1.0mm depth coating layer, (d) With 1.5mm depth coating layer and (e) With 2.0mm depth coating layer.

According to Figure B33, the signal of non-coating thickness is highest compared to the signal at 10 KHz frequency and it is affected by measuring the actual depth of defect when it integrates with a differential probe. By following the signal, it decreases as the thickness of the coating layer increases. The signal is inversely proportional to thickness. In (a) the signal of the absolute probe is very high without the coating layer, (b) is the signal with the 0.5mm coating layer depth, (c) is the signal with the 1.0mm coating layer depth, (d) is the signal with the 1.5mm coating layer depth, and lastly (e) is the signal with the 2.0mm coating layer depth.

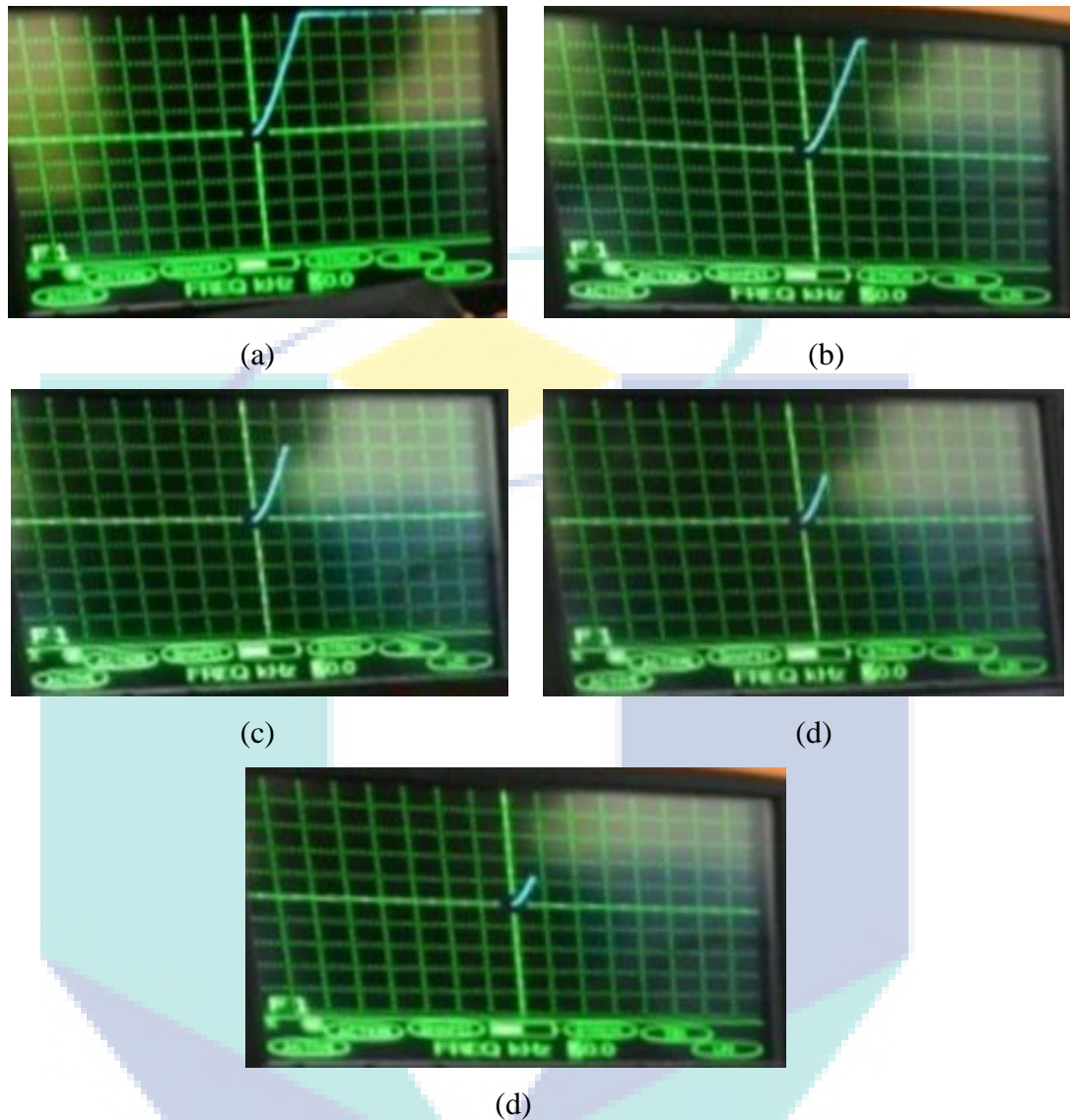


Figure B10 Signal with 20 KHz (a) Without coating layer, (b) With 0.5mm depth coating layer, (c) With 1.0mm depth coating layer, (d) With 1.5mm depth coating layer and (e) With 2.0mm depth coating layer.

B7. Publication

Year	Title	Publication
March 2017	Hybrid Eddy Current Testing Error Compensation Based On Mamdani-Fuzzy Coupled Differential and Absolute Probes	Neurocomputing Journal Impact Factor 2.392 NEUCOM-D-17-00793
Nov 2016	A Review on System Development in Eddy Current Testing and	IET Circuit Devices and System (IEEE Journal) CDS-SI-2016-0327 Impact Factor 0.590

	Technique for Defect Classification and Characterization.	
Dis 2016	AC Excitation Signal Test Frequency for Locating Surface Defect of Heat Treated Brass Calibration Block Using Eddy Current Technique	Journal of Engineering and Apply Sciences Scopus Index
Dis 2016	Multi-Excitation Signal for Depth Crack Defect in Eddy Current Testing	Fluidsche2017 Scopus Index
2016	A Review on Structures and Non-Destructive Eddy Current Testing Applications, Sensors journal, ISI(Q1):2.47 impact factor.	Giant Magnetoresistance Sensors
2017	Eddy Current Testing Platform System Based on the Optimized ECT Probe Design for Pipe Defect Inspection ,Sensors journal, ISI(Q1):2.47	Giant Magnetoresistance Sensors
2016	Defect Signal Analysis for Nondestructive Testing	ARPN Journal of Engineering and Applied Sciences. Scopus indexed
2016	Subsurface Defects Evaluation Using Eddy Current Testing	Indian Journal of Science and Technology (Indjst), ISI indexed
2015	Non-destructive evaluation of depth of subsurface defects using Eddy Current Testing	International Academic Conference (IAC)
2015	Investigating the Optimum Frequency and Gain for Calibration Copper Block Using Eddy Current Technique,	International Conference on Smart Sensors and Application (ICSSA)